Validating Greatwall kinase as a potential target in cancer therapy

Aimee Eckert

A thesis submitted to the University of Sussex for the degree of Doctor of Philosophy

September 2018

Genome Damage and Stability Centre
University of Sussex

DECLARATION

I hereby declare that this thesis has not been submitted in this or any other form to any other university for the award of a degree. The work described here is my own except where otherwise stated.

Aimee Eckert

September 2018

Acknowledgements

I would like to thank everyone who has made this work possible and who has helped me get this far. Firstly, thank you to the Medical Research Council for funding this project. Sincere and endless thanks to Helfrid Hochegger for offering me the opportunity to do a PhD in his laboratory. Without his expertise, feedback, guidance and bottomless reserve of patience, I would not be writing this. Sincere thank you to all our collaborators, especially Chris Lord of the ICR, who helped to make this work possible. Thank you to everyone past and present in the Hochegger group who are a constant source of wisdom, support and humour. Thank you to Nadia for always finding time to help.

Thank you to everyone in the Genome Centre for making it such a lovely place to work. I am indebted to Katie, Zuza and Annie for invaluable advice and amazing humour about science, life and everything in general. Thank you for all the ‘Breakdown Tuesday’s’. You are wonderful humans and incredible friends.

Endless thanks, praise and apologies to my brilliant parents Sarah and Piere. Thank you for always believing in me and putting up with me. Thank you for never telling me that I couldn’t do something.

Thank you to Rob for loving and cheering me on from Cork, and for laughing at my terrible jokes.

I also owe a great deal to my luminous science communication family. Thank you all for the laughs, opportunities and support.

For Simon Eckert.

University of Sussex

Aimee Eckert – Doctor of Philosophy

Validating Greatwall kinase as a potential target in cancer therapy

SUMMARY

All cancers have deregulated cell proliferation. Therefore, full understanding of cell cycle control is needed to identify protein targets that can lead to the development of novel therapies, as well as improving our knowledge and use of existing ones. Greatwall kinase (GWL), a protein essential for mitotic entry in human cells, is gaining interest in cancer research as it has been shown to be upregulated in various cancers. My research aims to decipher the mechanisms of Triple Negative breast cancer (TNBC) cell sensitivity to GWL knockdown, as this information could provide scope for the development of novel drugs to be synergised with existing treatments. We have shown that depletion of GWL via shRNA in certain TNBC cell lines causes harmful cell proliferation defects. Surprisingly these effects coincided with significant depletion of replicating cells, rather than pronounced mitotic defects. This suggests that certain cancer cells are especially reliant on GWL and that GWL may have other functions apart from its known role in suppressing mitotic PP2A activity. To further investigate these novel functions, we have performed a siRNA cell viability screen comparing cells lacking and expressing GWL. This led to the identification of a novel synthetic lethality between CDK4 (a kinase whose activity is restricted to G1-S phase) and GWL (canonically active in mitosis). Further analysis revealed that this synergy of GWL and CDK4 does not involve the known downstream substrates of GWL: ENSA and ARPP19, suggesting that GWL acts in this pathway in a non-canonical way. Taken together, this thesis presents the discovery of a novel biological pathway in the control of the G1/S transition that could be exploited in cancer therapy to treat TNBC patients.

TABLE OF CONTENTS

List of figures

List of tables

Abbreviations

ADP	Adenosine diphosphate
APC/C	Anaphase-promoting complex/cyclosome
APS	Ammonium persulphate
ARPP19	cAMP-regulated phospho-protein 19
ATM	Ataxia telangiectasia mutated kinase
ATP	Adenosine triphosphate
ATR	Ataxia telangiectasia and Rad-3-related kinase
BEG	PP2A-B55α/ENSA/Greatwall pathway
BSA	Bovine serum albumin
CAK	CDK-activating kinase
cAMP	Cyclic adenosine monophosphate
Cdc	Cell division cycle
CDK	Cyclin dependent kinase
CDK	Cyclin dependent kinase
CENPF	Centromere protein F
CKI	CDK-inhibitor
CSF	Cytostatic factor
DAPI	4', 6-diamidino-2-phenylindole
DDR	DNA Damage Response
DDK	Cdc7/Dbf4 kinase, or Dbf4-dependent kinase
dH_2O	Distilled water
DNA	Deoxyribonucleic acid
Dox	Doxycycline
DSB	Double strand breaks
ECL	Enhanced chemiluminescence
EDTA	Ethylenediaminetetraacetic acid
ENSA	α-Endosulfine
FACS	Fluorescence Activated Cell Sorting
FCS	Foetal Calf Serum
GFP	Green Fluorescent Protein
GWL	Greatwall kinase
HEK	Human embryonic kidney

HRP	Horseradish peroxidase
INK	Inhibitors of CDK
L	Litre
MAP	Mitogen activated protein
MASTL	Microtubule associated serine/threonine-like
MAT1	Ménage à trois-1
Mcm	Mini-chromosome maintenance
MPF	Maturing/Mitosis Promoting Factor
mL	Millilitre
mM	Millimolar
mm	Millimetre
mRNA	Messenger RNA
NEB	Nuclear envelope breakdown
nM	Nanomolar
ORC	Origin recognition complex
PAGE	Polyacrylamide gel electrophoresis
PDX	Patient derived xenograft
PI	Propidium iodide
PKA	cAMP-activated protein kinase
PKC	Protein kinase C
PLK1	Polo-like kinase 1
PP1	Protein phosphatase 1
PP2A	Protein phosphatase 2A
Rb	Retinoblastoma
RC	Replication complex
ROI	Region of interest
Rpm	Revolutions per minute
RNA	Ribonucleic acid
RPA	Replication protein A
SCC	Squamous cell carcinoma
Ser	Serine
SAC	Spindle assembly checkpoint
SDS	Sodium dodecyl sulphate
siRNA	Short interfering RNA

SRB	Sulforhodamine B
Thr	Threonine
TEMED	N,N,N',N'-tetramethylethylenediamine
TNBC	Triple Negative Breast Cancer
TGF-β	Transforming growth factor-β
TRE	Tetracycline Response Element
Tyr	Tyrosine
µg	Microgram
µL	Microlitre
µM	Micromolar
UK	United Kingdom
US	United States of America
WT	Wild-type

Chapter 1. Introduction

1.1 The mammalian cell cycle

The cell is the fundamental building block of all living things. With the exception of the very first cells on Earth around 3.5 billion years ago, all cells have arisen from other cells via cell division. The first description of the cell is generally credited to Robert Hooke who, whilst studying a slice of cork under a microscope, noted small and regular units that he described were like an empty honeycomb, or the cells monks would sleep in at that time (W. Turner 1890; Mazzarello 1999). The discoveries and contributions of many scientists, including Louis Pasteur, Robert Remak, Rudolf Virchow, Matthias Schleiden and Theodor Schwann, together led to the disproval of Spontaneous Generation Theory, and the wide acceptance of Cell Theory.

Cell division can create new cells in two slightly different ways. The word mitosis describes a cell division in which a single cell duplicates its DNA (and organelles, if the cell possesses these) and divides once to create two identical cells. This process is used in asexual reproduction, and for growth and repair in multicellular organisms. The other type of cell division is meiosis, which is exclusively used to create gametes by organisms that reproduce sexually. In meiosis, chromosomal crossover followed by two cell divisions creates four genetically different cells. The process that co-ordinates these highly complex cell division events is the cell cycle, and in this thesis, I will be focusing on the mitotic cell cycle.

The fundamental task to allow cellular proliferation is ensuring accurate genome duplication and segregation of the duplicated genome. In bacteria there is no strict separation of these two processes, but the evolution of a separate nuclear compartment in eukaryotes appears to have necessitated the introduction of an ordered sequence of events termed the cell division cycle. In most animal cells the typical progression of this cycle involves the separation of the DNA synthesis phase (S phase) by two 'gap' phases (G1 and G2) from the segregation and division phase (M phase, mitosis). The stages comprising of G1, S and G2 phases can also be referred to as interphase (Howard & Pelc 1986). During interphase, a cell co-ordinates and interprets signals from its environment and may receive sufficient pro-growth signals to enter a new round of mitosis, which means the cell will prepare to synthesise a copy of its DNA, and this phase is termed G1. DNA replication takes place in S phase, and G2 is the second gap phase in which cells check that DNA replication has been done properly and prepares to begin mitosis (Alberts et al. 2002; Morgan 2007). Although mitosis is the shortest of the cell cycle phases, it is so dynamic in nature that the mitotic phase can be further divided into several additional phases: Prophase, in which the nuclear envelope is broken down (Nuclear Envelope Breakdown, NEB) and the chromosomes begin to condense. The next two phases are prometaphase and metaphase, in which the mitotic spindle is assembled and the chromosomes line up on the equator of the cell, called the metaphase plate, and the sister chromatids are attached via their kinetochore to a spindle pole. Then in anaphase the sister chromatids are pulled and separated to each spindle pole, and this is followed by telophase in which a new nuclear envelope starts to form, and the chromosomes begin to de-

condense. After this mitotic stage, the cell undergoes cytokinesis by pinching its cytoplasm and cleaving into two to form two daughter cells (Alberts et al. 2002; Morgan 2007).

Cells decide whether or not to divide by interpreting the signals they receive from their surroundings. This is true for unicellular organisms such as yeasts as well as multicellular organisms. However, in multicellular life the cells are formed into tissues and organs, and so all cells must co-operate to maintain organisation for the benefit of the organism. Thus, almost all types of normal human cells will not proliferate unless prompted to do so by mitogenic factors (Blagosklonny 2004; Duronio & Xiong 2013). Other signalling proteins such as transforming growth factor-β (TGF-β), are able to overrule the pro-growth messages conferred by mitogenic factors and stop cell proliferation (Kubiczkova et al. 2012; Li et al. 2014). These conflicting signals are collected by many different cell surface receptors, and somehow processed into a binary decision: to divide, or not divide? After a round of mitosis and cytokinesis, the cell must decide soon after whether it will enter another cycle of division or enter a un-proliferative state. The un-proliferative state can be reversible, which is known as quiescence or G_0 (G zero); or it can be irreversible, which is called senescence and is especially associated with fully differentiated cells (Cheung & Rando 2013). In 1974, Pardee provided evidence for the quiescent state and demonstrated the existence of a restriction point (R-point) in G1 that determines cell fates: cells in G1 are able to become quiescent before the R-point but after the R-point, they are committed to enter a mitotic cell cycle. Transition of the restriction point has been proposed to be determined by accumulation of a

labile protein (R-protein) whose synthesis is sensitive to growth factors, and must accumulate to a critical amount before a cell can pass the restriction point and proceed towards DNA synthesis (Campisi et al. 1982). However some studies suggest that both terminally differentiated and senescent cells are able to re-enter the cell cycle by inhibiting tumour suppressors such as p53 and RB (Beauséjour et al. 2003; Pajcini et al. 2010).

1.2 CDKs and Cyclins

A significant part of the cellular machinery that decides in G1 phase whether a cell enters a proliferative state, as regulating many processes throughout the cell cycle as a whole, is a group of serine/threonine protein kinases, collectively called the Cyclin-dependent kinases (CDKs). The nature of these kinases, as suggested in their name, is that they never act alone. They require regulatory subunits called Cyclins for proper function. Various CDK-Cyclin complexes are largely responsible for transmitting signals to hundreds if not thousands of targets to move the cell through growth and division, and so form the 'engine' or 'master regulators' of the cell cycle machinery. During G1 phase, the activities of two CDKs – CDK4 and CDK6 are guided by the D Cyclins (D1, D2 and D3). After the R-point in late G1, the E Cyclins (E1 and E2) associate with CDK2 to enable the phosphorylation of the substrates required for entry into S phase (Bertoli et al. 2013). As cells enter S phase, the A Cyclins (A1 and A2) replace the E Cyclins as the binding partners of CDK2, allowing S phase to progress. Later in S phase, the A Cyclins now switch partners and bind with CDK1. As the cell moves further into G2 phase, the A Cyclins are replaced as the binding

partners of CDK1 by the B Cyclins (B1 and B2). At the start of M phase, the CDK1-Cyclin B complexes trigger the events that together make up the complex, dynamic movements of mitosis (Morgan 2007; Malumbres & Barbacid 2009; Hochegger et al. 2008). After the metaphase–anaphase transition, Cyclin levels start to decline, and CDK-controlled phosphorylations begin to be reversed by phosphatases to drive mitotic exit (Barr et al. 2011; E. S. Johnson & Kornbluth 2012). The events in each phase of the cell cycle will be covered in more detail later.

The activities of the CDK-Cyclin complexes must be modulated to have control over the different cell cycle stages. It is the fluctuating levels of Cyclin proteins, via rounds of intermittent Cyclin gene expression and proteolysis, that induce fluctuations in their corresponding CDK activities, as CDK protein levels remain fairly constant (Minshull et al. 1989; Minshull et al. 1990). **Figure 1.1** summarises this process, with panel **A)** indicating which CDK partners with which Cyclin and at what cell cycle stage, and panel **B)** indicating how the different Cyclin protein levels in the cell rise and fall during the cell cycle phases.

The first member of the CDK family to be identified (now designated CDK1, especially in human cells) was discovered via genetic screens in *S. pombe* and *S. cerevisiae* mutants with defects in their cell division cycles (Russell & Nurse 1986). This protein, named Cdc2 in *S. pombe* and Cdc28 in *S. cerevisiae*, was shown to be essential for cell-cycle progression. Then, homologs of Cdc2 were identified in human cells by their abilities to rescue

yeast mutants (M. G. Lee & Nurse 1987; Draetta et al. 1987). Cyclins were discovered during studies of the sea urchin cell cycle (Evans et al. 1983; Pines & Hunt 1987), and are so named because their concentration within the cell rises and falls in a cyclical fashion throughout the cell cycle. In budding yeast, a single CDK termed Cdc28 drives the progression through the cell cycle by interacting with cell cycle phase-specific Cyclins. In higher eukaryotes, these functions of CDK1 have been distributed among different homologues of the kinase that interact with specific Cyclins at a given time and place in the cell as described earlier and illustrated in **Figure 1.1**. Studies of cell cycle control mechanisms across a variety of eukaryotes have found that the networks that underpin the cell cycle and the topology of the cell cycle control proteins are remarkably conserved, even if individual protein amino acid sequences can be very different (Cross et al. 2011). For example, the human Cdc2 can be a substitute for Cdc2 in *Schizosaccharomyces pombe* (M. G. Lee & Nurse 1987) and for the CDK1/CDC28 in *Saccharomyces cerevisiae* (Wittenberg & Reed 1989). Also, human Cyclins can substitute for *S. cerevisiae* Cyclins (Lew et al. 1991).

Cyclins act as allosteric activators of CDKs. When docking with its Cyclin partner, the CDK protein undergoes a conformational change that rearranges the activation loop, or T-loop, so that the kinase's active site is exposed. This allows important amino acid residues to be moved into place for optimal ATP

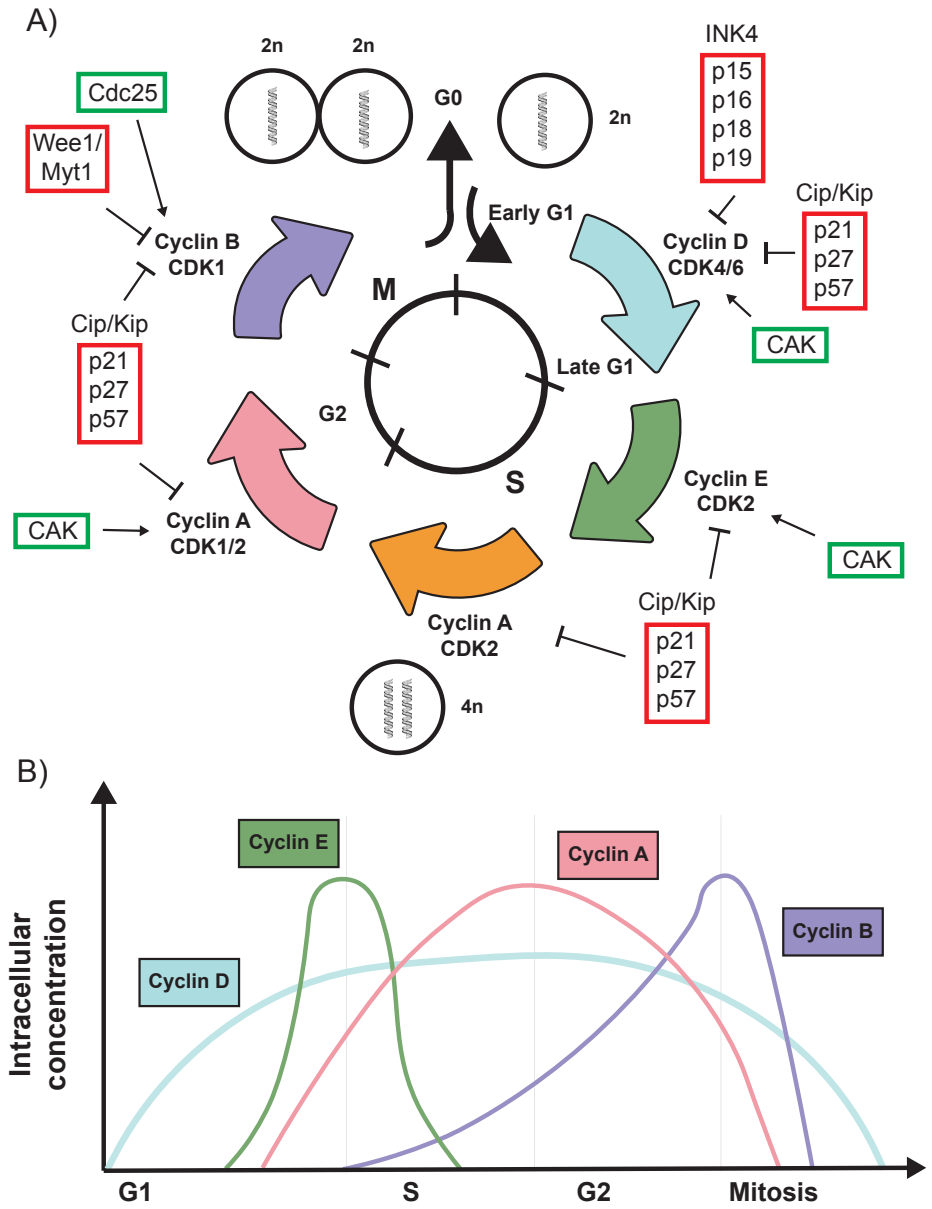

Figure 1.1 Control of the mammalian cell cycle by CDK-Cyclin complexes
A) A schematic representation of the CDK-Cyclin complexes that regulate mammalian cell cycle progression throughout the different cell cycle phases. Activating regulators are in green boxes, inhibitory regulators are in red boxes. CAK is the trimer of CDK7/Cyclin H/MT1. Adapted from Malumbres et al. 2010. B) Cyclin expression during the cell cycle. D-type Cyclin levels are relatively stable throughout the cell cycle, and E-type Cyclins are expressed at G1/S to drive S phase entry. A-type Cyclins allow progression into mitosis from S phase and the B-type Cyclins are primarily responsible for mitosis. Adapted from Morgan, 2007.

binding (Jeffrey et al. 1995; Russo et al. 1996). In contrast, Cyclins have no enzymatic activity but contain binding sites for substrates, in addition to the CDK binding site (Petri et al. 2014; Dorée & Hunt 2002). It is important to note that **Fig. 1.1** does not tell a complete story, as firstly CDKs can be promiscuous in their Cyclin binding, with CDK1 and CDK2 being able to bind Cyclins A, B, D and E, in comparison to CDK4 and CDK6 only partnering with D-type Cyclins (Hochegger et al. 2008). Secondly, other post-translational modifications are required for a CDK's activity to peak. In addition to Cyclin binding, an activating threonine phosphorylation is added by the CDK-activating kinase (CAK) complex, which is in itself a CDK-Cyclin complex: CDK7/Cyclin H (Fesquet et al. 1993; Poon et al. 1993; Fisher & Morgan 1994) but also includes the ménage a trois 1 (MAT1) protein to form a trimeric complex (Kaldis et al. 1998). However, unlike most other CDK-Cyclins, CDK7/Cyclin H was found to be active throughout the cell cycle with no detectable oscillation in its activity (Matsuoka et al. 1994; Poon et al. 1994; A. J. Brown et al. 1994).

In human cells, there are at least 20 different CDKs that interact with at least 29 Cyclins and Cyclin-related proteins, though not all of them are directly involved in the cell cycle (Fung & Poon 2005; Malumbres & Barbacid 2009). This means that it is likely that there is some redundancy between the CDKs and their Cyclins. The most extreme examples of this are genetic studies with knock out mice that produced embryonic fibroblasts lacking CDK2, CDK3, CDK4 and CDK6 (Santamaría et al. 2007; Barrière et al. 2007). Likewise, a 2010 study from the Nurse lab produced a functional cell cycle in *S. pombe* relying on a single Cyclin/CDK complex (Coudreuse & Nurse 2010). From these genetic

studies a minimal-threshold model of cell cycle control emerged. In this model, the differences between the interphase and mitotic CDKs does not rely on substrate specificity, but simply results from a higher threshold activity for mitosis than for interphase (Hochegger et al. 2008). Thus, the CDK activity threshold appears to differentiate between cell cycle phases rather than substrate specificity alone. This is possibly due to the high amino acid sequence identity between the CDKs which may prevent failsafe substrate binding site specificity (for example between CDK4 and CDK6 amino acid sequence homology is 71% (Ferrer et al. 2006)). The evolution and conservation of specific CDKs in higher eukaryotes does, however, suggest qualitative differences between these complexes must exist that contribute to fitness and have therefore been conserved. CDK2, for example does not play any essential role for the development and life span of mice, but is essential for fertility (Ortega et al. 2003; Berthet et al. 2003). These qualitative functions of specific CDK/Cyclin complexes remain largely unexplored.

1.2.1 CDK-Cyclin complexes are regulated by CDK inhibitors

Another layer of cell cycle control, which occurs in G1 phase, is done through the Cyclin dependent kinase inhibitors (CKI). The INK4 gene family of CKIs encodes $p16^{INK4a}$, $p15^{INK4b}$, $p18^{INK4c}$, and $p19^{INK4d}$, all of which bind to CDK4 and CDK6, and inhibit their kinase activities by interfering with their association with D-type Cyclins (Sherr & Roberts 1999). In contrast, the Cip/Kip family of CKIs bind to both Cyclin and CDK subunits, and can modulate the activities of Cyclin D-, E-, A, and B-CDK complexes (Sherr & Roberts 1999). The CKI

proteins play an important role as tumour suppressors. They prevent phosphorylation of the retinoblastoma protein (RB) in G1 until sufficient mitogenic signals cause increased Cyclin D expression to permit sufficient CDK4/6 activity that allows the cell cycle to continue (Sherr & Roberts 1999). The RB protein will be talked about in more detail later. The members of the INK4 and Cip/Kip protein families and where they act in the cell cycle are noted in **Figure 1.1**.

1.3 Initiation of cell cycle entry and cell cycle checkpoints

To safely navigate the complex procedure of cell division, there are rigid cell cycle checkpoints in place. The term 'cell cycle checkpoint' refers to the mechanisms by which a cell actively pauses cell cycle progression until it can ensure that an earlier process, such as DNA replication or mitosis, is complete (Hartwell & Weinert 1989). This means the cell cycle checkpoints act as a means of surveillance and protection, to ensure that genomic stability is maintained and to prevent aberrant cells from proliferating. Whilst these layers of protection are extremely effective at preventing the emergence of cancerous cells, it is not failsafe and misregulation or mutations in the cell cycle checkpoint proteins are very common in cancer cells (Malumbres & Barbacid 2009). The role of the cell cycle in cancer cell formation will be discussed later. Most adult human cells are differentiated and in a quiescent state, which occurs via hypo-phosphorylated RB and other proteins repressing cell cycle gene expression through the binding and inhibition of the E2F family of transcription factors (Infante et al. 2008). However, quiescent cells are able to re-enter the cell cycle

under certain conditions. When mitogenic signalling pathway activation leads to the induction of Cyclin D and E expression in G1 phase, this permits the formation of active Cyclin -CDK4/6 and -CDK2 complexes, respectively. These active Cyclin-CDK molecules can then add inhibitory phosphates to RB, thus inactivating it.

This releases the E2F transcriptional activators and allows the transcription of genes required for cell cycle progression to begin (Bandara et al. 1991; Malumbres 2011). The activation of these E2F dependent transcription programs is the key event that commits cells to enter the cell division cycle, and a schematic of this process is shown in **Figure 1.2**. As previously mentioned, this point of no return in G1 phase is also termed the restriction or R-point.

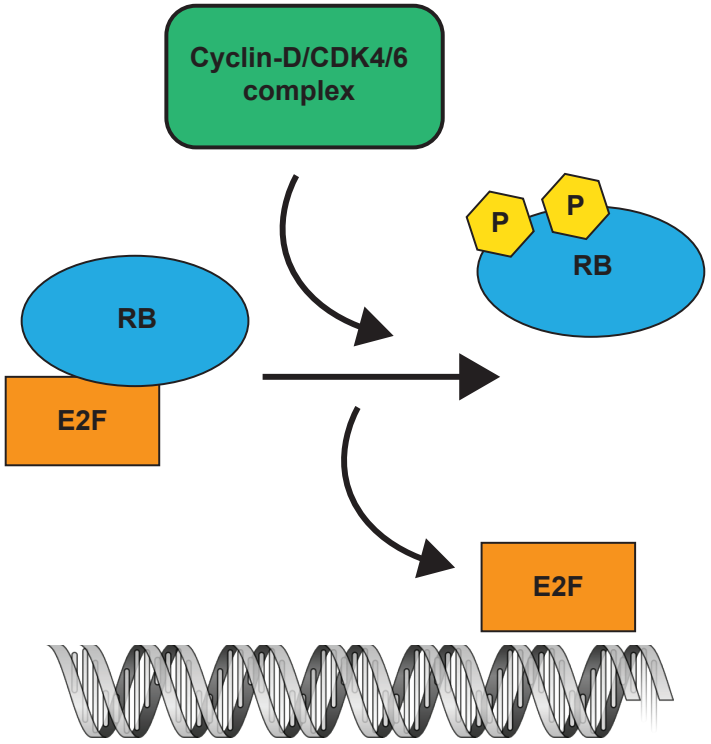

Figure 1.2 Activation of E2F by Cyclin D-CDK4/6 in G1 phase A summary of how the transcription factor E2F is activated to permit the progression from G1 to S phase. Cdk4 or Cdk6 complexed with Cyclin D hyper-phosphorylates RB, released E2F from RB binding. E2F is now free to transcribe genes required for cell cycle progression.

1.3.1 G1/S transition and checkpoint

If the cell has progressed past the restriction point, then this means it will commit to replicating its DNA even if the mitogenic growth factors are removed from the environment (Elledge 1996). Recent work by the Meyer lab has redefined this commitment point as the inactivation of the APC/Cdh1 ubiquitin ligase that is activated at the end of mitosis, and maintains Cyclin degradation until it is turned off in mid G1 phase (Cappell et al. 2016). The restriction point, also known as the G1/S checkpoint, operates to monitor the transition between the quiescent or G0 phase, and the proliferative state. This checkpoint assesses whether a cell is ready to enter S phase and replicate the genome, by monitoring for the presence of growth factors and DNA damage. During the entirety of the cell cycle the DNA damage response (DDR) will be constantly monitor for and detect DNA damage; and will only allow the cell cycle to progress if conditions are acceptable. The DNA damage checkpoint can arrest the cell cycle in mid S phase or in late G2 phase (Y. Zhu et al. 2004; Ciccia & Elledge 2010; Heijink et al. 2013).

Several mechanisms have evolved to prevent cell cycle progression once this checkpoint is activated. The major pathway relies on the p53 tumour suppressor that induces the transcription of p21, thereby preventing CDK activation and origin firing (He et al. 2005). However other mechanisms, such as the regulation of the CDK2 Y15 dephosphorylation by Cdc25A (Gu et al. 1992), also appear to play a role but are less well understood. A key effector of the G1/S checkpoint is DNA damage, but other factors such as cell size, metabolism and cellular stress

signalling may also result in activation of this pathway (Barnum & O'Connell 2014).

The major events past this point that lead to the initiation of S phase concern mainly the licensing and firing of DNA replication origins, which are initiated during G1 phase (Araki 2010; Yekezare et al. 2013). DNA replication starts from defined genomic regions termed origins. In bacteria, DNA replication generally initiates at a single, well-defined origin on a circular chromosome. In contrast, eukaryotic cells replicate their genomes from multiple origins that are distributed on multiple chromosomes (Yekezare et al. 2013). Replication origins are sequence specific in budding yeast, but appear to be only loosely defined in higher eukaryotes (Goldar et al. 2009; Barberis et al. 2010). To guide DNA synthesis, the origins of replication are bound by the Origin Recognition Complex (ORC), which serves as a foundation for the assembly of the pre-replication complex (pre-RC) which is comprised of the Mcm2-Mcm7 complex and the licensing factors Cdt1 and Cdc6 (H. Rao & Stillman 1995; Rowley et al. 1995; Speck et al. 2005). This reaction can only occur during a period of low CDK activity, thereby preventing relicensing after CDK activity rises, until the cell cycle is complete and Cyclins are degraded at the end of M phase (Hochegger et al. 2008). Origin firing involves the activation of the Mini-Chromosome Maintenance (Mcm) complex that leads to a melting of the DNA strands allowing the initiation of DNA polymerisation. This process requires CDK activity, but also the activity of another kinase - Cdc7/Dbf4 (Jares et al. 2000; Masai & Arai 2002).

1.3.2 S phase

S phase refers to the synthesis of the cell's DNA prior to mitosis. Here, the Cyclin E-CDK2 and Cyclin A-CDK2 complexes are the main kinases that drive the cell through this DNA replication phase. Appropriate CDK activity ensures that accurate DNA replication takes place and also ensures that replication of the genome occurs only once per cell cycle. Cyclin E/A-CDK2 activity peaks during S phase entry (**Fig 1.1**), where it has two main functions (Woo & Poon 2003): Firstly, it participates in the release of the transcription factor E2F from RB, to enable transcriptional control of certain genes required for S phase and driving S phase entry (Lundberg & Weinberg 1998) (**Fig. 1.2**). Secondly, it phosphorylates components required for the initiation of DNA replication. Replication of the genomic DNA during S phase is a well-choreographed, highly ordered process involving numerous different proteins (Bell & Dutta 2002; S. Tanaka & Araki 2010), and preparation for DNA synthesis begins in G1 phase with the licensing of the replication origins which was mentioned earlier. In G1 phase these origins are licensed, but the helicase is still inactive and initiating activation requires the additional binding of multiple cofactors and two kinases in order to start unwinding the DNA double helix; Dbf4-dependant kinase (DDK) and CDK (Masai et al. 2000; Diffley 2004). The activation of the pre-RC and initiation of DNA replication is known as origin firing. Among the cofactors required for DNA replication to begin is a protein called Cdc45. Cdc45 interacts with the pre-RC and induces loading of Replication Protein A (RPA) and DNA polymerase α to initiate origin firing (Zou & Stillman 2000). Phosphorylations by Cyclin E/A-CDK2 and DDK are essential for Cdc45 loading onto the origins, although it is not clear whether it is Cyclin E or A that is involved. However there

is evidence that both can functionally compensate for each other in S phase (Woo & Poon 2003; Hochegger et al. 2008). The expression of Cyclin E peaks before Cyclin A at the start of S phase (**Fig. 1.1**), which indicates that Cyclin E-CDK2 probably dominates in early S phase and are replaced by Cyclin A-CDK2 complexes later in S phase (H. Zhao et al. 2012). Together, these kinase activities regulate the formation of the initiation complex and the initiation of replication of licensed origins at the beginning of S phase.

Once DNA replication has begun, bidirectional replication forks are established and both DDK and Cyclin E-CDK2 are dispensable for the completion of S phase (Bousset & Diffley 1998; S. Tanaka & Araki 2010). This means these proteins are in theory only essential for the initiation of DNA replication. The inactivation of RB promotes transcription of genes required for subsequent cell cycle stages, including Cyclins A and B. Also, the activity of Cyclin A-CDK2 increases as S phase progresses (**Fig. 1.1**) (Woo & Poon 2003). The Cyclin A-CDK2 complexes phosphorylate various targets required for completion and exit from S phase, which include targets that promote activation of pre-RC complexes and also targets that allow elongation and inhibit the formation of new pre-RC complexes (Lundberg & Weinberg 1998; Harbour & Dean 2000; Malumbres & Barbacid 2001).

In 1970, cell-fusion experiments carried out by Johnson and Rao indicated the presence of a re-replication block (P. N. Rao & R. T. Johnson 1970). The results indicated that only G1 cells are competent to carry out DNA replication, while cells that have already completed this process, i.e. the G2 cells, were

unable to re-replicate their DNA. This re-replication block is key to limiting replication to only once per cell cycle, and so preventing genomic instability. It is now understood that this occurs due to the two-step nature of the activation of DNA replication (Woo & Poon 2003; Remus & Diffley 2009). The first step is that CDK activity is relatively low for most of G1 phase, and thus is permissive to pre-RC assembly and origin licensing. The second step is, as CDK activity increases in S phase, and active Cyclin A-CDK2 complexes predominate, DNA replication is initiated, and the pre-RCs are activated. Now the high CDK activity inhibits the formation of further pre-RC complexes, thus preventing their reformation and CDK activity remains high until the end of mitosis. Different thresholds of CDK activity which activate different steps of the cell cycle, is therefore critical to ensuring that genomic DNA is replicated exactly once per cell cycle and is thus transmitted stably over many cell generations (Hochegger et al. 2008). The CDK-mediated inhibition of pre-RC formation occurs in several ways. The CDK initiation of origin firing disassembles the pre-RC leaving an unlicensed origin and high CDK activity then inhibits the formation of new pre-RC by several mechanisms: These include the phosphorylation of free Cdc6, causing its export from the nucleus and the phosphorylation of the ORC complex and Cdt1, leading to their dissociation from the chromatin and/or their degradation (V. Q. Nguyen et al. 2001; Takeda & Dutta 2005).

The end of S phase is marked by the completion of the DNA replication. The cell then moves into the next phase, G2, in which the cell prepares to equally divide its newly doubled complement of chromosomes.

1.3.3 G2/M checkpoint

The cell cycle can be arrested at the G2/M transition in response to DNA damage and incomplete replication (X. W. Wang et al. 1999; Vairapandi et al. 2002; Furukawa-Hibi et al. 2002; Kastan & Bartek 2004). Mirroring the restriction point in G1 phase, once a cell has progressed past the antephase point in G2 phase, then it is committed to undergoing mitosis (Pines & Rieder 2001). The major effectors of this checkpoint are the ATM/ATR kinases via their downstream targets CHEK1 and Chk2 (Abraham 2001; Bartek & Lukas 2003; Maréchal & Zou 2013). The major mechanism by which a cell cycle stop is introduced by these kinases is the prevention of Cdc25 mediated activation of CDK1. Both Cdc25 and Wee1 are direct targets of CHEK1/2 kinases, but there is also indirect control via protein stability, localisation and complex formation. It remains unclear, if this effects exclusively CDK1, or if CDK2 activity is also downregulated by the checkpoint. Both incomplete replication and DNA damage signal to the replication checkpoint and recent studies support a model whereby ongoing replication intrinsically prevents entry into mitosis via constitutive ATR activation (Lemmens et al. 2018; Saldivar et al. 2017).

1.3.4 G2/M transition

To make sure that cell division produces healthy daughter cells with complete, undamaged DNA, the cell has an additional checkpoint before M phase, called the G2 checkpoint. At this stage, the cell will check for DNA integrity and complete DNA replication. If errors or damage are detected, the cell will pause here, and the cell attempts to either complete DNA replication or repair the damaged DNA. If the damage is irreparable, the cell may undergo apoptosis.

Once DNA replication is complete, cells prepare for sister-chromatid segregation and cell division, and enter a cell cycle phase that Walther Flemming discovered in the late 19th century and termed mitosis based on the Greek word for thread, “mitos” (Rieder 2003). The use of a word for thread refers to the appearance of the condensed chromosomes at the onset of mitosis, which is one of the many prominent changes the cell undergoes in this transition. In fact, almost every cellular compartment is dramatically affected by mitotic entry. The nuclear envelope melts into the ER, the Golgi body disassembles, the centrosomes separate and start emanating rapidly growing and shrinking microtubule fibres, the cell cortex contracts and rounds up, and still there are many more examples of mitotic specific changes in the cell (Morgan 2007).

These rapid changes are driven by the activation of CDK1, bound to mitotic Cyclins (A and/or B). There are three different Cyclin B proteins in mammalian cells. Cyclin B3 expression is limited to developing germ cells, and the adult testis (T. B. Nguyen et al. 2002). Cyclin B2 is found in cycling adult cells, is non-essential for mouse development and associates with the Golgi apparatus (Jackman et al. 1995; Brandeis et al. 1998). Cyclin B1 is essential for the early embryonic cell cycle in developing mice, and is thought to be responsible for most of the other actions of CDK1 in the cytoplasm and nucleus during the mitotic transition (Brandeis et al. 1998; Strauss et al. 2018). However, siRNA depletion of Cyclin B1 in human cells shows a surprising lack of phenotypic outcome (Gong & Ferrell 2010), and unpublished work in our lab suggests that Cyclin A can compensate most mitotic functions of B-type Cyclins. For simplicity

I will call the mitosis promoting activity of CDK1, CDK1/M-Cyclin for the rest of this section.

Activation of CDK1 is, thus triggering a critical cellular switch that must be extremely tightly regulated. This is achieved at various levels of control. Firstly, the expression of M-Cyclins is repressed until required by tight transcriptional control via various transcriptional control elements. For example, the promoters of Cyclins B1 and B2 (and A1) contain CCAAT-boxes. These DNA sequences sequester the transcription factors required for efficient gene expression, for example the trimeric nuclear transcription factor Y (NF-Y), (Katula et al. 1997; Bolognese et al. 1999; Manni et al. 2001). During mitosis Cyclin B1 can continue to be expressed because the chromatin containing the Cyclin B1 gene remains in an open formation, and its promoter continues to be bound by NF-Y (Sciortino et al. 2001). The transcription factors of Cyclin B – NF-Y, FOXM1 and B-MYB, are controlled by CDK activity. This means transcription of Cyclin B is only done efficiently once the activity of Cyclin A-CDK2 is sufficiently high during S and G2 phases (Bolognese et al. 1999; Fung & Poon 2005). So, the Cyclin B levels begin to rise during S phase (**Fig. 1.1**) and continue to increase during G2 phase and remain high in early mitosis. Cyclin B must reach sufficiently high a concentration in order to form a high concentration of fully active Cyclin-B/CDK1 complexes to drive mitotic entry (Fung & Poon 2005). In addition, to become fully active CDK1 requires an activating phosphorylation. This is carried about by a Cyclin activating kinase (CAK) on Thr16 in the T-loop to create a fully active kinase (Tassan et al. 1994). As mentioned briefly earlier, the CAK of CDK1 includes a CDK-Cyclin binding pair: CDK7/Cyclin H (Fesquet

et al. 1993; Poon et al. 1993; Fisher & Morgan 1994). The identity of the CAK that carries out this phosphorylation varies between organisms, but in humans this kinase is composed of a trimeric complex: CDK7, Cyclin H and MAT1 (ménage à trois 1) (Kaldis et al. 1998). This CAK complex is also responsible for the activating phosphorylations of CDK2, CDK4 and CDK6 (Lolli & L. N. Johnson 2005; Schachter et al. 2013).

The critical step in M-phase/CDK1 activation is the removal of an inhibitory phosphorylation by Cdc25 phosphatases. CDK1 is kept inactive throughout interphase by phosphorylations on Threonine (Thr) 14 and Tyrosine (Tyr) 15, which are added by the kinases Wee1 (Parker & Piwnica-Worms 1992) and Myt1 (Mueller et al. 1995). Switch like activation of this kinase requires a rapid removal of these inhibitory phosphates. This is achieved by a positive feedback loop. The activated CDK1 can phosphorylate and thus inhibit its own inhibitors Myt1 and Wee1, and activate its activator Cdc25 (Perry & Kornbluth 2007). This process is included in **Figure 1.1**. In turn, these enzymes are also controlled by DNA damage checkpoints, which delay the onset of mitosis in the presence of unreplicated or damaged DNA (Nigg 2001). Finally, spatial distribution of various mitotic proteins is also a key feature of mitotic control (Álvarez-Fernández et al. 2013). Cyclin B, for example is mainly cytoplasmic throughout interphase, but translocates to the nucleus shortly before mitotic entry (Toyoshima 1998; Hagting et al. 1999). Other examples of spatial control include nuclear Wee1, cortical Myt1, cytoplasmic Cdc25 and others. The precise impact of this spatial control of mitotic entry remains to be determined, but preliminary evidence suggest that it plays an important role (Santos et al.

2012; Lindqvist et al. 2007; Lindqvist et al. 2009). These factors together generate a high concentration of highly active CDK1/M-Cyclin that triggers the start of mitosis.

Once active, CDK1/M-Cyclin phosphorylates hundreds of target proteins (Dephoure et al. 2008) to cause the transition from interphase to mitosis. These CDK1 dependent phosphorylation events orchestrate the dramatic cellular rearrangements, including the assembly of a mitotic spindle to enable equal separation of the genetic material to two daughter cells.

1.3.5 Spindle Assembly Checkpoint

Once cells have entered mitosis there is one last opportunity for a checkpoint to protect the genome, which is called the spindle assembly checkpoint (SAC). This checkpoint avoids unequal chromosome segregation by delaying the onset of anaphase until all 92 kinetochores of a human cell have attached to microtubules extending from opposite spindle poles. This state is called sister kinetochore bi-orientation or chromosome bi-orientation (Rieder et al. 1995; T. U. Tanaka 2005). Because the separation of the sister chromatids during anaphase is an irreversible step, the cycle will not proceed until all the chromosomes are firmly attached to at least two spindle fibres from opposite poles of the cell.

1.4 Greatwall kinase and its function in mitotic regulation

Greatwall kinase (GWL), the major subject of this thesis, named in humans as microtubule-associated serine/threonine-protein kinase-like (MASTL) (Voets & Wolthuis 2010), was first discovered in *Drosophila* in 2004 (J. Yu et al. 2004). The human GWL/MASTL will be referred to as just GWL in this thesis. Mutations of this kinase in flies give rise to abnormal mitotic entry with cells failing to stabilise a stable mitotic state. This inspired the name of GWL since this kinase is required to overcome a barrier to enter mitosis. Further biochemical work in Xenopus egg extracts suggested that GWL was working via downregulation of PP2A activity to facilitate mitotic entry (Castilho et al. 2009). Subsequent work in human cells and conditional knock-out mouse suggested that this function of GWL is conserved although the depletion of GWL in mammalian cells appears to cause only minor delays in mitotic entry (Álvarez-Fernández et al. 2013). This discrepancy has remains poorly understood. Since the currently major known function of GWL lies in the CDK1 activation switch, the context of this signalling cascade at the G2/M transition shall be described first. In animal cells, two kinases (Myt1 and Wee1) work together to inhibit CDK1 before mitosis via the phosphorylation sites Thr 14 and Tyr 15 on CDK1 (Welburn et al. 2007). The activities of Myt1 and Wee1 are high for the majority of the cell cycle, but then rapidly decrease during mitosis to allow the dephosphorylation and thus activation of CDK1 by members of the Cdc25 phosphatase family (Welburn et al. 2007). These dramatic changes are generated in part by the positive feedback loops described previously. Initially, the models that described this switch system only focused on the direct feedback loops between Wee1, Cdc25 and CDK1. However, this model does

not consider the role of the phosphatases that counteract these kinase driven feedback systems. Over the past decade it has become apparent that the regulation of phosphatases plays a major role in the G2/M transition (Mochida et al. 2009; Mochida et al. 2010) and that GWL has a critical function in this signalling network (Vigneron et al. 2009). In the first paper to describe GWL, mutating the essential *Drosophila* GWL gene disrupted cell cycle progression (J. Yu et al. 2004). The GWL mutant cells took much longer to traverse through the period of chromosome condensation from late G2 phase through to nuclear envelope breakdown. This means that the chromosomes remain persistently under-condensed, and anaphase is delayed due to prolonged activity of the spindle checkpoint (J. Yu et al. 2004). To ensure that these phenotypes were not artefacts of problems that arose during G1 or S phase and too see what happens in vertebrate cells, further experiments were done in *Xenopus* egg extracts, taking advantage of GWL's conservation in vertebrates (Human GWL shows 60.5% homology with *Xenopus* GWL) (J. Yu et al. 2004). Depletion of GWL from mitotic *Xenopus* egg extracts rapidly lowers Maturation Promoting Factor (MPF) activity because of the accumulation of inhibitory phosphorylations on Cdc2 kinase (the equivalent of human CDK1). Also, GWL depletion prevented the Cycling extracts from entering M phase. These results suggest that GWL participates in an auto-regulatory loop that generates and maintains sufficiently high MPF activity levels to support mitosis.

The inactivation of Cyclin B-CDK1 was prevented in mitotic *Xenopus* egg extracts by the immunodepletion of the inhibitory kinases Wee1 and Myt1, and the subsequent immunodepletion of GWL from these extracts still

promoted mitotic exit (Vigneron et al. 2009). This exit from mitosis was accompanied by a dephosphorylation of most of the substrates of Cyclin B-CDK1 despite the high activity of this kinase. However, this massive dephosphorylation was not observed when the mitotic egg extracts were submitted to a co-depletion of GWL and PP2A. These were the first data suggesting a role of GWL in the inhibition of PP2A (Vigneron et al. 2009). Soon after, multiple research groups also established that GWL maintains the mitotic state not by regulating the Cyclin B–Cdc2 activation loop, but by regulating the phosphatase PP2A-B55 (Castilho et al. 2009; Mochida et al. 2009). Later, two groups in particular established the elusive substrates of GWL that mediate this phosphatase inhibition as α-Endosulfine (ENSA) and cyclic adenosine monophosphate (cAMP)-regulated phospho-protein 19 (ARPP19) (Mochida et al. 2010; Gharbi-Ayachi et al. 2010). The Mochida *et al.* (2010) study identified the GWL substrate, ENSA, from interphase Xenopus egg extracts, while the Gharbi-Ayachi et al. (2010) study identified ARPP19 using biochemical fractionation of Cytostatic factor (CSF) Xenopus egg extracts and in vitro Greatwall kinase assays. Whether ARPP19 and ENSA have distinct and separate roles in this particular pathway remains to be established (Lorca & Castro 2012) but it is clear from the data from several groups that both these proteins can act downstream of Greatwall to inhibit PP2A to allow correct mitotic entry and progression. This allows the CDK1 activity to predominate and drive entry into mitosis.

Further studies in *Xenopus* egg extracts found that GWL can promote recovery from DNA damage and that GWL is directly inhibited by the DNA damage

response (DDR) (Peng et al. 2010). Immuno-depletion of GWL increased the DDR, whereas addition of wild-type, but not kinase-dead GWL, inhibited the DDR (Peng et al. 2010). The removal of damaged DNA from the egg extracts caused recovery from checkpoint arrest and mitotic entry, which was impaired by GWL depletion and enhanced by GWL overexpression (Peng et al. 2010). A later *Xenopus* study found that GWL is able to promote checkpoint recovery independently of CDK1 or Plx1 (the *Xenopus* homolog of polo-like kinase 1) (Peng et al. 2011). A direct interaction between GWL and Plx1 was found in which Plx1 phosphorylates GWL and that this GWL interaction and phosphorylation by Plx1 appears elevated during checkpoint recovery(Peng et al. 2011). So overall, synergy between Plx1 and GWL are required for reactivation of these kinases from the G2/M DNA damage checkpoint and efficient checkpoint recovery (Peng et al. 2011). More work has now been carried out to try and understand the exact role of GWL in mammalian and human cells. In agreement with the results described above, in human cells GWL also indirectly inhibits PP2A-B55 via phosphorylation of ENSA and ARPP19 (Cundell et al. 2013; Álvarez-Fernández et al. 2013).

The human GWL protein is stably expressed throughout the cell cycle but is phosphorylated and most active during mitosis (Dephoure et al. 2008; Voets & Wolthuis 2010; Olsen et al. 2010). Depletion of GWL expression in human cells causes problems in mitotic progression including defects in chromosome condensation and separation (Burgess et al. 2010; Álvarez-Fernández et al. 2013). It has been found that depleting human cell lines of GWL using siRNA caused a delay in mitotic entry, chromosome alignment defects and metaphase

delay (Burgess et al. 2010) and aberrant chromosome segregation resulting in polyploidy. In addition, depletion of GWL by siRNA in the human cell lines RPE, U2OS and HeLa delays the G2/M transition, and is associated with an extended mitosis period, failures in sister chromatid segregation and mitotic cell death (Voets & Wolthuis, 2010). The phenotypes of GWL overexpression or depletion in model organisms and common experimental human cell lines are listed in **Table 1.1**.

Species/Human cell line	**Protein**	**Normal function**	**Mutation, knockdown and/or overexpression phenotypes**	**Ref**
Schizosaccharomyces pombe	Ppk18	Not essential for mitosis. Regulates nitrogen starvation-induced G_0 entry and maintenance	Overexpression of *ppk18* causes cell-cycle delay in G1. Moderate overexpression of *ppk18* only affects G2/M and not the G1/S size control.	(Aono et al. 2018) (Chica et al. 2016)
Saccharomyces cerevisiae	Rim15	Required for proper entry into stationary phase (G_0). Involved in cell proliferation in response to nutrients.	Null mutation shortens chronological lifespan, causes increased apoptosis and decreased autophagy in response to nitrogen starvation.	(Swinnen et al. 2006) (Cao et al. 2016) (Bisschops et al. 2014) (Weinberger et al. 2007)
Drosophila melanogaster	Greatwall kinase	Mitotic entry. Required for proper chromosome structure and segregation in mitosis and meiosis.	Mutation in larvae: Irregular chromosome condensation; mitotic arrest; long prophase. Hemizygosity leads to a failure of meiosis I characterised by	(J. Yu et al. 2004)

			premature loss of sister chromatid cohesion. The *Scant* mutation, a dominant allele of GWL that introduces a K97M amino-acid substitution; results in a hyperactive kinase that causes developmental failure. Can be rescued by increasing maternal Polo dosage, indicating that coordination between the two mitotic kinases is crucial for mitotic progression.	(Archambault et al. 2007) (Archambault et al. 2007)
Caenorhabditis elegans	Genome does not contain evident GWL ortholog. Does encode an Endosulfine protein with a well-conserved GWL target site.	n/a	Deletion of GWL target site from Endosulfine has no obvious effects on cell divisions, viability or reproduction under normal laboratory conditions.	(M.-Y. Kim et al. 2012)
Xenopus laevis	Greatwall kinase	Required for the positive feedback loop that removes inhibitory tyrosine phosphate from the central mitotic regulatory	Depletion prevents egg extracts from entering or maintaining M phase (accumulation of inhibitory phosphorylations on Thr14 and Tyr15 of Cdc2). Activated GWL both accelerates the mitotic G2/M transition in cycling	(Y. Zhao et al. 2008) (Castilho et al. 2009) (Vigneron et al. 2009) (Gharbi-Ayachi et al. 2010) (Mochida et al. 2010)

		kinase Cdc2	egg extracts and induces meiotic maturation in G2-arrested *Xenopus* oocytes in absence of progesterone. Activated Greatwall can induce phosphorylations of Cdc25 in the absence of the activity of Cdc2, Plx1 (*Xenopus* Polo-like kinase). The effects of active Greatwall mimic in many respects those associated with addition of the phosphatase inhibitor okadaic acid (OA) GWL can promote checkpoint recovery independently of Cdk1 or Plx1, whereas depletion of GWL from extracts exhibits no synergy with that of Plx1 in delaying checkpoint recovery, suggesting a distinct but related relationship between Gwl and Plx1.	(Peng et al. 2011)
Mus musculus	Greatwall kinase or MASTL	Promotes normal G2-mitosis transition by inhibiting PP2A-B55 via ARPP19 and ENSA	Embryonic lethal, but one allele sufficient for healthy, normal mice. Conditional knockout of mouse GWL indicates that mouse embryonic fibroblasts can enter mitosis without GWL but display mitotic collapse after nuclear envelope breakdown.	(Álvarez-Fernández et al. 2013) (Diril et al. 2016)
HeLa (cervical carcinoma)	Greatwall kinase or MASTL	Promotes normal G2-mitosis transition by	Depletion induces a G2 arrest. Partial depletion induces multiple mitotic defects	(Burgess et al. 2010)

		inhibiting PP2A-B55 via ARPP19 and ENSA	that affect spindle-assembly checkpoint and cytokinesis. GWL possibly required for G2 DNA damage responses. GWL overexpression accelerated mitotic entry. GWL downregulation delayed mitotic entry after DNA damage, and caused premature activation of APC/C.	(Wong et al. 2016)
U2OS (osteosarcoma)	Greatwall kinase or MASTL	Promotes normal G2-mitosis transition by inhibiting PP2A-B55 via ARPP19	siRNA depletion delays the G2/M transition; extended mitosis; failures in sister chromatid segregation and mitotic cell death	(Voets & Wolthuis 2010)
RPE (retinal pigment epithelial)	Greatwall kinase or MASTL	Promotes normal G2-mitosis transition by inhibiting PP2A-B55 via ARPP19	siRNA depletion delays the G2/M transition; extended mitosis; failures in sister chromatid segregation and mitotic cell death	(Voets & Wolthuis 2010)
MDA-MB-231 (TNBC)	Greatwall kinase or MASTL	Promotes normal G2-mitosis transition by inhibiting PP2A-B55 via ARPP19 and ENSA	Overexpression increases cell proliferation, migration and invasion. GWL knock out cells did not show a defect in mitotic entry but showed significant increase in the duration of mitosis accompanied by abnormal or lack of chromosome segregation resulting in tetraploid cells.	(Vera et al. 2015) (Álvarez-Fernández, Sanz-Flores, Sanz-Castillo, Salazar-Roa, Partida, Zapatero-Solana, Ali, Manchado, Lowe, VanArsdale,

			GWL knockdown reduced cell proliferation, prevented invasion and metastasis both in vitro and in xenografts.	Shields, Caldas, Quintela-Fandino & Malumbres 2018a) (Rogers et al. 2018)
MCF10a (immortalised breast epithelial)	Greatwall kinase or MASTL	Promotes normal G2-mitosis transition by inhibiting PP2A-B55 via ARPP19 and ENSA	Both knockdown and knockout of GWL in MCF10a cells impaired their proliferation. MCF10a cells have been reported to be less sensitive to GWL depletion to some breast cancer cell lines according to levels of cleaved PARP, cell viability assay and cell cycle analysis. GWL overexpression promotes cell transformation and increases invasive capacities of cells via AKT hyperphosphorylation. GWL overexpression caused loss of contact inhibition and partial epithelial–mesenchymal transition, which disrupted migration and allowed cells to proliferate uncontrollably in 3D culture. Also increased DNA damage, delayed interphase and aberrant mitotic divisions resulting in increased micronuclei formation.	(Álvarez-Fernández, Sanz-Flores, Sanz-Castillo, Salazar-Roa, Partida, Zapatero-Solana, Ali, Manchado, Lowe, VanArsdale, Shields, Caldas, Quintela-Fandino & Malumbres 2018a) (Yoon, Choe, Jung, Hwang, Oh & J.-S. Kim 2018a) (Vera et al. 2015) (Rogers et al. 2018)

Primary human fibroblasts	Greatwall kinase or MASTL	Promotes normal G2-mitosis transition by inhibiting PP2A-B55 via ARPP19 and ENSA	GWL overexpression induced the senescence checkpoint and promoted cell proliferation and anchorage-independent cell growth.	(Vera et al. 2015)

Table 1.1 A summary of known phenotypes of GWL depletion and overexpression in some model organisms and human cell lines.

In summary, the main mitotic role of GWL in human cells is to inhibit the phosphatase PP2A–B55 that permits the maintenance of the phosphates on mitotic substrates of Cyclin B-CDK1. This is important because this enormous phosphorylation event is essential to promote the complex, dynamic events of mitosis. A visual depiction of the consensus of GWL signalling during mitotic entry can be seen in **Figure 1.3**.

1.5 PP1 and PP2A as regulators of mitosis

The role of the phosphatases that are in opposition the kinase signalling events is starting to be more appreciated as a crucial aspect of the control of mitotic entry and exit (Bollen et al. 2009; De Wulf et al. 2009). Studies are now revealing that the timely ordering of mitotic events, in fact, appears to be a result of a delicate interplay between both the kinases and their counteracting phosphatases (Domingo-Sananes et al. 2011). Previously, phosphatases were given less appreciation because they were thought of as indiscriminate and broad acting in their dephosphorylation. Indeed, phosphatases are broad-acting *in vivo*. For instance, PP1 controls processes as diverse as glycogen

metabolism, cell polarity, DNA damage, transcription, and cell cycle progression (De Wulf et al. 2009). This suggests that the roles of phosphatases within mitosis are hidden by secondary phenotypes. In addition, the gene numbers encoding kinase and phosphatase activities are disproportionate.

Approximately 500 human genes have been estimated to encode protein kinases, whilst only about 40 appear to code for serine/threonine phosphatases (which make up 98% of phosphorylations in mammalian cells) (Manning et al. 2002; Moorhead et al. 2007; Wlodarchak & Xing 2016). The consensus is now changing and phosphatases are seen as highly specific inhibitors of precise signalling pathways and feedback loops that are critical for the control of mitotic events (De Wulf et al. 2009; Domingo-Sananes et al. 2011). For example, the down-regulation of CDK1 is not sufficient for mitotic exit in human cells. Human cells with reduced CDK1 activity do not progress past metaphase when the protein phosphatases PP1 and PP2A are selectively inhibited (L. Zhu & Skoultchi 2001). Also, it is well known in biology that gene number does not necessarily reflect protein number or complexity, as some of the serine/threonine phosphatases form a large number of diverse oligomeric complexes. In particular, PP2A forms ~100 heterotrimeric holoenzymes and protein phosphatase 1 (PP1) forms ~400 heterodimeric holoenzymes meaning that these are not single enzymes but rather a family of enzymes (Ruvolo 2016; Wlodarchak & Xing 2016). PP2A is a trimeric enzyme with common catalytic (C) and A (‘scaffolding’) subunits but variable B (regulatory) subunits, and PP2A isoforms are identified by the B regulatory subunit they contain, which also determines the substrate specificity and cellular localisation of the resulting PP2A isoform (Ruvolo 2016).

The large diversity of holoenzyme structure that can be achieved means that PP2A has been suggested or confirmed to dephosphorylate over 300 substrates, most of which are involved in cell cycle regulation (Wlodarchak & Xing 2016). PP2A has been implicated in preventing of premature separation of chromosomes in anaphase. PP2A, in complex with the regulatory B56 subunit, is recruited to the centromeres by the Shugoshin protein and keeps cohesion subunits in an unphosphorylated state, counteracting Plk1 phosphorylation (Kitajima et al. 2006; Tang et al. 2006; Barr et al. 2011). Also PP2A, in complex with is regulatory B55α subunit, has been implicated in Golgi reassembly after mitotic exit (Schmitz et al. 2010). The role of PP2A which is of most importance to this thesis is that is has been discovered to be an important part of the signalling network required to allow timely mitotic progression, specifically PP2A-B55 (Mochida et al. 2009; Castilho et al. 2009; Vigneron et al. 2009; Lorca & Castro 2012). Also, the dephosphorylation and thus the activation of the anaphase spindle protein PRC1 is controlled by a PP2A-B55 isoform (Cundell et al. 2013).

In addition, B55 has been implicated in reassembly of the Golgi apparatus and nuclear envelope during mitotic exit (Schmitz et al. 2010). As mentioned previously, PP2A-B55 is inhibited in mitosis by ENSA and ARPP19 (Gharbi-Ayachi et al. 2010; Mochida et al. 2010). Together, these components form the BEG (B55–ENSA–Greatwall) pathway controlling mitotic exit (Cundell et al. 2013). Because Cyclin B-CDK1 activates GWL, the PP2A-B55 inhibition is maintained until Cyclin B is degraded (Castilho et al. 2009; Gharbi-Ayachi et al. 2010; Mochida et al. 2010).

Once all chromosomes have aligned and are under tension on the metaphase spindle, the anaphase-promoting complex triggers destruction of Cyclin B and the separase inhibitor securin. This leaves an interesting problem of how PP2A-B55 is reactivated and Greatwall kinase is inhibited during mitotic exit. The current models of the phosphatase regulation during the metaphase anaphase transition suggest that PP1 first inactivates Greatwall (Heim et al. 2015) by dephosphorylating a C-terminal site that is thought to be essential for kinase activity. Once Greatwall is inactive, PP2A-B55 itself dephosphorylates its inhibitor ENSA/ARPP19. Removal of the ENSA–Greatwall inhibitory system results in constitutive B55 activity, causing mitotic catastrophe and unequal chromosome segregation because of precocious central spindle formation and cytokinesis (Manchado et al. 2010; Voets & Wolthuis 2010; Cundell et al. 2013).

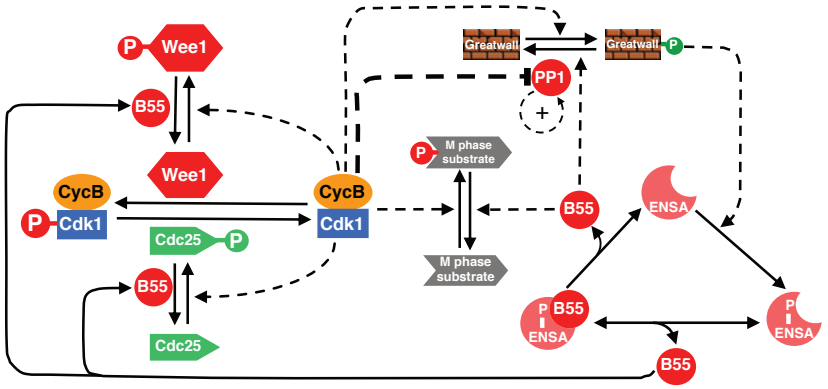

Figure 1.3 The Greatwall kinase pathway A diagram of the current consensus of GWL signalling during mitotic entry in mammalian cells. GWL is activated in late G2 phase and phosphorylates its targets, ENSA and Arpp19 (for simplicity, just ENSA is shown on this schematic), which in turn bind to and inhibit the PP2A-B55 phosphatase. This prevents PP2A-B55 from prematurely dephosphorylating substrates of CDK1. This allows mitotic phosphorylations to accumulate and drive cells through mitosis. It is possible that PP1 phosphatase, as well as PP2A-B55, can inactivate GWL. Adapted from Hégarat et al. 2014.

1.6 The cell cycle and cancer

Cells have evolved to cope with both metabolic and external sources of DNA-damaging agents through the development of elegant DNA repair mechanisms. This is called the DNA damage response (DDR), which is a collective term for the huge network of an estimated 450 proteins (Pearl et al. 2015) that seek to detect and repair DNA damage. This also includes events that lead to cell-cycle arrest, regulation of DNA replication, and the repair or bypass of DNA damage. In the event of sufficient DNA repair not being possible or suboptimal, the DDR can also impact on downstream cell fate decisions, such as cell death or senescence (D'Adda Di Fagagna et al. 2003; Kang et al. 2015; M. J. O'Connor 2015). Such mechanisms are vital for life, because DNA is under constant attack by agents that can directly damage the nucleotide bases or the phosphodiester backbone of the DNA molecule. For example, free oxygen radicals, arise as a consequence of normal cellular metabolism or can be formed when the organism is exposed to ionizing radiation in the environment (Kastan & Bartek 2004). In metazoans, it could be said that the cell cycle checkpoints and DNA repair mechanisms exist as a method of protection against cancer.

However, deregulating the cell cycle is a primary agenda for the emerging cancer cell, as this tightly regulated process controls cell growth. Multiple checkpoints are in place that assesses a cell's extracellular growth signals, its size, and DNA integrity at all times. If a cancer cell is to grow to become a clinically relevant tumour, cancer cells have to overcome the cell cycle control machinery. Cancer cells also display many additional differences to normal

cells as well as unscheduled proliferation – such as genomic instability (increased DNA mutations and chromosomal aberrations), chromosomal instability (changes in chromosome number), loss of differentiation and increased invasiveness (Hanahan & Weinberg 2011). Markers of DNA damage can often be a phenotype of genetically unstable cancer cells. For example, certain markers of double strand breaks (DSBs), such as nuclear γH2AX foci (a histone phosphorylation event that occurs on chromatin surrounding a DSB), are markedly elevated in some precancerous lesions (Lord & Ashworth 2012). Taken together, these alterations of normal cells, cause both proliferative advantages and increased susceptibility to the accumulation of further mutations or genetic misregulation that contribute to tumour progression and acquisition of more oncogenic phenotypes. The three cell cycle defects that are essential for the growth of cancer cells - unscheduled proliferation, genomic instability and chromosomal instability, are mediated, directly or indirectly, by the misregulation of Cyclin-dependent kinases (Malumbres & Barbacid 2005).

As mentioned earlier, CDK activity is regulated by two groups of inhibitors: the INK4 family, and the Cip and Kip family, composed of p21, p27 and p57 (Sherr & Roberts 1999; Malumbres & Barbacid 2009). These CKI proteins are able to block the proliferation of adult stem cells in various tissue types (Malumbres & Barbacid 2009). Also, knock-in mice expressing a mutant p27 protein are unable to bind Cyclin-CDK complexes, display increased stem and progenitor cell populations and a range of tumour susceptibilities (Besson et al. 2007). The key regulators of G1 phase progression are perturbed in

most human cancers. For example, deregulation of CDK4 and CDK6 activities and their substrates (mostly RB) have been implicated in a wide variety of tumours (Ortega et al. 2002; Malumbres & Barbacid 2005). RB function can be lost through mutation of the *RB1* gene, with tumours such as retinoblastomas, osteosarcomas and small-cell lung carcinomas displaying particularly high occurrences of *RB1* mutation (Chinnam & Goodrich 2011; Di Fiore et al. 2013). RB loss of function can also occur after a cell is infected with Human Papilloma Virus (HPV), as the viral oncoprotein E7 can bind to RB and prevent interaction with E2F. This prevents RB from inhibiting cell cycle progression, and HPV infection plays a key role in the development of the vast majority of cervical carcinomas (Yim & Park 2005; Munger & D. L. Jones 2015).

Another strategy that cancer cells employ to deregulate cell cycle control is through the MYC transcription factor. When MYC is deregulated, it is an oncoprotein. Elevated levels of Myc protein are found in many different types of human cancer and may be deregulated in as many as fifty per cent or more of all tumours (Kalkat et al. 2017; Chen et al. 2018). MYC belongs to a family of basic helix-loop-helix (bHLH) transcription factors that act as heterodimers to influence the transcription of a large number of target genes that possess E-box sequences (S. Jones 2004). The Mad-Max complexes repress transcription, whereas Myc-Max complexes act to promote transcription, and the protein products of many of these target genes influence the cell cycle. For example, the Myc-Max heterodimer can induce expression of the growth-promoting proteins E2F, Cyclin D and CDK4 (Obaya et al. 2002; Liao et al. 2007). Also,

Myc-Max can cause expression of Cul1, which is responsible for degrading the CDK inhibitor $p27^{Kip1}$ (Grandori et al. 2000). Another binding partner of Myc - Miz1 - can repress expression of the CDK inhibitors $p15^{INK4b}$, $p21^{Cip1}$ and $p27^{Kip1}$ (Wiese et al. 2013). Overall there are several ways in which an excess of the Myc oncoprotein can act to deregulate the cell cycle machinery, and so facilitate pre-cancerous or cancerous cells through their growth and division cycles.

In general, basic regulators of G1 progression are altered in most human cancers. Genetic alterations usually affect CDK4 and CDK6, their positive (mainly cyclin D1) and/or negative (INK4A and INK4B) regulators and their substrates (mainly RB). Even if the Rb protein itself is not mutated, alterations to other gene products are common events in tumourigenesis. Repression of the RB gene by methylation at its promoter (Stirzaker et al. 1997; Feinberg & Tycko 2004), inactivation by viral oncoproteins as mentioned previously (Yim & Park 2005; Munger & D. L. Jones 2015), elevated levels of Cyclin D1 (Arnold & Papanikolaou 2005), and suppression of CDK inhibitor activity (Malumbres & Barbacid 2001). The different types of G1 regulator mutations and in what tumours they are found in are extensively classified in this review (Malumbres & Barbacid 2001).

There have been analyses of the genes deregulated in chromosomally unstable tumours which have found that misregulation of genes involved in G2 and M phases is also common (Perez de Castro et al. 2006; Carter et al. 2006). These genetic signatures include overexpression of CDK1 and some

of its regulators such as Cyclin B1 and B2, as well as components of the centrosome and chromosome segregation machinery, such as NEK2, Aurora kinase A, Aurora kinase B, Cdc20, CENPF (Centromere protein F), Separase, and Securin (Carter et al. 2006).

Since CDKs, other cell cycle kinases, and their binding partners and substrates are frequently hijacked in the context of cancerous cells; this raises the question of how to devise therapeutic strategies based on knowledge of the cell cycle machinery and how certain cancer cells manipulate it. Though caution must be taken, as cell cycle control is so broadly important for multi-cellular life and there are numerous highly proliferative tissues in the body; therapeutics designed to target cell cycle control should aim to be as selective for tumour cells as possible.

However, despite this challenge, cancer therapeutics that target the cell cycle are already in clinical use. One group of drugs targets the cytoskeleton, with the aim of interfering with chromosome separation and mitosis in cancerous cells to limit their proliferation. For example, Paclitaxel (or Taxol) stabilises the microtubule polymer and inhibits its disassembly. This means Paclitaxel-treated cells are unable to form the metaphase spindle configuration that is required to pass the SAC (Bharadwaj & H. Yu 2004; Brito et al. 2008). In contrast, other cytoskeleton-targeting chemotherapy drugs such as Demecolcine and Vinblastine can work either by depolymerising the microtubules or by preventing their assembly, depending on the concentration used (Jordan & Wilson 2004).

Additionally, recent research has shown therapeutic potential kinases that facilitate DNA replication and repair. For example, Ataxia telangiectasia mutated kinase (ATM), Ataxia telangiectasia and Rad3-related kinase (ATR), and Checkpoint 1 and 2 kinases (CHEK1 and CHEK2). CHEK1, CHEK2, ATM and ATR have roles in arresting the cell cycle in the event of DNA damage (J.-H. Lee & Paull 2007; E. J. Brown & Baltimore 2003). The ATM–CHEK2 pathway is activated in response to ionizing radiation treatment and agents that cause double-strand DNA breaks. ATM phosphorylates and activates CHEK2, which in turn phosphorylates Cdc25c at Serine 216. This promotes binding of the members of the 14-3-3 protein family, nuclear export, and cytoplasmic sequestration of Cdc25c. This suppression of the Cdc25c phosphatase activity and its nuclear exclusion prevents it from activating Cyclin B-CDK1, and so preventing mitotic entry (Boutros et al. 2007; Matheson et al. 2016). The ATR–CHEK1 pathway is activated by regions of single stranded (ss)DNA that have been complexed with RPA (Smith et al. 2010; Bartek & Lukas 2003). Single stranded breaks can arise from a broad range of genotoxic stresses. In response to ssDNA damage, ATR phosphorylates and activates CHEK1, which then phosphorylates Wee1 and Cdc25c, thereby simultaneously activating Wee1 kinase activity and inactivating Cdc25c phosphatase activity. This allows Wee1 to phosphorylate the Tyrosine 15 residue, which inactivates Cyclin B-CDK1, causing cell-cycle arrest in G2 phase (Matheson et al. 2016; Do et al. 2013; N. Johnson et al. 2009; Jazayeri et al. 2005).

Therefore these DDR pathways act in a tumour suppressive manner, so whilst it is not surprising that mutations and/or deletions of ATM and Chk2 are often

found in a range of human cancers (Manic et al. 2015; Antoni et al. 2007), it is interesting to note that the opposite seems to be true in the case of the ATR-CHEK1 axis (Manic et al. 2015). The incidence of ATR or CHEK1 gene loss or mutations in human cancers is generally quite low, but with some notable exceptions. For example, CHEK1 has found to be frequently overexpressed in Triple Negative breast cancers (TNBC) (Verlinden et al. 2007; Albiges et al. 2014). Cancer cells with defects in the G1/S checkpoint are thought to rely more on the ATR-CHEK1 pathway, so even though these cells are upregulating a DDR pathway, this means they are more vulnerable to its inhibition (Garrett & Collins 2011; Fokas et al. 2014; McNeely et al. 2014). Interestingly, inhibitors of ATR and CHEK1, are the only two classes of compounds from the proteins discussed in this paragraph that have so far entered clinics (Manic et al. 2015).

The inhibitory kinase Wee1 that inactivates CDK1 in response to various types of DNA damage, as explained above, is also a subject of clinical cancer research. Wee1 is expressed in high amounts in a range of cancers, including breast, liver, cervical and lung cancers (Masaki et al. 2003; Iorns et al. 2009). The rationale of Wee1 as a therapeutic target is that cancer cells that overexpress Wee1 may be more reliant on an intact G2/M checkpoint for survival and mitosis. Therefore, inhibition of Wee1 activity may sensitise cancers dependent on a functional G2/M checkpoint to DNA-damaging drugs. Since Wee1 inhibition promotes mitosis, this propagates further genomic instability in cancer cells by forcing the cell through successive replication cycles, with the aim to induce apoptosis from mitotic catastrophe. Therefore, the inhibition of Wee1 could increase the efficacy of existing conventional DNA-

damaging therapies (Matheson et al. 2016; Do et al. 2013). There is a Wee1 inhibitor, AZD1775, which has progressed into clinical trials in combination with DNA-damaging therapies (Matheson et al. 2016; Do et al. 2015; Schellens et al. 2011).

When it was discovered over 30 years ago that CDK holoenzymes are the key drivers of cell cycle specific events (M. G. Lee & Nurse 1987), CDK inhibitors were developed as potential cancer therapeutics. The first-generation CDK inhibitors were rather unspecific in their mechanism of action and so are also referred to as ‘pan-CDK inhibitors’, one example in particular being flavopiridol (Sedlacek et al. 1996) which carried high expectations and featured in over 60 clinical trials, but showed low efficacy in Phase II clinical trials (Asghar et al. 2015). The next generation of CDK inhibitors sought to increase specificity for CDK1 and CDK2, but only a few molecules progressed past Phase I clinical trails (Misra et al. 2004; Payton et al. 2006; Parry et al. 2010; DePinto et al. 2006). The reasons why such pan-CDK inhibitors were unsuccessful can be attributed to: lack of understanding of the mechanism of action, no knowledge of biomarkers to find subpopulations of patients who could benefit most from the treatment, and finally the broad action of these drugs meant the therapeutic window was small, and so very little discrimination between normal and cancerous cells (Asghar et al. 2015). The described disadvantages to these pan-CDK inhibitors means that improved understanding of which CDK holoenzymes are active and when *in vivo* as well as greater CDK specificity is needed if CDK inhibitors are to be successful as cancer therapeutics.

CDK4/6 inhibitors have emerged as appealing therapeutic target. The mechanism of action is well understood, as the primary mode of action would be suppression of RB phosphorylation and so inhibiting proliferation by enforcing cell cycle arrest in G1 phase. However, depending on the cell type and the transforming event, some RB-positive cells undergo quiescence and others undergo senescence when treated with CDK4/6 inhibitors so more needs to be understood about the circumstances that bring about these two different non-proliferative states (Baughn et al. 2006; Kovatcheva et al. 2015; Choi et al. 2012; Michaud et al. 2010). Also, patients could be stratified for tumours that have deregulated components of this pathway, with the exception of RB-negative tumours (Klein et al. 2018; Pernas et al. 2018; Asghar et al. 2015). There is evidence the Cyclin D-CDK4/6 axis is hyperactive in a range of breast cancers which makes targeting CDK4/6 a promising therapeutic strategy (Arnold & Papanikolaou 2005; Q. Yu et al. 2001; Q. Yu et al. 2006). The first CDK4/6 inhibitor to enter clinical use was Palbociclib (Finn et al. 2016) followed by Ribociclib and Abemaciclib (Gelbert et al. 2014; Tripathy et al. 2017). More about CDK4/6 inhibition in cancer therapy is described in **Section 1.8**.

1.7 Greatwall Kinase in triple negative breast cancer

Approximately 12 to 17% of female breast cancer patients (Foulkes et al. 2010) and 6% of male breast cancer patients (Plasilova et al. 2016) are diagnosed with Triple-negative breast cancer (TNBC). TNBC is distinctive by its lack of expression of common breast cancer cell growth drivers, as it is defined as a

breast tumour that lacks expression of the oestrogen receptor (ER), progesterone receptor (PR) and the Human epidermal growth factor receptor 2 (HER2) (Foulkes et al. 2010; Stockmans et al. 2008).

So not only does TNBC represent a heterogeneous group of tumours, but also TNBC lacks the targets required for treatment with hormone therapies or drugs that target the HER2 receptor, therefore treatment options for TNBC are currently limited to chemotherapy and surgery. This fact combined with the aggressive nature of TNBC tumours mean that prognosis is often worse for TNBC than other breast cancer types, (Gadi & Davidson 2017; Stockmans et al. 2008; P. Sharma 2016). TNBCs are associated with a 4-fold increased risk of metastases and a significantly shorter overall survival (Marmé & Schneeweiss 2015).

Current research efforts are focused on identifying targets and agents that could bring benefit specifically to the TNBC subtype. In addition, optimising existing treatments for TNBC is ongoing as knowledge grows regarding use of current chemotherapy agents and regimes (Liedtke et al. 2008). For example, some patients with primary TNBC tumours that express a high proportion of basal-like genes have a high likelihood of response to chemotherapy, but if the tumour is not chemo-sensitive, then they have a worse outlook given the reliance on chemotherapy (Marmé & Schneeweiss 2015; Schneider et al. 2008). Improved understanding in what drives TNBC cell growth and identification of different molecular subtypes of TNBC may aid in further

tailoring treatment for this type of breast cancer (P. Sharma 2016; Schneider et al. 2008).

Studies have shown that GWL is often overexpressed in a range of human cancers, including breast cancer (L. Wang et al. 2014) (Rogers et al. 2018). It has also been shown that GWL protein expression levels can vary dramatically across different Squamous Cell Carcinoma (SCC) cell lines (L. Wang et al. 2014). GWL overexpression also encouraged transforming behaviour in immortalised, non-transformed cells and can increase *in vitro* and *in* vivo tumour cell proliferation (Vera et al. 2015). Therefore it may be that GWL is not required in large amounts to maintain CDK1 activity during a normal, unperturbed cell cycle, but instead is required more urgently in order to reach more robust levels of CDK1 activation in certain situations (Álvarez-Fernández et al. 2013). For example, during checkpoint recovery following cell cycle arrest after DNA damage events (Peng et al. 2010).

A caveat with the current body of knowledge about GWL is that most of the research has been done in cancer cell lines. Therefore, it is largely unknown what effects GWL inactivation or depletion has on the health and survival of non-transformed cell lines. For example one study could not detect GWL mRNA in a range of human tissues including the brain, thalamus, pituitary gland, heart, spinal cord, stomach, lung, testis, ovary and kidney (H. J. Johnson et al. 2009), which is contradictory to the theory that GWL is a key player in mitotic entry (Voets & Wolthuis 2010). It is possible that the human GWL protein is more important for genetically unstable and constantly dividing cancer cells, which

makes GWL an attractive target in cancer therapy research because there is a possibility that its inhibition may not be too harmful to non-cancerous proliferating cells in the body. It thus could be possible that cancer cells, being more genetically damaged and unstable than normal cells, are more reliant on GWL.

1.8 CDK4/6 inhibition in triple negative breast cancer

Traditionally, CDK4/6 inhibition has been viewed as a poor therapeutic target for TNBC, because these tumours often show loss of the *RB1* gene or RB function (Herschkowitz et al. 2008). CDK4/6 inhibition has shown to be a promising monotherapy agent in hormone sensitive breast cancers (DeMichele et al. 2015; Finn et al. 2015; N. C. Turner et al. 2015; Hortobagyi et al. 2016; Finn et al. 2016), and the CDK4/6 inhibitors Palbociclib (IBRANCE®) and Ribociclib (Kisqali®) are in clinical use for breast cancer patients in the UK and US (Iacobucci 2017; Kmietowicz 2017; Finn et al. 2016; Hortobagyi et al. 2016). A third CDK/6 inhibitor, Abemaciclib, is under investigation in clinical trials and has been recently approved by the US Food and Drug Administration (FDA) (Polk et al. 2017; Patnaik et al. 2016). However, as previously mentioned, TNBC is a molecularly heterogeneous cancer known for its genomic instability, high expression of cyclin E1 (Network et al. 2012) and has shown resistance to single-agent CDK4/6 inhibition (DeMichele et al. 2015; Finn et al. 2009). However, because of the urgent need to find targets that could be beneficial to TNBC patients, it would be beneficial identify biomarkers that could identify situations in which it would be effective to inhibit CDK4/6 in certain TNBC

tumours. It has been found that some types of TNBC cell are resistant to CDK4/6 inhibition (Asghar et al. 2017). However this study found some exceptions, for example CDK4/6 inhibition was effective in the luminal androgen receptor (LAR) subtype of TNBC *in vitro* and *in vivo* (Asghar et al. 2017). Also, if a certain type of cancer cell is resistant to a particular monotherapy, there could be novel combinations of therapies that are highly effective against TNBC. For example, the crosstalk between the CDK4/6 and the PI3K–AKT–mTOR pathways, including many negative feedback loops, has yielded strong rationale for combining inhibitors through these pathways to inhibit tumour growth, and this strategy has been effective in ER-positive and HER2-postive breast cancer cells which were previously resistant to CDK4/6 inhibition alone (Vora et al. 2014; Goel et al. 2016; Herrera-Abreu et al. 2016). A synergistic effect between PI3K and CDK4/6 has also been observed in TNBC cells. In a panel of TNBC cells, both the combination of Palbociclib with Taselisib (in PIK3CA-mutant TNBC cells) or of Ribociclib with Alpelisib resulted in enhanced cell cycle arrest and apoptosis, than either drug alone (Asghar et al. 2017; Teo et al. 2017). In the study by Asghar and colleagues, the synergy between PI3K and CDK4/6 inhibitors sensitised some TNBC cell types to CDK4/6 inhibitor sensitivity (Asghar et al. 2017).

Such research means that there is a strong pre-clinical rationale for researching CDK4/6 inhibitors in different molecular subtypes of breast cancer, including TNBC, and for testing new combinations of treatments alongside CDK4/6 inhibitors.

1.9 Thesis aims

At the beginning of this project I was planning to focus my studies on how GWL contributes to tumourigenesis, and perhaps try and establish a biomarker that predicts the dependency of cancer cells on elevated GWL expression. As time progressed, other research groups studying GWL in the context of cancer published results that, whilst supportive of the work we have done in this thesis, meant that our own strategy had to be flexible to avoid too much repetition. The work in this thesis addresses two themes of GWL biology in TNBC cells: The first chapter establishes the GWL depletion phenotypes in a panel of breast cells, and the second theme, which forms multiple chapters, explores a key result from a siRNA and drug screen, which found a novel synthetic lethality between GWL and CDK4/6. After validating this screen hit experimentally, we decided to explore the mechanism of this relationship because not only is it novel and exciting from a basic biology perspective, but also combined with the fact that there are successful CDK4/6 inhibitors in clinical use, so this information could bear fruit for future translational work.

Chapter 2. Materials & Methods

2.1 Materials

2.1.1 Human cell lines and cell culture

The cell lines used in this project are listed below in **Table 2.1.** Before experiments began, the cell lines were tested for mycoplasma contamination and their identities authenticated using a short tandem repeat (STR) DNA profiling service. Cell lines were tested for mycoplasma contamination regularly throughout the project.

Cell line	Origin
MDA-MB-231	Breast (adenocarcinoma; Triple Negative; Basal B)
MDA-MB-436	Breast (invasive ductal carcinoma; Triple Negative; Basal B)
MDA-MB-468	Breast (adenocarcinoma; Triple Negative; Basal A)
HS578T	Breast (carcinosarcoma; Triple Negative; Basal B)
MCF10a	Breast (immortalised fibrocystic epithelia)

Table 2.1: Cell lines used in project Information about the phenotype of the cell lines was obtained from the American Type Culture Collection and a study by Chavez *et al.* (Chavez et al. 2010).

All cancer cell lines were cultured in Dulbecco's modified Eagle Medium (DMEM) (Life Technologies) supplemented with 10% Tetracycline-free FBS (PAN Biotech). The immortalised breast epithelial cell line MCF10a was cultured in DMEM/F12 (Life Technologies) supplemented with 10% Tetracycline-free FBS (PAN Biotech), 20ng/mL EGF (Peprotech), 0.5mg/mL Hydrocortisone (Sigma), 100ng/mL Cholera Toxin (Sigma) and 10 μg/mL Insulin (Sigma).

The media of all cells was supplemented with 100U/mL penicillin and 0.1mg/mL streptomycin (Life Technologies). All cells were cultured in a 37°C, 5% CO_2 incubator.

The number of cells per mL of media was calculated using a haemocytometer.

2.1.2 Drugs

- Doxycycline (Sigma); stored in powder form at 4°C protected from light. Aliquots dissolved in water, stored at -20°C protected from light.
- CDK4/6 inhibitor Lee011/Ribociclib (Selleckchem). Aliquots dissolved in DMSO, stored at -20°C protected from light.
- CDK4/6 inhibitor Palbociclib (Selleckchem). Aliquots dissolved in DMSO, stored at -20°C protected from light.

2.1.3 Buffers

4x Sample Buffer for Immunoblotting

10 mL	Working concentration 1x
2.0 mL 1M Tris-HCl, pH 6.8	50 mM
0.8 g SDS	2%
4.0 mL 100% glycerol	10%
0.4 mL 14.7 M β-mercaptoethanol	1%
1.0 mL 0.5 M EDTA	12.5 mM
8.0 mg bromophenol blue	0.02%
2.6 mL dH_2O	

10x SDS running buffer for SDS-PAGE

Per litre dH_2O:

121.1 g Tris Base

576.5 g Glycine

40 g SDS

Diluted to 1x with dH_2O prior to use

Immunoblotting buffers

Anode 1: 300 mM Tris, 20% methanol, pH 10.4

Per litre:

200 mL methanol

36.3 g TRIZMA base (Fisher)

Made up to 1 L with dH_2O

Anode 2: 25 mM Tris, 20% methanol, pH 10.4

Per litre:

200 mL methanol

3.02 g TRIZMA base (Fisher)

Made up to 1 L with dH_2O

Cathode: 25 mM Tris, 40 mM 6-aminohexanoic acid, 20% methanol, pH 9.6

Per litre:

200 mL methanol

3.02 g TRIZMA base (Fisher)

5.24 g 6-aminohexanoic acid (Sigma)

Made up to 1 L with dH_2O

2.1.4 Primary antibodies

The names, sources and the dilutions of the primary antibodies used are listed in **Table 2.2**. Primary antibodies stored at -20°C.

Antigen	Source (catalogue number)	Species	Dilution (assay)
Greatwall kinase / MASTL	Sigma (HPA054273)	Rabbit	1:500 (IB); 1:200 (IF)
α-Tubulin	Abcam (ab7291)	Mouse	1:10,000 (IB); 1:1000 (IF)
p-γH2AX (Ser 139)	Millipore (05-636)	Mouse	1:1000 (IF)
α-Endosulfine (ENSA)	Abcam (ab125873)	Rabbit	1:1000 (IB)

PP2A-B55	Santa Cruz (sc-18330)	Goat	1:1000 (IB)

Table 2.2 Primary antibodies used in project IB, immunoblot; IF, immunofluorescence

2.1.5 Secondary antibodies

All horseradish peroxidase (HRP)-conjugated secondary antibodies were obtained from Dako/Agilent and stored at 4°C protected from light.

- Goat anti-rabbit
- Goat anti-mouse
- Rabbit anti-goat

For IF experiments, all secondary antibodies were used at 1:2000. For IB experiments, secondary antibodies were used at 1:2500 with the exception of detecting α-Tubulin where the concentration of the secondary antibody was 1:4000.

2.1.6 siRNA 0ligonucleotides

The names and sources of the siRNA oligonucleotides used are listed in **Table 2.3**. Stored at -20°C protected from light.

Target	Source (catalogue number)
Negative Control	QIAGEN AllStars (SI03650318)
PP2A-B55α subunit (PPP2R2A)	QIAGEN FlexiTube (GS5520)

PP2A-B55δ subunit (PPP2R2D)	QIAGEN FlexiTube (GS55844)
α-Endosulfine (ENSA)	Dharmacon ON-TARGET plus SMARTpool (L-011852-00-0005)
ARPP19 (cAMP regulated phosphoprotein 19)	Dharmacon ON-TARGET plus SMARTpool (L-015338-00-0005)

Table 2.3 List of siRNA oligonucleotides used in project

2.2 Methods

2.2.1 Production of lentivirus particles containing shRNA constructs

4.5 μg each of plasmids encoding the viral components VSV-G1 and psPAX2, plus 3 μg of either the shGWL or shScr plasmid constructs (depending on which viral vector was being made) was diluted in 1.5 mL Opti-MEM™ media (Gibco) and mixed gently. In a separate tube, 36 μL Lipofectamine 2000 (Invitrogen) was added into 1.5 mL Opti-MEM™ and mixed gently. The Lipofectamine mixture was incubated at room temperature for 5 minutes. After this, the viral plasmids and the shRNA plasmids were combined with the Lipofectamine solution, mixed gently and incubated at room temperature for 20 minutes.

Meanwhile HEK293FT cells were trypsinised and re-suspended at a concentration of 1.2 x 10^6 cells/mL in antibiotic-free DMEM. Then the transfection mixture (3 mL total) was added to a 10 cm plate and then 5 ml of 1.2 x 10^6 cells/mL were added to give 6 x 10^6 cells total in 8 ml. The cells and transfection mixture were gently combined by rocking the plate and placed in a

cell culture incubator. 24 hours later, the media was aspirated and replaced with 8 ml antibiotic-containing media. 48 hours following transfection, the cells were checked for GFP expression. In the event of GFP positive HEK293FT cells, the media was carefully harvested and centrifuged at 3000 rpm for 5 min to pellet any HEK293FT cells present. The supernatant containing the virus was divided into 1 mL cryovials and stored at -80°C.

2.2.2 shRNA-lentivirus based transfection

A small batch of DMEM supplemented with 6 μg/μL Polybrene (Sigma) (to aid viral transfection efficiency) was prepared, and to each well of a 6-well plate the following viral dilutions were set up (**Table 2.3**)

Dilution	Volume of lentivirus titre (μL)	Volume of complete DMEM supplemented with 6 μg/μL Polybrene (μL)
0	0	1500
1:3	500	1000
1:5	300	1200
1:10	150	1350

Table 2.4 Lentiviral transfection dilutions used in project

To each well, a suspension of 50,000 cells/mL in complete DMEM was added. The cells and the virus particles were left to incubate for 48-72 hours, and then inspected for GFP production. Cells that displayed a good transfection efficiency, i.e. glowing green from GFP expression, were harvested and frozen

in cryovials at -80°C before being sent to Alice Shea at Bart's Cancer Institute (BCI) for GFP-sorting to select for the population of cells that express the higher amounts of GFP. Within the shRNA plasmid, the GFP gene is coupled to the Tetracycline Response Element (TRE) via a T2A ribosome-skipping element **(Figure 3.3)**. This means the level of GFP expression will be proportional to the level of shRNA expression.

2.2.3 siRNA lipid-based transfection

For siRNA-based depletion assays, the transfection reagent Lipofectamine RNAiMAX (Invitrogen) was used.

Per siRNA transfection, 500 μL Opti-MEM™, 5 μL of RNAiMAX and 2.5 μL of each appropriate siRNA molecule (**Table 2.3**) were mixed gently together and incubated at room temperature for 15 minutes. This mixture was then added dropwise to the well of a 6-well plate containing a freshly counted and re-suspended solution of cells.

2.2.4 Total cell extracts

Cells were counted and lysed in a volume of 4x Sample Buffer (Final concentration at 1x working dilution 50 mM Tris-HCl pH 6.8, 2% SDS, 10% glycerol, 1% β-mercaptoethanol, 12.5 mM EDTA, 0.02% bromophenol blue) that yielded a concentration of 100,000 cells per 10 μL.

2.2.5 SDS-PAGE and Immunoblotting

Samples were briefly sonicated with a Vibra-Cell™ sonicator (VWR) to shear DNA, and then boiled at 95°C for 5 minutes before separation by SDS-PAGE.

Running gels comprised of 10% bisacrylamide for detection of most proteins such as GWL, PP2A-B55 and α-Tubulin; a 15% bisacrylamide gel was used to sufficiently resolve ENSA, plus 125 mM Tris-HCl [pH 6.8], 0.1% SDS, 0.1% ammonium persulphate (APS) and 0.1% N,N,N',N'- tetramethylethylenediamine (TEMED). Resolving gels comprised 10% bisacrylamide, 375 mM Tris-HCl [pH 8.8], 0.1 % Sodium dodecyl sulphate (SDS), 0.1% Ammonium persulphate (APS) and 0.05% TEMED.

A lane of Color Prestained Protein Standard, Broad Range (11–245 kDa) marker (New England Biosciences) was included on all gels to confirm band sizes and to ensure completion of the electrophoresis protein separation. The SDS-PAGE gels were run at 150 V using a PowerPac™ Basic (Bio-Rad) until the blue front of the sample buffer had reached the bottom of the gel.

Protein was transferred by a semi-dry transfer onto a Hybond™ PVDF membrane (GE Healthcare Amersham) (that had been previously soaked in methanol) using a Trans-Blot® Turbo™ (Bio-Rad). The buffers used for the semi-dry transfer are listed in **Section 2.1.3**.

Proteins of interest were detected using the concentrations of primary antibody as indicated in **Table 2.2** in 5% milk/PBS solution. A loading control was

detected using a 1:10,000 dilution of anti α-Tubulin antibody (Abcam) in 5% milk/PBS solution. Membranes and primary antibodies were incubated overnight at 4°C.

The next day the primary antibody solution was removed, and the membranes washed 5 minutes in 0.1% NP-40/PBS x3. After washing, the appropriate HRP-conjugated secondary antibody (**Section 2.1.5**) was added to the membranes in a 5% milk/PBS solution and incubated at room temperature for 1 hour. After this incubation the membrane was washed x3 with 0.1% NP-40/PBS as before and then placed in PBS without detergent whilst the chemilluminescence substrate was prepared.

2.2.6 Chemilluminescence detection

The chemilluminescence substrate is comprised of:

- Luminol solution (0.1 M Tris-phosphate [pH 8.6]; 0.5 mg/mL Luminol Sodium Salt (Sigma))
- Enhancer solution (1.1 mg/mL p-Coumaric acid dissolved in DMSO (both from Sigma)
- Hydrogen peroxide (Fluka)

And is prepared in the following ratio per mL:

- Luminol 1 mL
- Enhancer 10 μL
- Hydrogen peroxide 3.1 μL

The chemilluminescence substrate was added to the membrane, and the results analysed by exposing the membrane to X-ray film (Amersham) and developed in a Xograph film developer. X-ray film exposure times were varied to optimise clarity and exposure of bands present.

2.2.7 Colony formation assay

Feeder layers were made by irradiating 6 x 10^4 cells per 10cm dish with 35 Gy radiation and plating out the cells and incubating them at 37°C, 5% CO_2 overnight to allow cells to adhere. Then fresh cells were counted, plated and incubated until discrete colonies could be seen. The media was removed, the plates washed with PBS and the cells fixed by adding 2 mL Methanol per plate and gently swirling. After aspiration of the Methanol, another PBS wash was carried out before staining the cells with 0.05% Crystal Violet solution (0.5 g Crystal Violet, 27 mL 37% formaldehyde, 10 mL Methanol in 963 mL PBS). After staining, the Crystal Violet was removed by submerging the plates and washing under gently running water until all background stain was removed.

2.2.8 Immunofluorescence and EdU staining for fixed cell microscopy

Cells were cultured on glass coverslips. If also staining for EdU, 10 μM EdU was added for 20 minutes prior to fixation. Cells were fixed with 1 mL 3.7% formaldehyde (Sigma-Aldrich) for 10 minutes at room temperature. Fixed cells were washed 3 times with PBS. Cells were then permeabilised with 1% NP-40 for 15 minutes and washed 3 times with PBS.

Optional step: If staining for EdU uptake, an appropriate volume of the Click-iT™ cocktail, made according to the manufacturer's instructions (Click-iT™ EdU Alexa Fluor™ 647 Flow Cytometry Assay Kit, Life Technologies) was prepared and 40 μL of the Click- iT™ cocktail applied to the coverslip. The coverslips were then incubated in the dark at room temperature for 30 minutes, and then gently washed twice with PBS.

The slides were then blocked for 30 minutes with 3% BSA/PBS (Sigma-Aldrich). Then, incubation with the primary antibody in 3% BSA/PBS for 1 hour at room temperature, followed by 2x PBS washes, then secondary antibody (1:2000 dilution) for 1 hour and then a final 2x PBS washes. Cells were then incubated with a 1:1000 DAPI solution in PBS for 10 minutes before being mounted onto standard laboratory slides face down using a drop of ProLong™ Diamond Antifade Mountant (Life Technologies) and allowed to set for at least 24 hours in the dark at room temperature.

2.2.9 Fixed and live cell microscopy

Images of cells were taken with an IX73 Inverted Microscope (Olympus) with a 40x oil immersion objective (Olympus). Images were collected by μManager software (Open Imaging). Fixed cell image figures were prepared with OMERO software. Nuclei were counted with ImageJ (NIH) with the Cell Counter plugin.

Movies of living cells were taken with an IX73 Inverted Microscope (Olympus) with an IXplore Live incubation chamber to maintain cell viability. Time frames

of cells were captured every 5 minutes over a 72-hour period. Cells and their divisions were tracked manually with ImageJ (NIH).

2.2.10 EdU labelling for Fluorescence Activated Cell Sorting

10 μM EdU was added for 1 hour prior to cell harvesting. Cells were trypsinised, spun down at 1500 rpm for 5 minutes and then washed with PBS before being spun down again. Then each sample pellet was re-suspended in 50 μL PBS and 750 μL 70% Ethanol and incubated at 4°C overnight.

Cells were spun down at 1500 rpm for 5 minutes and the supernatant removed. Then the cells were washed twice with 500 μL of 1% FCS/PBS. After the final wash, the pellet was resuspended into 40 μL of the prepared Click-iT™ cocktail, made according to the manufacturer's instructions (Click-iT™ EdU Alexa Fluor™ 647 Flow Cytometry Assay Kit, Life Technologies). The reaction was allowed to develop in the dark at room temperature for 30 minutes. Cells were spun down again at 1500 rpm for 5 minutes, the supernatant removed, and the cells washed twice with 500 μL of 1% FCS/PBS, before being spun down again.

The cells were resuspended in 500μL of 1% FCS/PBS containing 5 μg/mL of Propidium Iodide (PI) and 250μg/mL of RNase A (Sigma). The PI stain and the ribonuclease digestion was left to develop overnight at 4°C. Before FACS analysis (Accuri BD Accuri™ C6), the samples were filtered through the cell strainer caps of into Falcon 5 mL round bottom polystyrene test tubes (Scientific Laboratory Supplies).

2.2.11 Generating GWL shRNA MDA-MB-231 cells expressing DHB-mCherry

The CSIIefAH-DHBVen vector (generously gifted from Sabrina Spencer) was digested with BamH1 to remove the mVenus tag and the coding sequence for mCherry was cloned into this site by Gibson assembly. Correct integration and absence of PCR related mutations were checked by DNA sequencing. Using the CSIIefAH-DHBmCherry plasmid we generated lentiviral particles in 293FT cells and infected the GWL shRNA MDA-MB-231 cells. Positive clones were isolated by FACS sorting and expression of DHV-mCherry was confirmed by fluorescent microscopy.

2.2.12 Analysing CDK2 activity using the DHB-mCherry probe

DHBmCherry expressing GWLshRNA MDA-MB-231 cells were either treated with 2 μg/mL Dox or left in Dox free medium. Following three days of shRNA induction the cells were plated on 96 well plates (Cell carrier, Perkin Elmer). 2 wells were used for Control and 2 for Dox treated cells. Lee011 was then added at 0.5 μM to one of the control wells and one of the + Dox wells. To obtain a counterstain, the cells were also treated with 0.5 μM SiR-DNA (Cytoskeleton, Inc.). Imaging was performed on an Operetta high throughput imaging device (Perkin Elmer) using a 40x water lens (NA=1.1). Time-lapse microscopy was performed at 10-minute intervals and 25 positions per well were imaged for 25 hours. For analysis, the images were exported and regions of interest (ROI) inside and outside the nucleus were measured manually in ImageJ in hourly intervals. With the help of Helfrid Hochegger, the data were imported as Pandas data frames and further analysed using Python 3.7. Graphs were generated

using the Python Seaborn methods package. For **Figure 6.5B**, there is some qualitative analysis, and levels of CDK2 activity are judged by eye which is demonstrated in **Figure 6.5C**. The medium CDK2 activity is when there is no discernable difference in fluorescence between inside and outside the nucleus. High CDK2 activity is when the cytoplasm shows high fluorescence and there is no fluorescence in the nucleus. Low CDK2 activity is when the nucleus clearly shows higher fluorescence than the cytoplasm.

2.2.13 Publicly available datasets

Information regarding mRNA expression of GWL in different molecular subtypes of breast cancer and the Kaplan-Meier plot plotting survival probability against GWL expression in breast cancer were obtained from: http://tumorsurvival.org/TCGA/Breast_TCGA_BRCA/. Additional Kaplan-Meir plots plotting survival probability against GWL expression in a pan-cancer wide study (PANCAN) as well as just breast cancer were obtained from https://xenabrowser.net/. GO analysis was carried out by the PANTHER classification system at www.pantherdb.org.

2.2.14 Statistical analysis

Statistical tests were performed with GraphPad Prism version 5.0. *P* values were two-tailed and considered significant if $P < 0.05$. Error bars represent SEM of three independent experiments, unless otherwise stated. Certain figures show two independent replicates and error bars of SEM, but without statistical tests. Such cases are indicated in the figure legends. The Estimation Statistics analysis (Shared Control) shown in Chapter 5 was carried out using the

following open source tool: http://www.estimationstats.com/#/analyze/shared-control (Ho et al. 2018)

Chapter 3. Characterisation of Greatwall kinase depletion in Triple Negative Breast Cancer cells

3.1 Introduction: Greatwall Kinase and cancer

The function of GWL as an essential mitotic kinase has been extensively characterized in *Drosophila*, *Xenopus*, and mammalian cells (J. Yu et al. 2004; Vigneron et al. 2009; Burgess et al. 2010; Álvarez-Fernández et al. 2013). In addition, previous studies have published thorough characterisations of GWL function, localisation and depletion phenotypes in human cancer cells. The human GWL protein appears to be essential for development (Álvarez-Fernández et al. 2013) is stably expressed throughout the cell cycle but is phosphorylated and most active during mitosis (Dephoure et al. 2008; Voets & Wolthuis 2010; Olsen et al. 2010).

More recently while this thesis was in preparation, there have been studies published regarding the role of GWL and its depletion phenotypes in human breast cancer cells which suggest that GWL may have clinical importance both as a potential therapeutic target and as a prognostic tool (Vera et al. 2015; Álvarez-Fernández et al. 2013; Álvarez-Fernández, Sanz-Flores, Sanz-Castillo, Salazar-Roa, Partida, Zapatero-Solana, Ali, Manchado, Lowe, VanArsdale, Shields, Caldas, Quintela-Fandino & Malumbres 2018b; Rogers et al. 2018). These studies have shown that GWL is often overexpressed in a range of human cancers, including breast cancer (L. Wang et al. 2014; Rogers et al. 2018), and that overexpressing GWL in non-cancerous cells can promote some of the transformational properties needed for cells to eventually become

cancerous such as AKT hyper phosphorylation (Vera et al. 2015). It has also been shown that GWL protein expression levels can vary dramatically across different Breast Cancer cell lines (Álvarez-Fernández, Sanz-Flores, Sanz-Castillo, Salazar-Roa, Partida, Zapatero-Solana, Ali, Manchado, Lowe, VanArsdale, Shields, Caldas, Quintela-Fandino & Malumbres 2018b) and Squamous Cell Carcinoma (SCC) cell lines (L. Wang et al. 2014). GWL overexpression also encouraged transforming behaviour in immortalised, non-transformed cells and can increase *in vitro* and *in* vivo tumour cell proliferation (Vera et al. 2015). It is, thus, tempting to speculate be that GWL is not only required to maintain CDK1 activity during a normal, unperturbed cell cycle, but can also be high jacked by tumour cells to supress the downstream activity of the phosphatase complex PP2A-B55. It is important to note that PP2A has been implicated as a tumour suppressor (Janssens et al. 2005; Manchado et al. 2010; Álvarez-Fernández, Sanz-Flores, Sanz-Castillo, Salazar-Roa, Partida, Zapatero-Solana, Ali, Manchado, Lowe, VanArsdale, Shields, Caldas, Quintela-Fandino & Malumbres 2018b). Alternatively, overexpression of GWL may simply help in boosting CDK1 activity during checkpoint recovery following cell cycle arrest after DNA damage events (Peng et al. 2010). Thus, it could be possible that cancer cells, being more genetically damaged and unstable than normal cells, are more reliant on GWL. Overall, a link between GWL overexpression and tumourigenesis is starting to emerge, however does require further mechanistic understanding.

3.2 Greatwall kinase over expression in triple negative breast cancer

I performed an analysis of clinical data from breast cancer patients confirms the previously mentioned published reports that there is a link between GWL expression and patient survival. Using publicly available data from The Cancer Genome Atlas (TCGA) databases and the web tools http://tumorsurvival.org/index.html and https://xenabrowser.net/; this data can be seen in **Figure 3.1**. Looking exclusively at breast cancer, the Basal/Triple Negative subtypes show the highest amount of GWL mRNA expression according to RNA-Seq. Across all breast tumour types sampled as well as a survey of all tumour types via the PANCAN study, the tumours that graded 'high' in GWL expression were associated with shorter survival (**Fig. 3.1**).

To analyse the role of GWL in cancer cells I chose TNBC cells as a model system due the strong link of this tumour class with GWL over expression (**Fig. 3.1**) (Álvarez-Fernández, Sanz-Flores, Sanz-Castillo, Salazar-Roa, Partida, Zapatero-Solana, Ali, Manchado, Lowe, VanArsdale, Shields, Caldas, Quintela-Fandino & Malumbres 2018b; Rogers et al. 2018) and the therapeutic need due to TNBC exhibiting a high degree of heterogeneity and lacking well-defined therapeutic targets, meaning that this tumour type is associated with poor prognosis (Dent et al. 2007; Haffty et al. 2006; Bianchini et al. 2016).

Cell line	**Origin**
MDA-MB-231	Breast (adenocarcinoma; Triple Negative; Basal B)
MDA-MB-436	Breast (invasive ductal carcinoma; Triple Negative; Basal B)

MDA-MB-468	Breast (adenocarcinoma; Triple Negative; Basal A)
HS578T	Breast (carcinosarcoma; Triple Negative; Basal B)
MCF10a	Breast (immortalised fibrocystic epithelia)

Table 3.1: Cell lines used in project Information about the phenotype of the cell lines was obtained from the American Type Culture Collection and a study by Chavez *et al.* (Chavez et al. 2010).

Our collaborator, Chris Lord of the Institute of Cancer Research (ICR), London, generated additional preliminary data for this project. A high-throughput siRNA-GWL screen was set up to measure cell viability after GWL depletion in a large panel of human cell lines, mostly cancerous cells, from a variety of organs and molecular subtypes within cancers of the same organ. The waterfall plot showing the Z-scores of the cell viabilities following GWL depletion as well as the table showing the identity of each cell line used and its corresponding Z-score is shown in **Figure 3.2**. The waterfall plot **(Fig. 3.2A)** indicates that there is a subset of cancer cells that are highly sensitive to GWL depletion, whilst there are other cells that are tolerant of this. Cancerous cells from a range of organs show sensitivity and resistance to GWL depletion, so this raises the question what features of a cell determine its sensitivity to GWL.

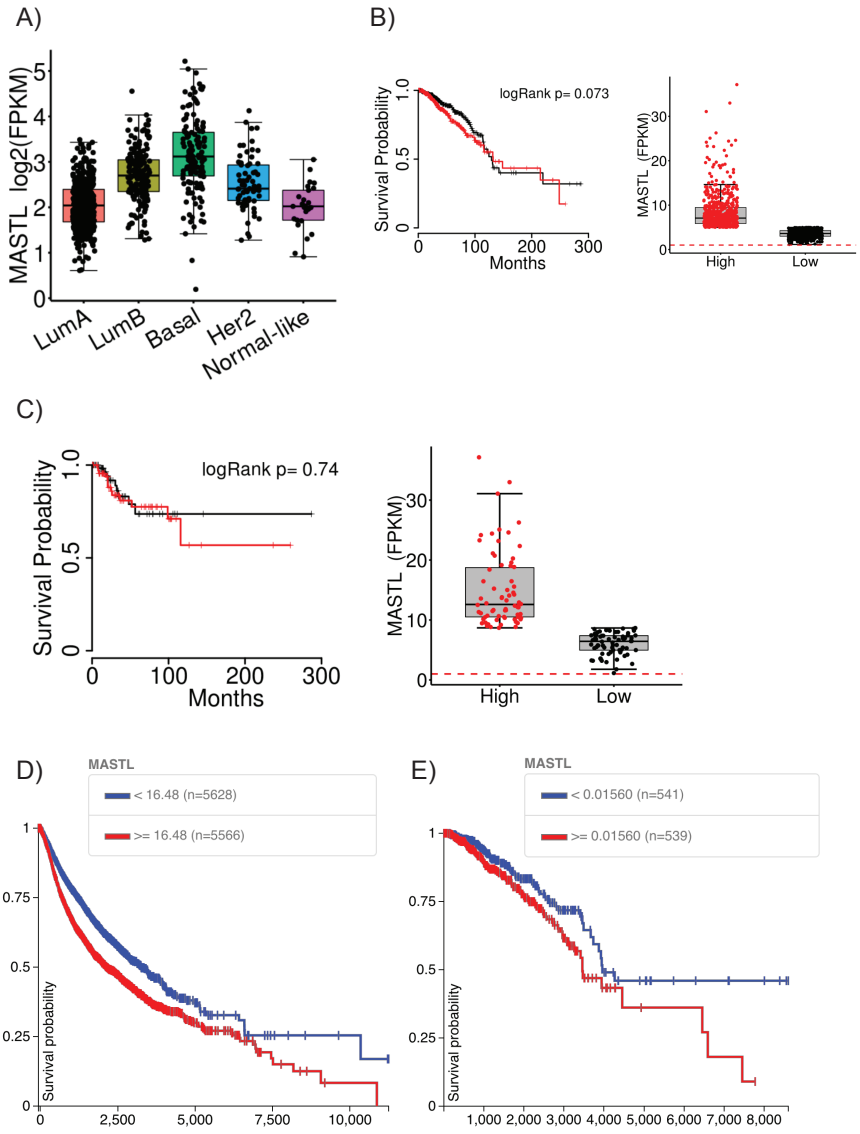

Figure 3.1 Clinical data from The Cancer Genome Atlas database shows a correlation between GWL overexpression and lower survival probability Red lines in survival plots signify GWL overexpression A) GWL (here as MASTL) mRNA expression across different breast cancer types B) Survival of patients with all breast tumour subtypes correlated with GWL mRNA expression C) Survival of patients with Basal (Triple Negative) breast tumours correlated with GWL mRNA expression D) PANCAN database (all tumour types) correlating patient survival with GWL expression E) Breast cancer patient survival correlated against GWL copy number.

A)

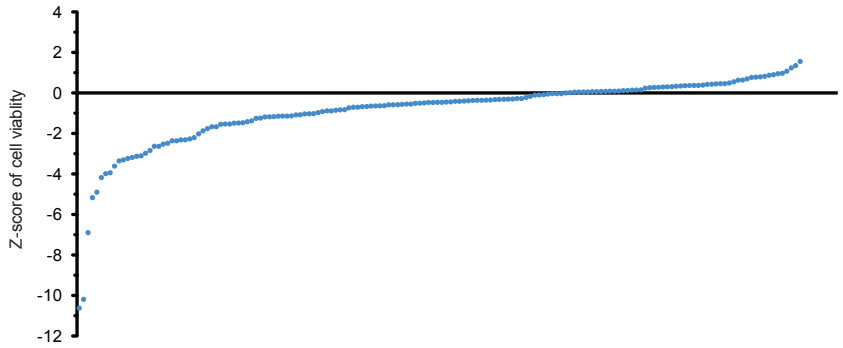

B)

Cell line	Z-score cell viability	Cell line	Z-score cell viability	Cell line	Z-score cell viability	Cell line	Z-score cell viability
SW48WT_COLORECTAL	-10.6229	OVMANA_OVARY	-1.242170739	MDAMB134_BREAST	-0.457172615	T47D_BREAST	0.118377237
MIAPACA2_PANCREAS	-10.18846188	SMOV2_OVARY	-1.181068118	CAL120_BREAST	-0.44680606	TE1_OESOPHAGUS	0.121768476
HCT116_ARID1A_HETEROZYGOUS	-6.897929601	MGHU3_BLADDER	-1.17744	H358_LUNG	-0.438072975	TE6_OESOPHAGUS	0.139017709
OCUM2M_GASTRIC	-5.16517	TKCC12_PANCREAS	-1.168304756	SUM44_BREAST	-0.411210476	MFM223_BREAST	0.147885779
OE19_OESOPHAGUS	-4.894437093	MDAH2774_OVARY	-1.147617515	A549_LUNG	-0.408349152	HS578T_BREAST	0.156385277
HCT116_ARID1A_HOMOZYGOUS	-4.176078148	HELA_CERVICAL	-1.140230969	OAW42_OVARY	-0.399925722	TE9_OESOPHAGUS	0.237577518
HCT116_ARID1A_PARENTAL	-3.98431951	OST_BONE	-1.137663955	OV56_OVARY	-0.381702528	SD_LYMPHOBLASTOMA	0.258695
A549DMSO_LUNG	-3.942	MDAMB468_BREAST	-1.130747385	PEO14_OVARY	-0.365409771	X143B_BONE	0.271924415
KOC7C_OVARY	-3.611883025	HCC70_BREAST	-1.078752952	KYSE70_OESOPHAGUS	-0.361712985	HCC1954_BREAST	0.279414203
AHEZ_LUNG	-3.351522673	TE11_OESOPHAGUS	-1.074389321	TE8_OESOPHAGUS	-0.361143565	H2342_LUNG	0.293890197
H727_LUNG	-3.304701858	LIM1215WT_COLORECTAL	-1.0312	JMSU1_BLADDER	-0.353683	MDAMB157_BREAST	0.300082985
MG63_BONE	-3.232651872	BEN_LUNG	-1.02733755	PL45_PANCREAS	-0.349390843	SUM159_BREAST	0.307510076
SKBR3_BREAST	-3.178653205	MCF12A_BREAST	-1.016138159	COV362_OVARY	-0.32146991	H292_LUNG	0.332206971
AC375_LUNG	-3.124900778	PACADD159_PANCREAS	-0.96916112	VP229_BREAST	-0.316461887	CASKI_CERVICAL	0.342963884
PACADD183_PANCREAS	-3.100002796	CROE33_OESOPHAGUS	-0.91861884	PACADD161_PANCREAS	-0.310115009	BT20_BREAST	0.360963089
RMG_OVARY	-2.976384363	CAMA1_BREAST	-0.884197763	TKCC09_PANCREAS	-0.303265352	COV504_OVARY	0.370119128
AC216_LUNG	-2.841890323	HPAC_PANCREAS	-0.883901447	TKCC15_PANCREAS	-0.299522226	KK_OVARY	0.372924087
KYAE_OESOPHAGUS	-2.635619194	HOS1_BONE	-0.857075855	RES186_GLIOMA	-0.273447422	NOS1_BONE	0.375563444
KYAE1_OESOPHAGUS	-2.635619194	CAL72_BONE	-0.828955432	SKOV3_OVARY	-0.27328583	H460_LUNG	0.386197099
TKCC27_PANCREAS	-2.526506093	ZR751_BREAST	-0.82391725	RT112M_BLADDER	-0.219322	X977_BLADDER	0.427191
ESO26_OESOPHAGUS	-2.481399022	TKCC18_PANCREAS	-0.73030125	PACADD119_PANCREAS	-0.169170752	MCF7_BREAST	0.429775476
TKCC10_PANCREAS	-2.363362292	TOV21G_OVARY	-0.700940393	TE14_OESOPHAGUS	-0.101229187	SF188_GLIOMA	0.456425518
MCF10A_BREAST	-2.357738986	TYKNU_OVARY	-0.70094	OVISE_OVARY	-0.095406745	OVAYSO_OVARY	0.45741
MFE296_ENDOMETRIUM	-2.319081004	TKCC05_PANCREAS	-0.677078204	TKCC26_PANCREAS	-0.080910817	OVTOKO_OVARY	0.458562384
BT549_BREAST	-2.30904	HMT3552_BREAST	-0.664599795	SJSA1OSA_BONE	-0.055389938	CAL51_BREAST	0.49999113
OE33_OESOPHAGUS	-2.267446764	RES259_GLIOMA	-0.649200938	SAOS2_BONE	-0.035084098	H1299_LUNG	0.551492773
AC295_LUNG	-2.202228179	AN3CA_ENDOMETRIUM	-0.64	JIMT1_BREAST	-0.034403736	SUM52_BREAST	0.634135
SNU16_GASTRIC	-2.01927	SCC47_HEADNECK	-0.633584431	H1650_LUNG	-0.029644015	HCC1143_BREAST	0.638193328
SIHA_CERVICAL	-1.865823778	SCC003_HEADNECK	-0.62776901	ZR7530_BREAST	0	MDAMB231_BREAST	0.699506734
DLD1_LARGE_INTESTINE	-1.76201	OVAS_OVARY	-0.581933262	SUM149_BREAST	0.019721022	CAOV3_OVARY	0.76564922
STELLATE_PANCREAS	-1.668301462	TOV112D_OVARY	-0.580605877	FLO_OESOPHAGUS	0.0433585	SCC36_HEADNECK	0.78406156
C33A_CERVICAL	-1.66665307	H1975_LUNG	-0.574923304	FLO1_OESOPHAGUS	0.049561541	HOSMNNG_BONE	0.794309124
KNS42_GLIOMA	-1.549852185	A427_LUNG	-0.558611298	H1838_LUNG	0.056286519	X93VU_HEADNECK	0.823145909
G292_BONE	-1.531742961	TKCC07_PANCREAS	-0.548058404	TE10_OESOPHAGUS	0.056670446	KATOIII_GASTRIC	0.874538
TKCC02_PANCREAS	-1.52909696	SCC90_HEADNECK	-0.546527264	H1793_LUNG	0.064686616	UW479_GLIOMA	0.903402576
ES2_OVARY	-1.4903238	TE5_OESOPHAGUS	-0.512663094	JHADESO1_OESOPHAGUS	0.064793109	HEC1A_ENDOMETRIUM	0.955189666
TKCC06_PANCREAS	-1.48276291	HUO3N1_BONE	-0.506369566	U2OS_BONE	0.07814788	OV90_OVARY	0.977538281
ASPC_PANCREAS	-1.470729155	TKCC22_PANCREAS	-0.490040753	BT474_BREAST	0.084746558	MDAMB453_BREAST	1.077007564
PL5_PANCREAS	-1.416185687	H11581_BLADDER	-0.469838	SKGT4_OESOPHAGUS	0.089437951	HOP62_LUNG	1.23647393
H2228_LUNG	-1.37413594	PANC_PANCREAS	-0.464974454	H23_LUNG	0.090121467	HCH1_OVARY	1.353872661
BXPC3_PANCREAS	-1.253319094	HCC202_BREAST	-0.460735545	PCI30_HEADNECK	0.096417354	OACP4C_OESOPHAGUS	1.559529896

Figure 3.2 A siRNA screen depleting GWL in a panel of human cancer cell lines indicates a therapeutic window Experiment by Chris Lord, ICR. A panel of human cancer cell lines was treated with GWL siRNA and their viability was assessed with CellTiter-Glo® assay. A) Cell viability was plotted as a Z-score B) List of cell lines and their corresponding Z-score. TNBC cell lines are highlighted in orange, and the hormone receptor positive and/or HER2 positive breast cancer cell lines are highlighted in green. The non-transformed human breast cell lines MCF10A and MCF12A are highlighted in blue.

As a first step in characterising GWL kinase in TNBC, I examined whether differences in GWL protein levels exist across a panel of TNBC cells and a non-transformed breast epithelial cell line. Four TNBC cell lines were used – MDA-MB-231 (MDA-MB-231), HS578T, MDA-MB-436 (MDA-MB-436), MDA-MB-468 (MDA-MB-468) and the non-cancerous breast cell line MCF10a. These cell lines are commonly used in cell culture and are well characterised, and more information about these cells can be found in **Table 3.1**.

Asynchronous whole cell extracts prepared from each of the five cell lines were analysed by Immunoblotting using antibodies against GWL and α-Tubulin, where α-Tubulin was used as a loading control. In **Fig. 3.3** the immunoblot bands that indicate GWL are the bands that are found nearest the 100 kilodalton (kDa) mark. The slightly lower bands that can be seen are believed to be non-specific. They do appear inconsistently in different blots and their appearance is not affected by siRNA or shRNA depletion. However, we cannot exclude that these bands constitute splicing variants of the kinase. A theoretical splicing variant with a size of 92 kDa is indeed documented in the UniProt database. **Fig. 3.3** clearly indicates that the TNBC cells have higher levels of GWL than the non-transformed MCF10a cells, which is in agreement with another study of breast cancer cells (Rogers et al. 2018) and also from data from cells of a different organ, SCC cells, where the non-transformed keratinocyte lines showed lower GWL protein levels than the SCC cell lines (L. Wang et al. 2014).

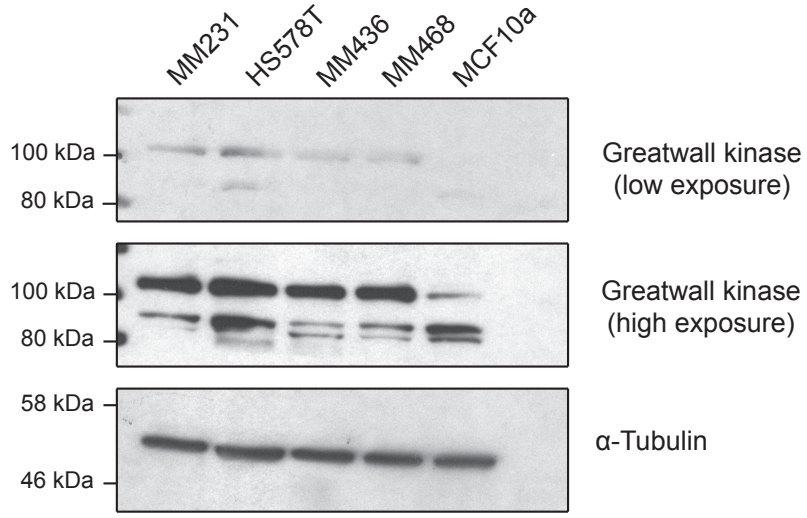

Figure 3.3 Expression of GWL in asynchronous human breast cell lines SDS-PAGE analysis of a panel of Triple Negative Breast Cancer cell lines as well as the non-transformed breast epithelial cell line MCF10a. Greatwall kinase expression levels were detected using the anti-Greatwall kinase antibody, and an anti-α-Tubulin antibody was used as a loading control.

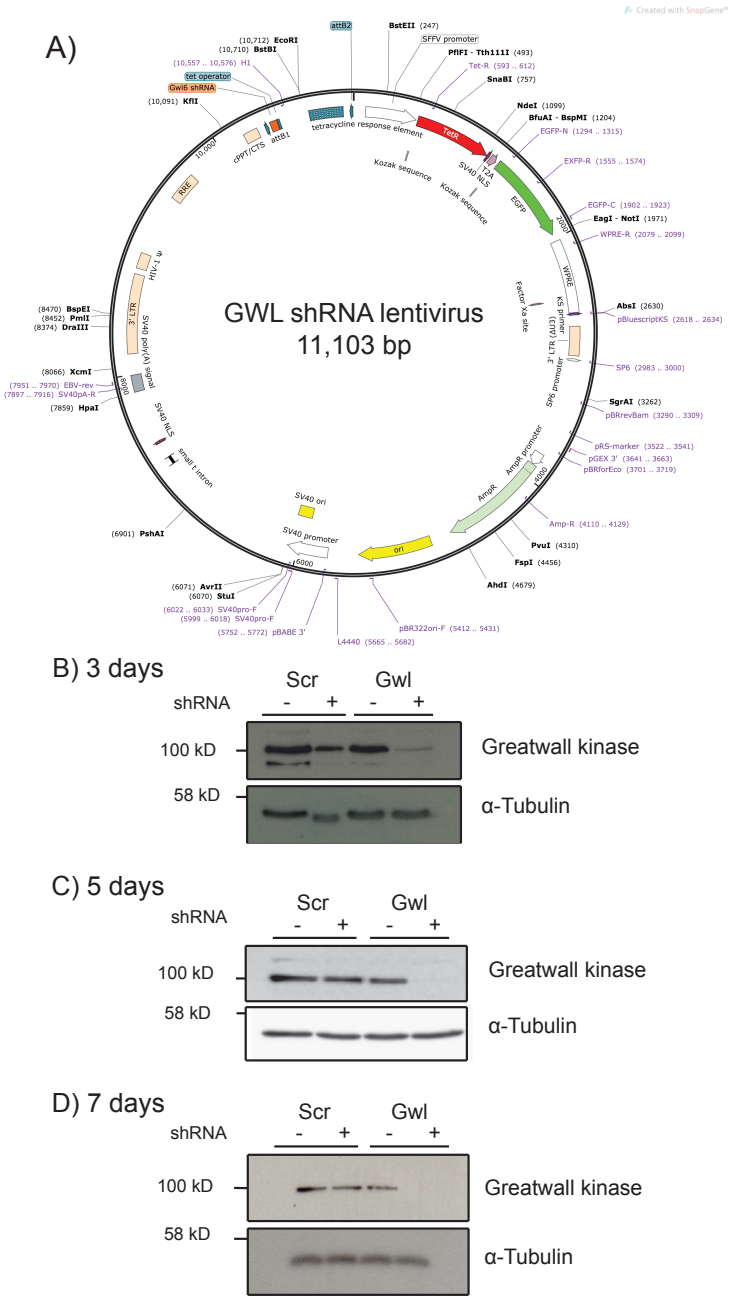

Fig. 3.4 Vector map of the inducible shRNA system and time course immunoblot depicting the knockdown of GWL A) Vector map of the plasmid containing the GWL-shRNA and GFP reporter gene. B)-D) SDS-PAGE analysis of the Doxycycline-inducible shRNA system to deplete GWL in MDA-MB-231 cells. A final concentration of 2 µg/mL Doxycycline was used to induce shRNA expression. B) GWL levels after 3 days of shRNA induction. C) GWL levels after 5 days D) GWL levels after 7 days.

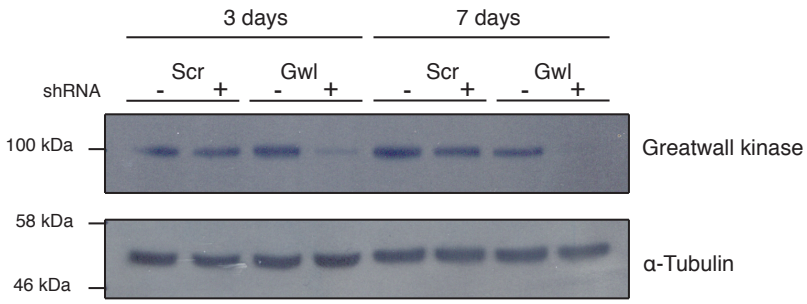

Fig 3.5 Testing the inducible shRNA system in HS578T cells SDS-PAGE analysis of the Doxycycline-inducible shRNA system to deplete GWL in HS578T cells. A final concentration of 2 µg/mL Doxycycline was used to induce shRNA expression.

3.3 A stable, Doxycycline-inducible shRNA system to study Greatwall kinase depletion

GWL has been shown to be essential in HeLa cells (Burgess et al. 2010; Voets & Wolthuis 2010). In mice, heterozygous mutants for functional GWL are viable and fertile but the homozygous knockout GWL mutants are embryonic lethal (Álvarez-Fernández et al. 2013). In the mammalian cell experiments in this paper, GWL appeared to be non-essential for mitotic entry alone (Álvarez-Fernández et al. 2013), but critical for long-term proliferation. Therefore, a conditional depletion approach is necessary for a comprehensive genetic analysis of GWL in in TNBC cells with a view to improve therapeutic knowledge. We decided to employ inducible shRNA expression as our method of choice for conditional depletion. Short hairpin RNA (shRNA) mediated knockdown methods have the advantage of having a lower turnover than siRNA and stably integrating the expression construct into the target genome for long-term expression. The use of a 'Tet-On' shRNA system with Doxycycline (Dox) allows for easy knockdown of GWL that is amenable for experiments that explore the effects of GWL depletion in a well-controlled and permanent manner.

We used a shRNA expression system published by Sigl *et al.* (Sigl et al. 2014). In this lentiviral construct, Green Fluorescent Protein (GFP) is coupled to a doxycycline-regulated transactivator protein (Tet-on) via a T2A ribosome-skipping element (Donnelly et al. 2001). This permitted fluorescence-based cell sorting of the cells with highest levels of Tet-on protein and is also useful for periodically checking that the cells had not rejected or deleted the construct from the genome. The shRNA is expressed from a promoter that is controlled

by a Tetracycline Response Element (TRE). Thus, addition of doxycycline allows expression of the shRNA and induces depletion of the target protein. The GWL shRNA sequence was cloned into this construct by a previous graduate student, Clare Vesely (unpublished results). The vector map can be seen in **Fig. 3.4**.

HEK293T cells were used to assemble the viral components into virus particles encasing the shRNA construct using a lipofectamine based transfection protocol. Wild-type cell lines were infected with the shRNA-containing lentivirus with the help of Polybrene. Full virus assembly and cell transfection protocols are found in Chapter 2 – Materials and Methods. Inclusion of a GFP reporter meant that following cell infection with lentivirus, selection of infected cells was carried out using two rounds of Fluorescence Activated Cell Sorting (FACS) to select and grow the cells expressing the shRNA construct the highest, to ensure the strongest possible GWL knockdown. Alice Shea at Bart's Cancer Institute (BCI) carried out the GFP FACS sorting, and cells were screened for Mycoplasma contamination before culture and use in experiments.

The next step was to test the efficacy of the shRNA-mediated GWL knockdown, as well as the Scr control by immunoblotting. In **Fig. 3.4** panels **B** to **D** show how the levels of GWL protein in MDA-MB-231 cells are decreased after 3 days exposure to 2 μg/mL Dox, and are undetectable by immunoblot after 5 days exposure, and this depletion is maintained after 7 days. **Figs. 3.4B** and **C** show most clearly how the presence of Dox in the Scr-shRNA cells does not affect the GWL protein levels. The decrease in GWL protein level in **Fig. 3.4A** in the

Scr + Dox lane is due to my unequal cell lysate loading, as shown by the corresponding α-Tubulin level. **Fig. 3.5** also shows that the shRNA-mediated knockdown of GWL works well in HS578T cells, the Scr-shRNA also does not affect GWL protein levels, and there is no detectable GWL protein after 7 days of shRNA induction.

To ensure that the shRNA-mediated depletion of GWL was effective and consistent, I used three separate immunoblots using three different cell extracts from each cell line to quantify the effectiveness of the GWL knockdown (**Figure 3.6**). Using the Image Studio Lite software (LI-COR Biosciences), I measured the band intensity of the bands corresponding to the shGWL no Dox lanes and the intensity of the bands corresponding to the shGWL plus Dox lanes. I then normalised these band intensity levels to the intensity of their corresponding α-Tubulin loading control bands. This allowed me to ensure that quantification of the immunoblot signal was linearly related to protein quantity and so was as accurate as possible.

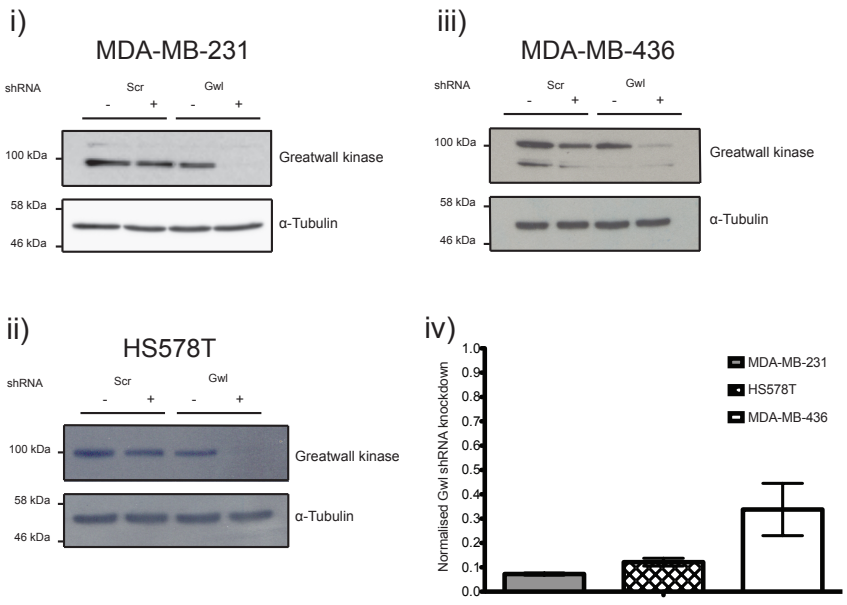

Figure 3.6 Quantifying the efficiency of the shRNA-mediated GWL knockdown in a panel of TNBC cells Panels i) to iii) are representative immunoblots of the indicated cell lines. iv) Quantification of the efficiency of the GWL knockdown. Each GWL + Dox knockdown lane was normalised to the corresponding loading control lane. N=3 biological repeats were used to generate the data. The error bars represent the Standard Error of the Mean (SEM) for each cell line.

3.4 Characterisation of Greatwall kinase depletion in human breast cells

Once it was established that the Doxycycline-inducible shRNA system to deplete GWL was effective, the next step was to look for GWL-loss phenotypes in the TNBC cells. Colony formation assays were used to assess the effect of GWL depletion on cell growth and survival over an extended period of time. Onto a layer of irradiated, senescent feeder cells in a 10 cm cell culture dish, 1000 live cells were plated with or without Dox treatment. After two weeks, with fresh Doxycycline being added every week, the cells were stained with Crystal Violet solution and the dishes photographed, and the number of colonies counted (**Fig 3.7**). I found that the cell lines MDA-MB-231 and HS578T were sensitive to GWL depletion in this context (**Fig. 3.7i)** to **viii**), with the GWL shRNA + Dox plates growing considerably less colonies than the three control plates. The MDA-MB-436 cells did not appear to suffer under this example of GWL depletion, with the GWL shRNA + Dox plate growing just as many colonies as the control plates. To quantify these results more thoroughly in addition to the representative photographs, I counted the number of colonies on each plate for each replicate. I then took the average counts for the Scr shRNA - Dox cell lines and set these averages as 1.0 in order to normalise the counts for the Scr + Dox cell lines and the GWL + Dox cell lines against their corresponding Scr - Dox counterparts (**Fig. 3.7xiii**). Counting the colonies and normalising to Scr - Dox shows that the MDA-MB-231 and HS578T cells are consistently sensitive to GWL loss, and the MDA-MB-436 cells are consistently insensitive to GWL loss, in a colony formation assay setting (**Fig. 3.7xiii**).

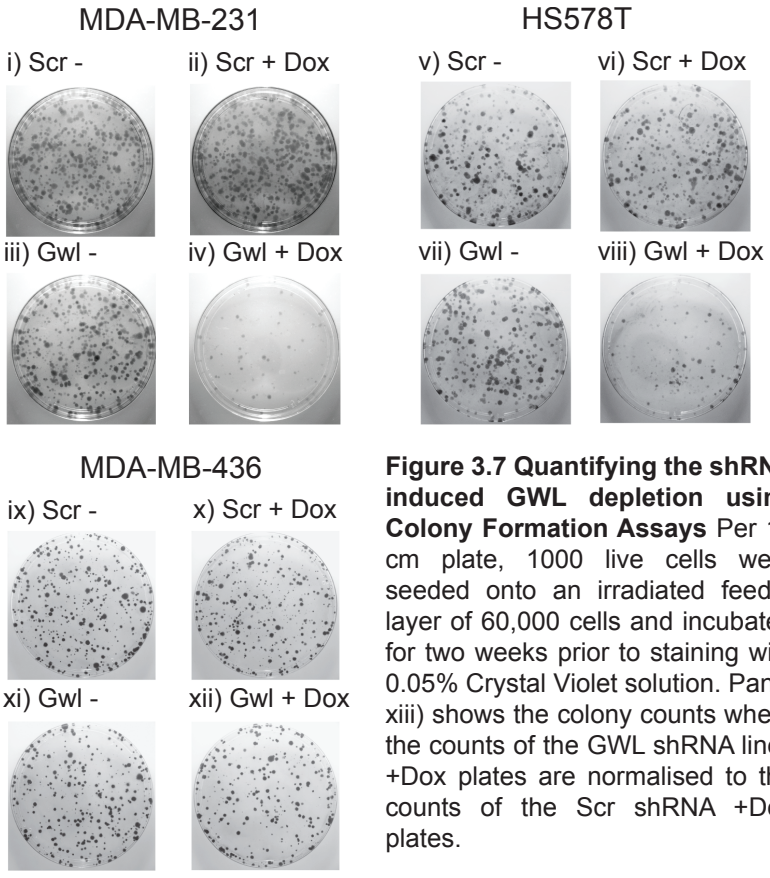

Figure 3.7 Quantifying the shRNA induced GWL depletion using Colony Formation Assays Per 10 cm plate, 1000 live cells were seeded onto an irradiated feeder layer of 60,000 cells and incubated for two weeks prior to staining with 0.05% Crystal Violet solution. Panel xiii) shows the colony counts where the counts of the GWL shRNA lines +Dox plates are normalised to the counts of the Scr shRNA +Dox plates.

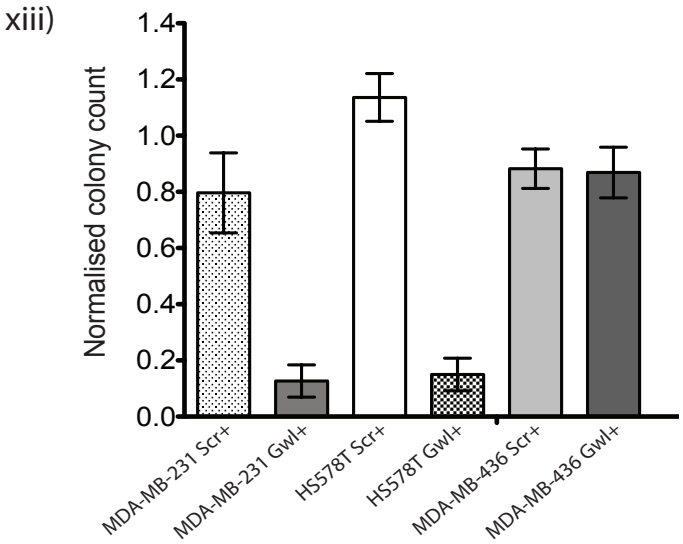

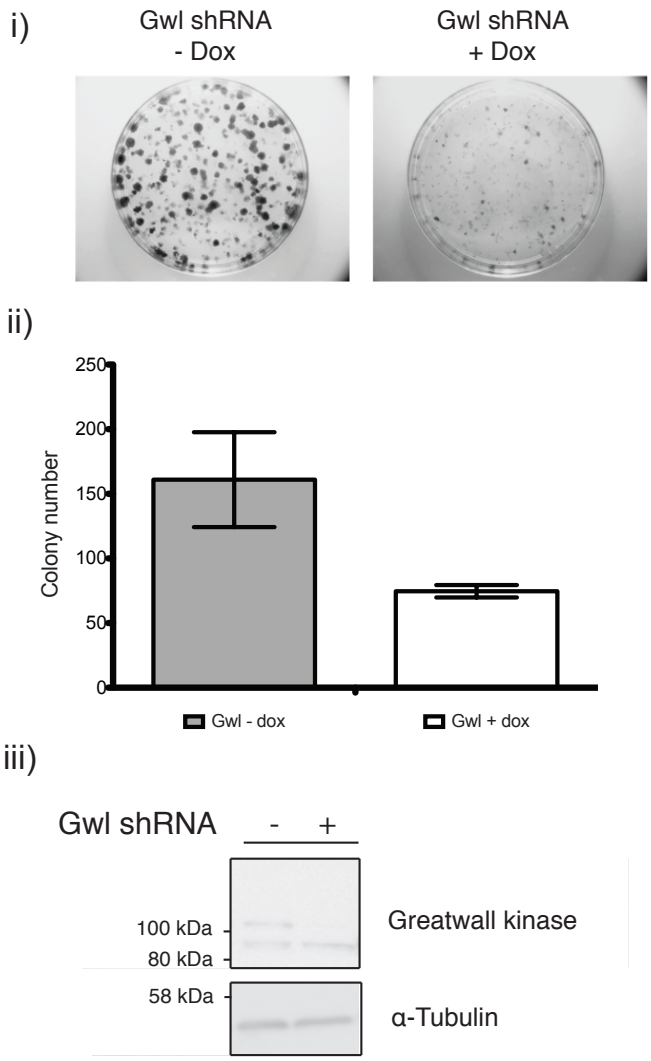

Figure 3.8 Analysing the effect of GWL knockdown on MCF10a cells i) Per 10 cm plate, 1000 live cells were seeded onto an irradiated feeder layer of 60,000 cells and incubated for two weeks prior to staining with 0.05% Crystal Violet solution. ii) Represents the mean counts of N=3 colony formation assay experiments. Error bars are SEM. iii) Representative immunoblot of the MCF10a GWL knockdown

This experiment was also carried out in MCF10a GWL shRNA cells, and the resulting colonies counted (**Fig. 3.8**). The GWL knockdown did have an intermediate effect on the colony growth of the cells, and there is a clear difference between the control and the Dox treated plates. **Fig. 3.8C** shows the knockdown of GWL in MCF10a GWL-shRNA cells after 7 days. The establishment of a Scr-shRNA control for the MCF10a cell line was attempted throughout this project but was unsuccessful and so this control is currently missing.

The next phase of the characterisation of GWL phenotypes in these cell lines was to look at the effect of GWL depletion on mitosis and the cell cycle using live cell microscopy (**Figures 3.9 – 3.11**). Filming live cells enabled me to observe when in the cell cycle the GWL knockdown caused problems, if any, and if so what the consequences of such problems are for these cells. Using the level of GWL knockdown shown in the time course immunoblots in **Figs. 3.4** and **3.5** as a reference, of the cells that were treated with Dox to induce GWL knockdown, these cells received the Dox treatment 48 hours prior to the start of filming. This ensured that GWL was beginning to be knocked down, so that I could see how the cells coped with the loss of GWL during imaging, rather than filming the aftermath, which may have been too late to observe how any phenotypes emerged. **Fig. 3.9A** and **B** show the results of a 50-hour filming period using MDA-MB-231 cells that had not been treated with Dox, and MDA-MB-231 cells that had been treated with Dox, respectively. The control cells in **Fig. 3.9A** consistently divide twice within the filming period with no significant mitotic problems. One triple division was observed, which is a normal feature of

cancerous cells. In the GWL knockdown movie using MDA-MB-231 cells (**Fig. 3.9B**), only two out of the ten cells tracked had daughter cells that divided again during filming. The other cells either did not divide again, or if they attempted mitosis, the mitosis time was longer (as shown by the length of the red bars representing M phase), or the cells showed cytokinesis failure or apoptosis. With the HS578T cells (**Fig. 3.10**), the control cells (**Fig. 3.10A**) more often than not divided only once during filming because most of the traceable cells did not divide until some way into the filming process, meaning that the second division was not able to be recorded. There was one cell that could be tracked early on in the movie whose daughter cells both divided, so like with the MDA-MB-231 cells it is possible for a HS578T cell to divide twice within 50 hours. In contrast, in the + Dox group (**Fig. 3.10B**), half of the cells underwent apoptosis after attempting mitosis. Some cells divided as normal, but there were no second divisions from their daughter cells. The third set of movies, shown in **Fig. 3.11** used the non-cancerous MCF10a cells. In the control movie (**Fig. 3.11A**), the MCF10a cells completed two rounds of mitosis without any significant problems. Most of these cells seemed to manage two divisions quickly, within the first 30 hours of filming, and then did not divide again. When GWL was depleted (**Fig. 3.11B**), just over half the cells seem to be unaffected, whilst the remainder did not undergo a second round of mitosis. Taking this information into account when looking at the colony formation assays, this suggests that in the MCF10a cell line when GWL is knocked down, the reduction in colony number seen could be due to the cells entering a quiescent or senescent state. This is in contrast with the MDA-MB-231 and HS578T cells that also show reduction in colony number after GWL knockdown but exhibited apoptosis during live cell

imaging. The difference could be that in the MCF10a cells, the cells cease dividing after GWL depletion, but in the MDA-MB-231 and HS578T cells, these cells are more likely to experience mitotic difficulties and cell death.

	MDA-MB-231 -Dox	MDA-MB-231 +Dox	HS578T -Dox	HS578T +Dox	MCF10a -Dox	MCF10a +Dox
# Daughter cells that did not divide again, but survived	0	13	18	10	3	9
# Daughter cells that divided again successfully	20	2	2	0	17	11
# Cell deaths & uncompleted divisions	0	3	0	5	0	0

Table 3.2 A count of the number of cells in the live cell imaging (Figures 3.9-3.11) that divided once, successfully divided twice, or underwent cell death

The number of cells that divided, and how often they divided, was counted; along with the number of cells that experienced cell death or failed divisions. This information is in **Table 3.2**. This helps to summarise the events in **Figs 3.9-3.11**, as it is clearer that the reduction in proliferation in the GWL depleted cells is due most of the tracked cells dividing once, and then not dividing again, rather than population depletion by cell deaths. Even with GWL depletion, the

MCF10a cells were more capable of undergoing two rounds of mitosis within the time frame compared to the two breast cancer cell lines. Only a few observed MDA-MB-231 and HS578T cells were seen committing a clear cell death, and cell death did not occur in any of the tracked MCF10a cells. The MDA-MB-231 cells with no GWL knockdown were the most proliferative, whereas the equivalent no Dox HS578T cells in this experiment were less likely to divide twice during filming.

A comparison of the mitotic time lengths between control and GWL depleted cells, and across the different cell lines is shown in **Figure 3.12**. The mitotic time was only recorded for cells that clearly and successfully completed mitosis, including cytokinesis. As a result, there are less data points in the GWL depleted conditions in all three cell lines tested, because there were fewer mitotic events. GWL knockdown caused a slight trend of increasing the length of time cells spent in mitosis, but the wide range in mitotic times and fewer mitotic events in GWL depleted cells makes this feature difficult to evaluate with this data alone. However, **Figure 3.12** suggests that GWL depletion is not always lethal to cells, and it can cause an increase in the mitotic duration.

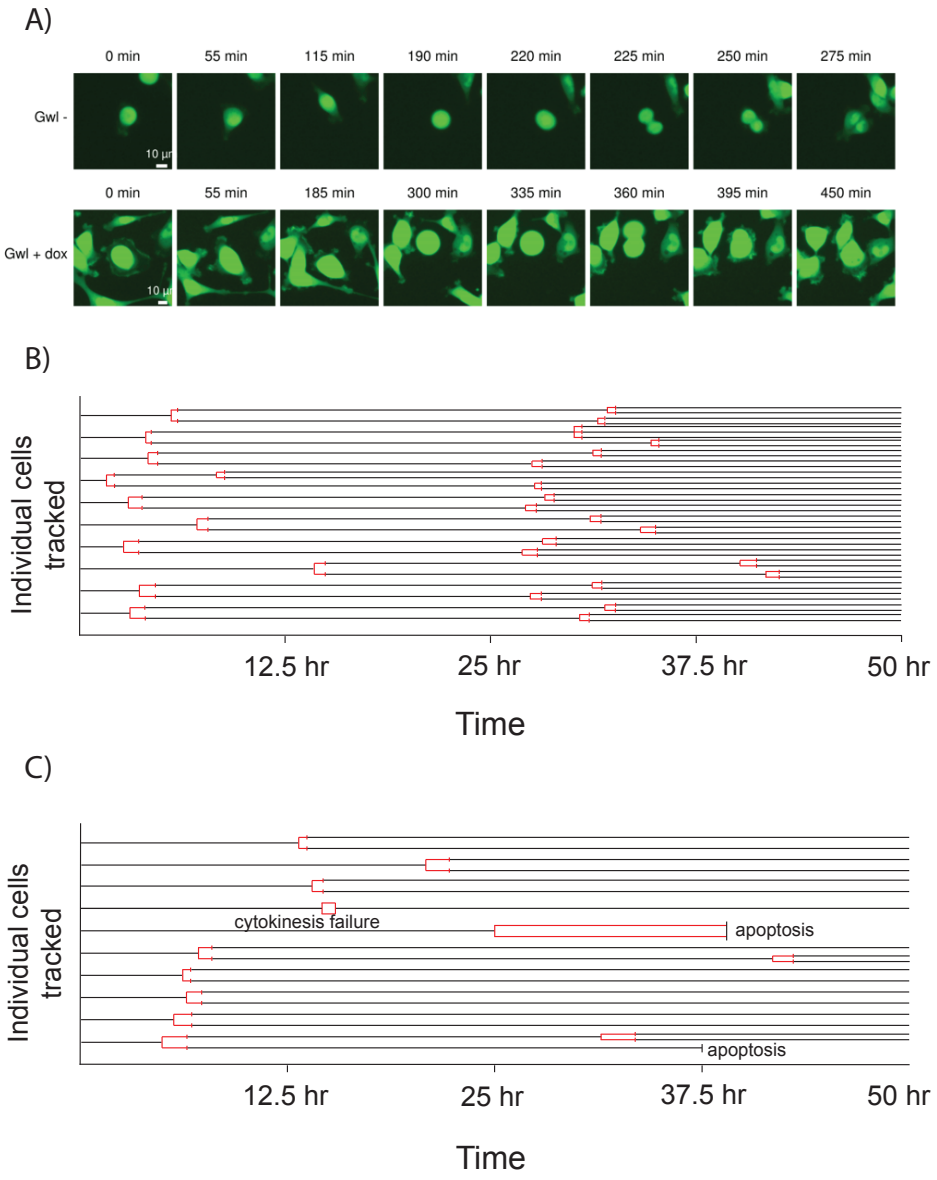

Figure 3.9 Investigating GWL depletion with live cell imaging in MDA-MB-231 cells Cells were plated onto a 2-well imaging chamber 48 hours prior to filming, and Dox added to one well to represent the GWL knockdown treatment. A) Frames of two representative cells undergoing mitosis with 10 µ M scale bar B) No Dox control C) GWL knockdown / plus Dox treatment. The horizontal red lines represent how long the cells stay in a rounded, mitotic state.

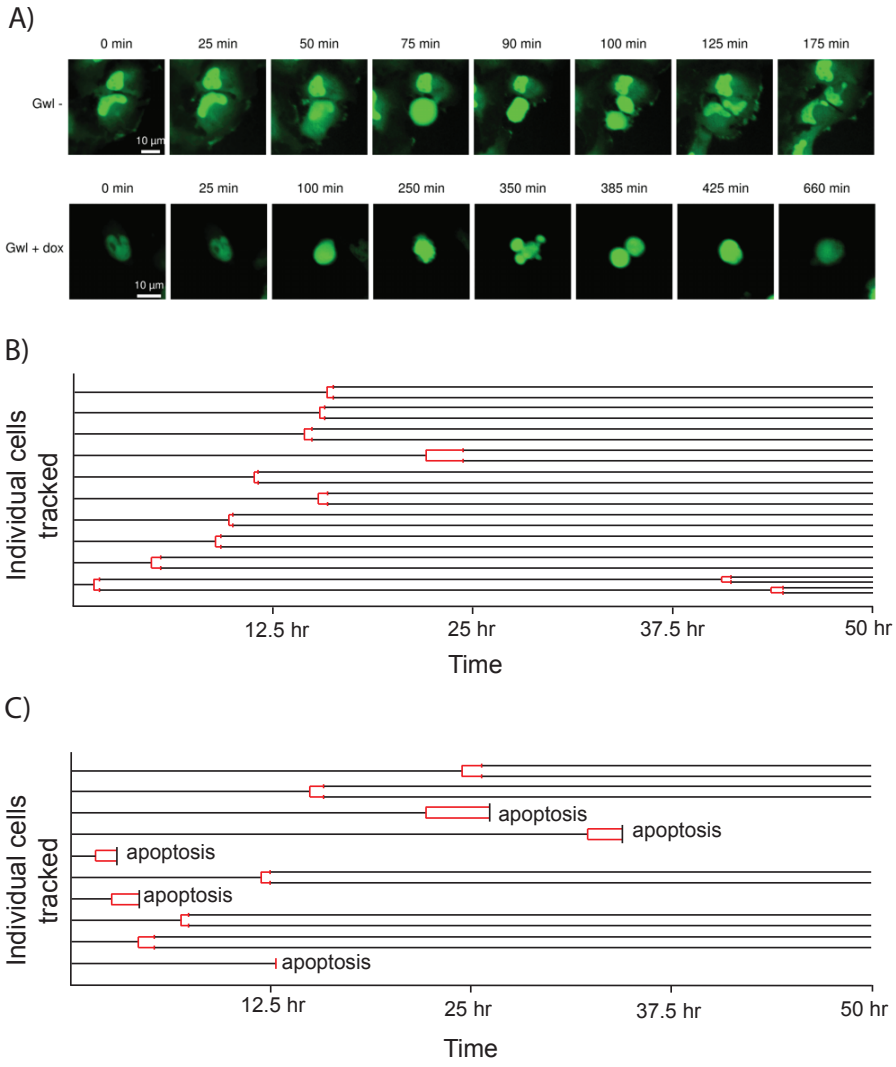

Figure 3.10 Investigating GWL depletion with live cell imaging in HS578T cells Cells were plated onto a 2-well imaging chamber 48 hours prior to filming, and Dox added to one well to represent the GWL knockdown treatment. A) Frames of two representative cells undergoing mitosis with 10 µM scale bar B) No Dox control C) GWL knockdown / plus Dox treatment. The horizontal red lines represent how long the cells stay in a rounded, mitotic state.

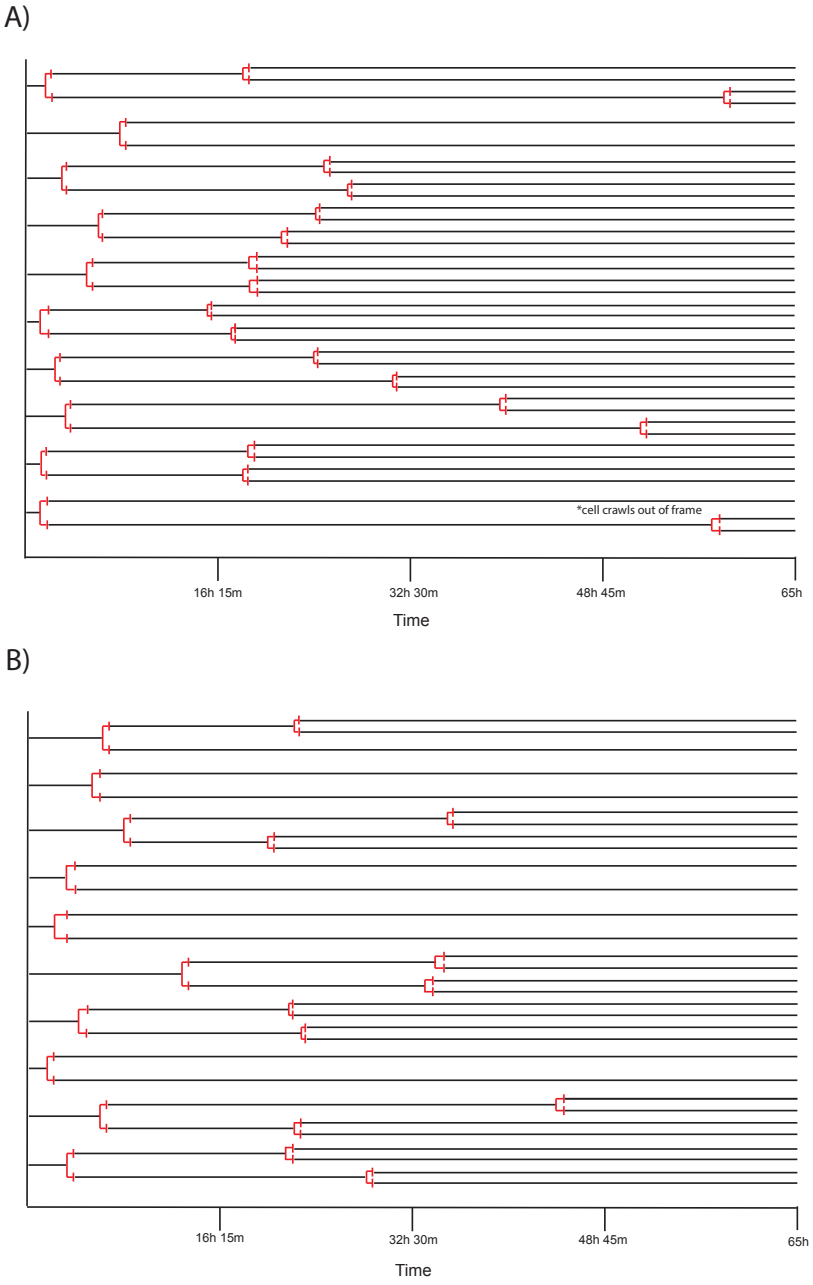

Figure 3.11 Investigating GWL depletion with live cell imaging in MCF10a cells Cells were plated onto a 2-well imaging chamber 48 hours prior to filming, and Dox added to one well to represent the GWL knockdown treatment. A) No Dox control B) GWL knockdown / plus Dox treatment.The horizontal red lines represent how long the cells stay in a rounded, mitotic state.

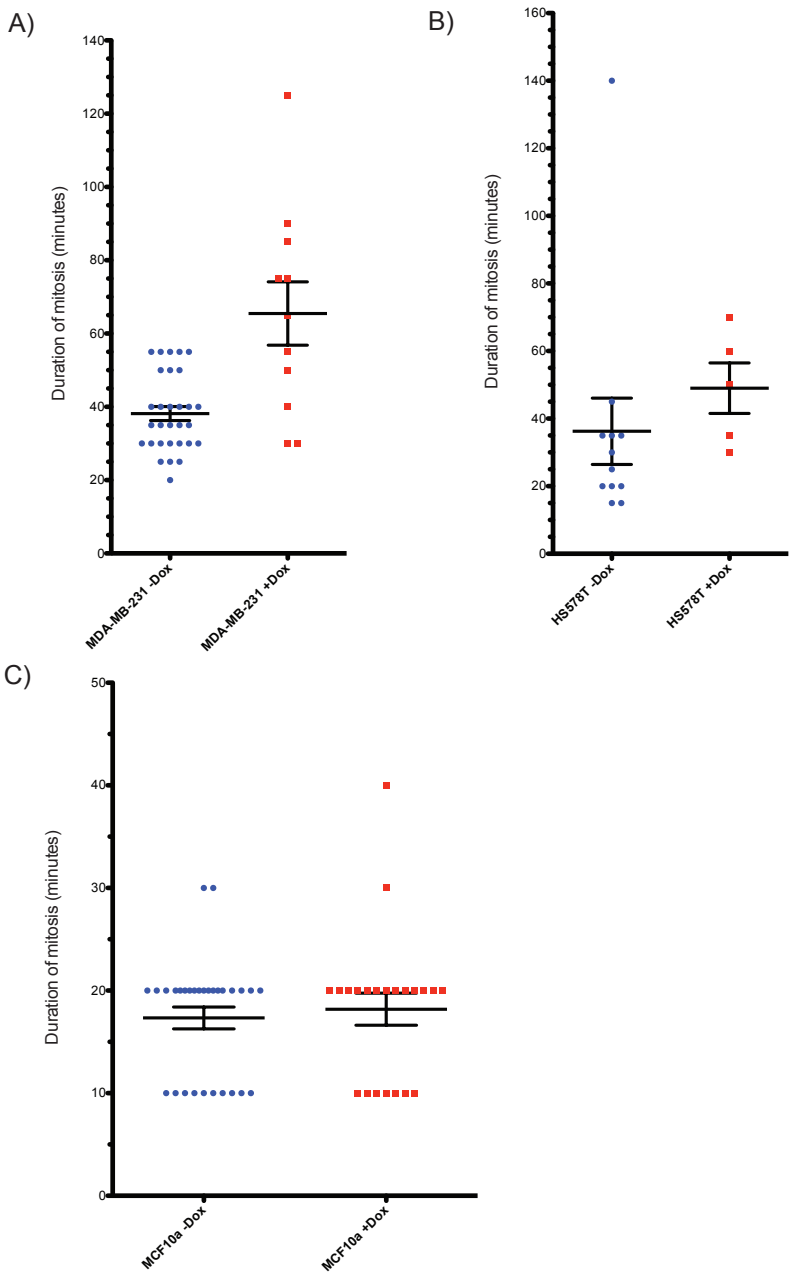

Figure 3.12 Plotting the duration of mitosis from live cell imaging
The length of time spent in a rounded up, mitotic state was recorded for each cell in **Figures 3.9-3.11** that completed mitosis successfully. A) MDA-MB-231 cells, with and without Dox B) HS578T cells, with and without Dox C) MCF10a cells, with and without Dox. Not every cell successfully completed mitosis, and there are less data points for +Dox experiments, because cells with depleted GWL divided less frequently.

To investigate how GWL depletion was affecting the cell cycle, I set up a series of fixed cell immunofluorescence (IF) experiments and analysed the images with ScanR software. Microscope slides were prepared after 3 days of Dox treatment, and further slides were made for each subsequent day to document the progressive effect of the GWL knockdown up to day 7 as well as a no Dox treatment control. Prior to cell fixing, I pulse labelled the cells with the modified nucleotide EdU followed by counter staining with an anti-CENPF antibody and DAPI nuclear stain. More details on this protocol are included in Chapter 2 – Materials and Methods. I imaged the slides on an Olympus IX-73 microscope with a 40x objective and used Micro-Manager software to instruct the computer and microscope to capture images in a 5 x 5 grid shape (25 images in total). This meant that 25 images containing thousands of cells in total could be analysed quickly and precisely with the ScanR software. The ScanR analysis was able to classify cells into cell cycle phases once appropriate detection thresholds were set.

If a cell was EdU positive it was in S phase, if it was CENPF positive it was in G2/M phase (Bomont et al. 2005; Loftus et al. 2017), and cells that were negative for both of these markers were in G1 phase. M phase is included as ‘G2/M’ in the analysis as CENPF is not degraded until late mitosis, mitotic cells represent only about 5% of a cell culture population, and many mitotic cells are washed off during the fixing process due to their rounding up. There were 2 biological replicates for this experiment but there should be reliability to the data due to the large number of cells counted. **Fig. 3.13** shows the data for this experiment using MDA-MB-231 cells. As the GWL protein begins to be knocked

down from Day 3 and as this depletion continues, the population of G1 phase cells increases and the S- and G2- phase populations decrease. This is most noticeable at Days 6 and 7 of Dox treatment. This data suggests that GWL knockdown causes prolonged G1 phase, rather than the expected increase in the G2/M population. This is curious, as current literature suggests that the most likely consequence of GWL depletion in human cells is G2 arrest (Burgess et al. 2010). I also chose to analyse the mean nuclear size and intensity of EdU staining after noticing that cells that had experienced GWL knockdown were often increased in size, and that in the EdU positive cells, the EdU staining itself seemed to be less bright. ScanR analyses was set up to measure nuclear size from the area of DAPI staining, and the average intensity of EdU staining per microscopy image. From the raw data I normalised each day of Dox treatment to the no treatment control. The graphs in **Fig. 3.13B** and **C** show the results of these analyses. **Fig. 3.13B** shows the results of the mean nuclear size analysis, and as GWL is depleted, the mean nuclear size increases. **Fig. 3.13C** shows that as GWL is depleted, the mean EdU staining intensity decreases in the remaining EdU positive population. Thus, in addition to a reduction in EdU positive/S phase cells in GWL depleted cells (**Fig. 3.13A**), the incorporation rate of EdU is dramatically reduced in the remaining S phase population. This suggests that the uptake of the EdU nucleotide, and thus DNA synthesis, might be happening at a slower or reduced rate compared to the control cells.

As an additional check to see if GWL knockdown was affecting entry into the cell cycle and the rate of cell proliferation, in MDA-MB-231 and HS578T shGWL cells I depleted GWL with Dox for 7 days before EdU pulse labelling, cell fixing

and processing. I then counted the total nuclei per image as well as the number of EdU positive cells with the aid of the ImageJ Cell Counter plugin to reduce human error. At least 200 cells were counted under each condition, and three biological replicates were made. The results from these experiments are shown in **Fig. 3.14**. In both the MDA-MB-231 and HS578T cells, a reduction in the EdU positive populations were seen after 7 days of GWL knockdown. To analyse the difference between the control cells and the cells treated with Dox, I carried out an unpaired t-test using GraphPad Prism software. Both MDA-MB-231 and HS578T cells showed significant differences in the S phase population, but this difference was greater in the MDA-MB-231 cells (**Fig. 3.14C** and **D**).

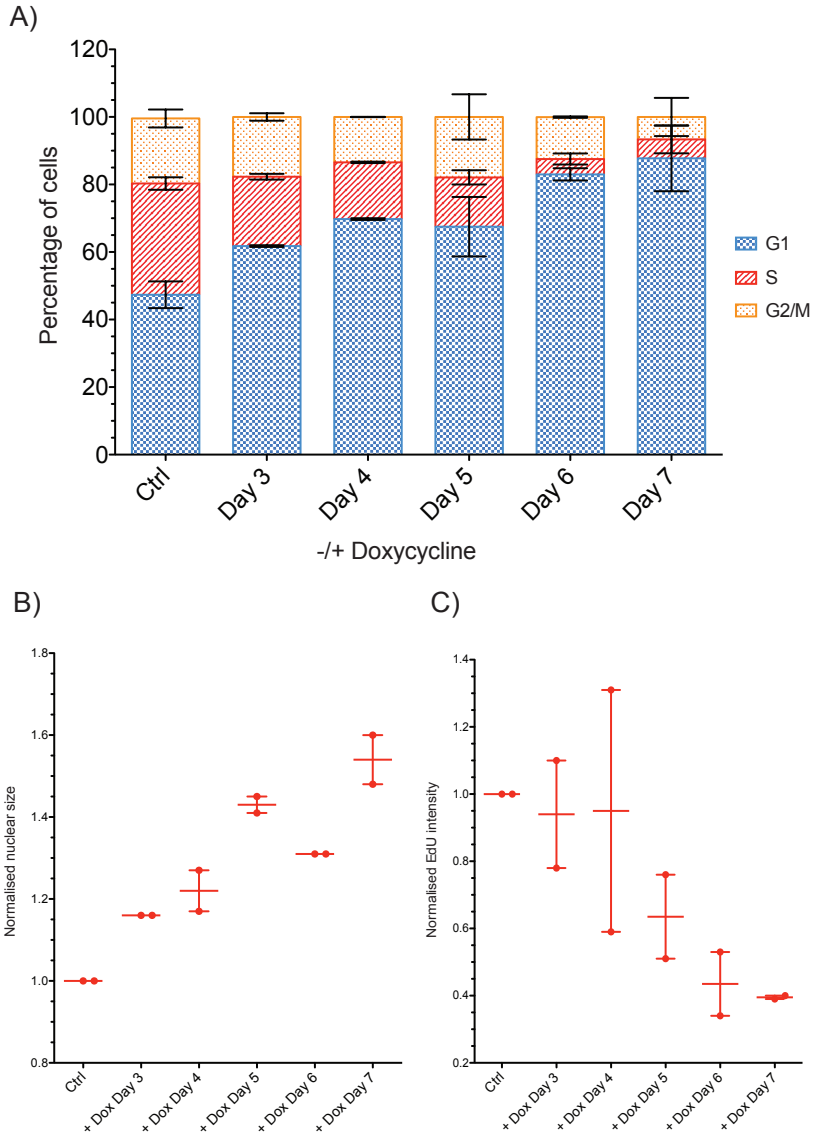

Figure 3.13 Using IF and ScanR analysis software to analyse effect of GWL depletion on cell cycle phase populations in MDA-MB-231 cells A) Using EdU as the S-phase marker and CENPF as the G2/M marker, cells were classified into cell cycle phases. B) Nuclear size determined by size of DAPI stain and normalised to the no treatment control. C) Mean EdU intensity normalised to the no treatment control. N=2 biological replicates.

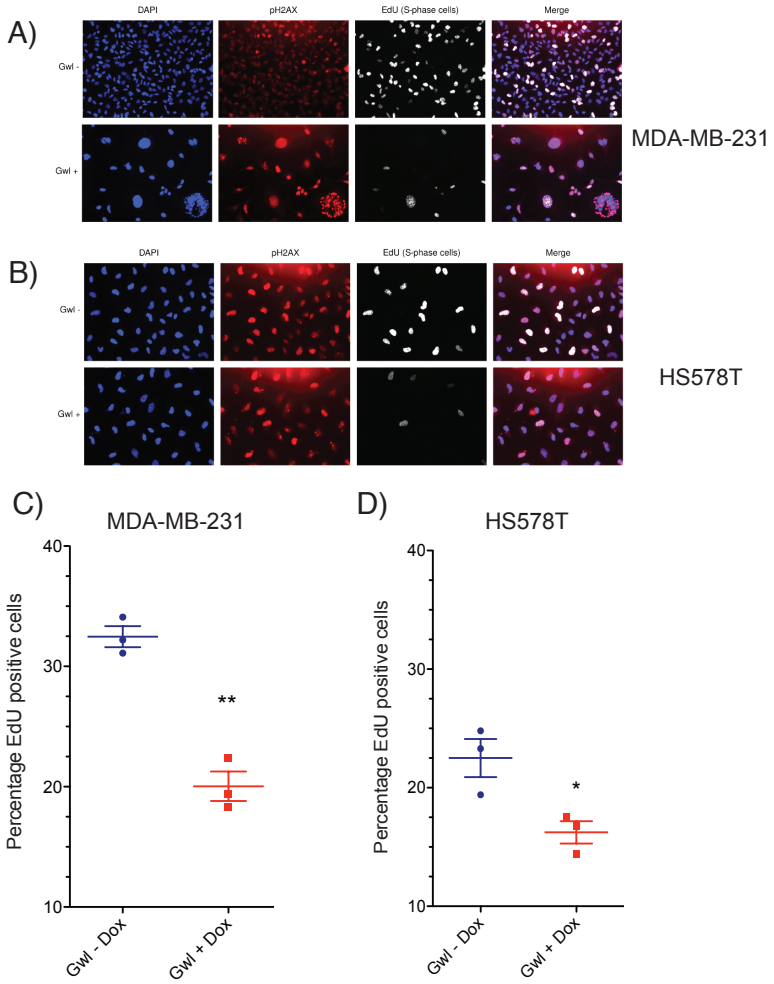

Figure 3.14 Analysing effect of GWL knockdown on S-phase population with fixed cell IF Cells were treated for 7 days with or without Dox and treated with 10μM EdU for 20 minutes prior to fixation with 3.7% paraformaldehyde. Fixed cells were stained for S-Phase cells with Click-iT® EdU Alexa Fluor® 647 kit, pH2AX (red) and DAPI (blue). A) Representative image of MDA-MB-231 cells 20x magnification B) Representative image of HS578T cells 20x magnification. C) Swarm plot of the EdU positive cells counted in MDA-MB-231 cells. D) Swarm plot of the EdU positive cells counted in HS578T cells. Unpaired t-test used to analyse the size of the difference in EdU positive cells in C) and D). In all samples >200 cells per biological replicate were counted. N=3

3.5 Conclusions and discussion

Here I tested a stable, Dox-inducible shRNA system to knock down GWL. This system allowed me to look for potential phenotypes of GWL depletion in a way that was simple to control and was effective over the course of a week (or longer with the addition of fresh Dox to the cell culture media).

I found that there are differences in GWL sensitivity between some different TNBC cell lines tested in the context of colony formation assays, live and fixed cell microscopy. The MDA-MB-231 and HS578T cells are highly sensitive to GWL loss, and in contrast the MDA-MB-436 cells are not sensitive to GWL loss. The non-cancerous breast epithelial cell line MCF10a also showed sensitivity to GWL knockdown. Previous work using cancer cell lines support this work, with evidence of GWL knockdown causing mitotic problems, cell cycle arrest and cell death (Burgess et al. 2010; Voets & Wolthuis 2010). The observation that the MDA-MB-231 cells are highly sensitive to GWL loss has also been recorded by (Álvarez-Fernández, Sanz-Flores, Sanz-Castillo, Salazar-Roa, Partida, Zapatero-Solana, Ali, Manchado, Lowe, VanArsdale, Shields, Caldas, Quintela-Fandino & Malumbres 2018b). Since GWL appears to have an important role in suppressing PP2A activity to ensure a timely completion of mitosis, it is not too surprising that GWL knockdown has deleterious effects on the non-cancerous cell line MCF10a. Though it remains to be elucidated under which contexts GWL is most important, as the urgency of GWL necessity may vary depending on developmental stage and cell type. In the live cell imaging however, this revealed that whilst the MDA-MB-231 and HS578T cells could either commit

apoptosis or stop dividing, the MCF10a cells did not show a similar response to acute GWL depletion.

In the siRNA GWL screen assessing cell viability when GWL is knocked down, **Fig. 3.2B** flags the TNBC cell line MDA-MB-231 as not sensitive to GWL depletion (Z-score 0.699). Based on the work in this chapter, as well this study showing that MDA-MB-231 cells show sensitivity to GWL loss (Álvarez-Fernández, Sanz-Flores, Sanz-Castillo, Salazar-Roa, Partida, Zapatero-Solana, Ali, Manchado, Lowe, VanArsdale, Shields, Caldas, Quintela-Fandino & Malumbres 2018b), then it is more plausible that the siRNA screen has some false positives and negatives and so the results should be interpreted with caution.

The most surprising finding of the work presented here is that the main effect of GWL depletion in MDA-MB-231 and HS578T cells appears to be on the G1 population. This is not the first reporting of a non-mitotic role in the GWL pathway. A recent study found that knocking down one of the downstream substrates of GWL, α-endosulfine (ENSA), caused a lengthening of S phase and reduced the density of replication forks in HeLa and U2OS cells (Charrasse et al. 2017). This phenotype was also seen when GWL was knocked down and was associated with a decrease in Treslin protein levels. Treslin helps to regulate DNA replication initiation via its interaction with TOPBP1 by participating in CDK2-mediated loading of CDC45L onto replication origins. The authors also found increased time spent in S phase was also rescued by

overexpression of Treslin when ENSA was knocked down and also that ENSA was located in the nucleus during S phase (Charrasse et al. 2017).

However, there are caveats to the work done in this chapter. In these experiments only one shRNA sequence was used, which means that any resulting cell phenotypes following shRNA induction could be as a result of off-target effects. Though in **Chapter 5**, an inducible CRISPR-GWL MDA-MB-231 cell line was tested. The results obtained from this cell line are in agreement with the results obtained from the shRNA-GWL MDA-MB-231 cell line. The relative lack of efficacy of the MDA-MB-436 shGWL knockdown in comparison to the high effectiveness of that seen in the MDA-MB-231 and HS578T cells is concerning (**Fig. 3.7**). Perhaps GWL has a powerful kinase activity that means that only a few GWL molecules are enough to inhibit PP2A effectively in a cell. This chapter also lacks analysis with a Scr-shRNA MCF10a cell line, however another study found that both knockdown and knockout of GWL in MCF10a cells also impaired their proliferation (Álvarez-Fernández, Sanz-Flores, Sanz-Castillo, Salazar-Roa, Partida, Zapatero-Solana, Ali, Manchado, Lowe, VanArsdale, Shields, Caldas, Quintela-Fandino & Malumbres 2018b). Another study reported in their experiments that the MCF10a cell line was less sensitive to GWL depletion to the breast cancer cell lines tested according to levels of cleaved PARP, cell viability assay and cell cycle analysis (Yoon, Choe, Jung, Hwang, Oh & J.-S. Kim 2018b).

A study that used a hyperactive version of GWL (the K72M mutant) has shown to encourage transforming behaviours such as overcoming cell-cell contact

inhibition and anchorage-independent growth (Vera et al. 2015) so it is not unreasonable to think that GWL knockdown has an anti-tumourigenic effect. To investigate further the difference in the S phase population and in EdU nucleotide uptake when GWL is knocked down it would be useful as a next step to analyse replication fork speed with DNA fibre assays and length of S phase with FACS analysis following thymidine release as per the experiments in (Charrasse et al. 2017).

Taken together, the data presented here indicate that GWL may have a more significant role in cell cycle control than we currently understand. The effect GWL knockdown has on the G1 and S phases in these experiments hints at a non-mitotic function of GWL, which has been suggested previously in the context of the S phase (Charrasse et al. 2017) and warrants further investigation.

Chapter 4. Using a siRNA and drug library to screen for synthetic lethality candidates in MDA-MB-231 Greatwall shRNA cells

4.1 Introduction

The observations described in the previous chapter raise the possibility that GWL depleted cancer cells display reduced proliferation rates not because of mitotic effects, but due to problems in S-phase. As previously discussed, these could be secondary effects, such as chromosome mis-segregation causing aneuploidy and cell stress. However, they could also reflect roles for GWL outside its canonical function as a mitotic kinase. Indeed, while work on this thesis was in progress, the Castro lab published a study suggesting that GWL dependent inhibition of PP2A-B55 could be important for S-phase progression via the stabilisation of Treslin (Charrasse et al. 2017). Treslin helps to regulate the initiation of DNA replication by promoting the pre-replication complex (pre-RC) to the pre-initiation complex (pre-IC) by binding with Topoisomerase Binding Protein 1 (TOPBP1) in a CDK2-dependent process, and the presence of this complex is essential for loading of Cdc45L onto replication origins (Kumagai et al. 2010). This new information combined with the discovery that GWL may have a role in regulating the AKT pathway (Vera et al. 2015) suggests that looking for non-mitotic roles of GWL can prove productive.

We decided to follow up the questions raised from Chapter 3 genetically and investigate synthetic lethal and synthetic resistant interactions of the kinase using both a siRNA depletion screen, and a small molecule drug screen. When

a synthetic lethal interaction exists between two genes, this means that the perturbation of either of these two particular genes individually is viable for the cell, but the disruption of both genes simultaneously causes loss of viability (Nagel et al. 2016; Beijersbergen et al. 2017). This is different to the idea of 'oncogene addiction', in which a cancer cell is dependent on a particular oncogene or oncogenic pathway for survival, such as the RAS pathway (Weinstein 2002; S. V. Sharma & Settleman 2007). A summary of synthetic lethality and oncogene addiction can be seen in **Figure 4.1**.

The class of drugs known as poly(ADP-ribose) polymerase (PARP) inhibitors are the first clinically approved drugs to be designed with synthetic lethality in mind (Lord & Ashworth 2017). Individuals with an inherited mutation in either the BRCA1 or BRCA2 gene are at a higher than average risk of developing breast or ovarian cancer (Miki et al. 1994; Wooster et al. 1995). Since the BRCA1 and BRCA2 proteins are required for homologous recombination during DNA repair and so are tumour suppressors, a loss of a functional copy increases the risk of genetic instability, a feature which is central to the development of all cancers (Venkitaraman 2002). It was found that BRCA1 and BRCA2 defective tumours are sensitive to PARP inhibitors, both in tumour models *in vivo* and in the clinic (Farmer et al. 2005; Evers et al. 2010; Rottenberg et al. 2008; Fong, P.C. et al. 2009) and to date three different PARP inhibitors have now been approved for the treatment of patients with BRCA-mutant ovarian cancer, and one for those with BRCA-mutant breast cancer. In addition, these agents have also shown promising results in patients with BRCA-mutant prostate cancer (Ashworth & Lord 2018). Overall,

the PARP-BRCA interaction provides the first example of a successful synthetic lethal approach that has reached the clinic.

Technologies such as high-throughput siRNA and CRISPR-Cas9 screening which allow large-scale screening directly in human cell culture, as well as bioinformatics predictions in theory should speed up the search for cancer-specific pathway alterations (Ashworth & Lord 2018). Such methods have identified many potential therapeutic targets but have also highlighted just how complex cancer cell signalling is, as cells in a tumour are heterogeneous in nature and exist in a complex microenvironment (O'Neil et al. 2017). Therefore, synthetic lethality candidates should be experimentally verified. This chapter will describe the results of the siRNA and drug screens that we carried out, thanks to our collaborator, Chris Lord at the Institute of Cancer Research (ICR).

A total of 63 drugs were screened for synthetic sensitivity and resistance with GWL. MDA-MB-231 shScr and shGWL cells were treated either with 2 μg/mL DMSO vehicle control or with 2 μg/mL Dox for 72 hours to induce shRNA, followed by 24 hours drug treatment, and then the cell viability was assessed via MTT assay. A spreadsheet showing the raw data from this screen, including the drug names and concentrations used, is listed in **Appendix 1**. The majority of the analysis was carried out on the siRNA screen by the Lord laboratory, and so this will be the focus of this chapter. The siRNA screen is described in more detail in **Section 4.2**.

Having a two-pronged approach as we have done here, screening for synthetic lethality candidates with both siRNA and a small molecule drug screen, means that more confidence can be had in hits that appear in both screening methods.

The sequential chapter will explore the experimental validation of one of the most convincing synthetic lethality candidates from the screens – CDK4/6.

4.2 siRNA screen hits that exhibit synthetic sensitivity with Greatwall kinase depletion

If the siRNA screen results are interpreted with caution and with experimental validation of the most interesting candidates, a synthetic lethality screen could provide us with much information on the cellular pathways that are affected by the loss of GWL that could be exploited therapeutically. We carried out an siRNA screen with MDA-MB-231 shScr and shGWL cells as shRNA control and to deplete GWL, respectively, against a siRNA library of 1535 proteins enriched for cancer-associated genes. To induce shRNA, 2 µg/mL Dox was added. In the wells where shRNA was not induced, cells were treated with 2 µg/mL DMSO vehicle control instead. The cells were treated with Dox (or DMSO) for 72 hours before addition of siRNA. siRNA induction was allowed for a further 48 hours, then cell viability was assessed via MTT assay. The results of the siRNA screen with GWL and Scr shRNA induction, shown as two technical repeats, can be seen in **Figure 4.2**. The viability of the GWL shRNA cells according to absorbance of MTT assay are on the y-axis, and the viability of the control Scr shRNA cells are on the x-axis of the graph. The closer a data point is to the bottom right corner of the graph, it means that the siRNA being tested had a greater, more adverse effect on the shGWL cell viability compared to the cells in which GWL was not also depleted. In both **Fig 4.2 A)** and **B)**, the red dot in each plot represents the siRNA against CDK4.

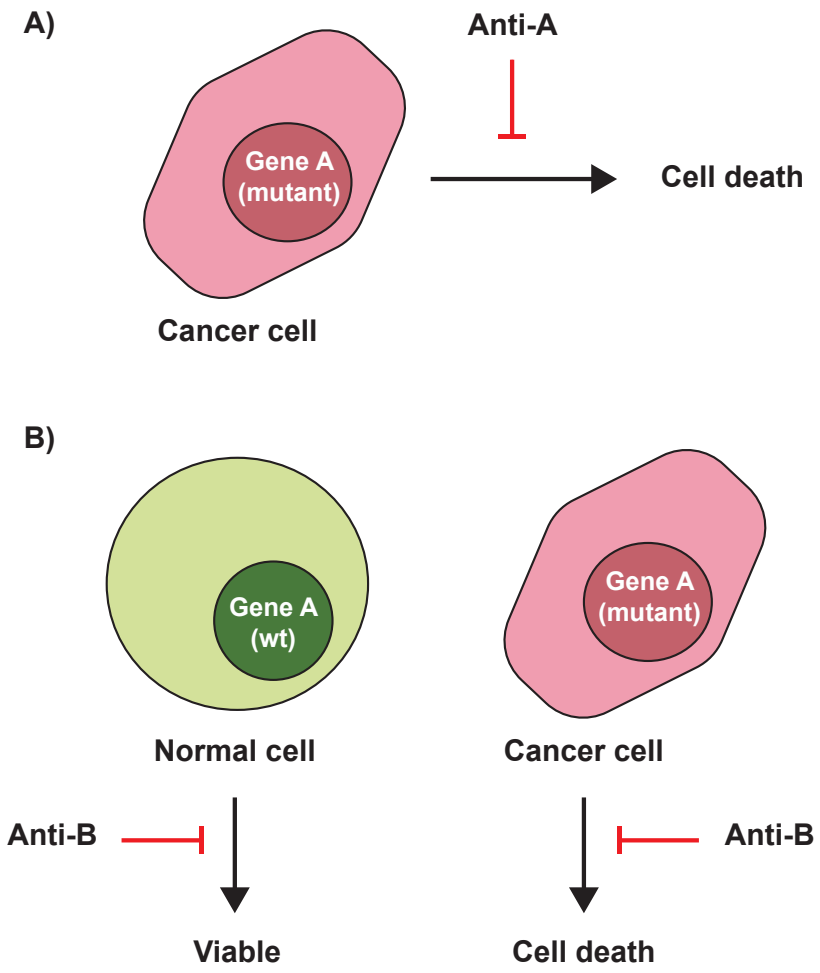

Figure 4.1 The difference between oncogene addiction and synthetic lethality A) Oncogene addiction. Cancer cells that have an activating mutation in Gene A can become addicted to the proliferative signal encoded by this gene and so can be hypersensitive to treatments that inhibit the pathway activated by Gene A. B) Synthetic lethality. If Genes A and B are synthetic lethal, then this means that the inactivation of Gene B will be lethal to cancer cells with a mutation in Gene A but not to normal cells with a wild-type Gene A. Adapted from Beijersbergen et al. 2017.

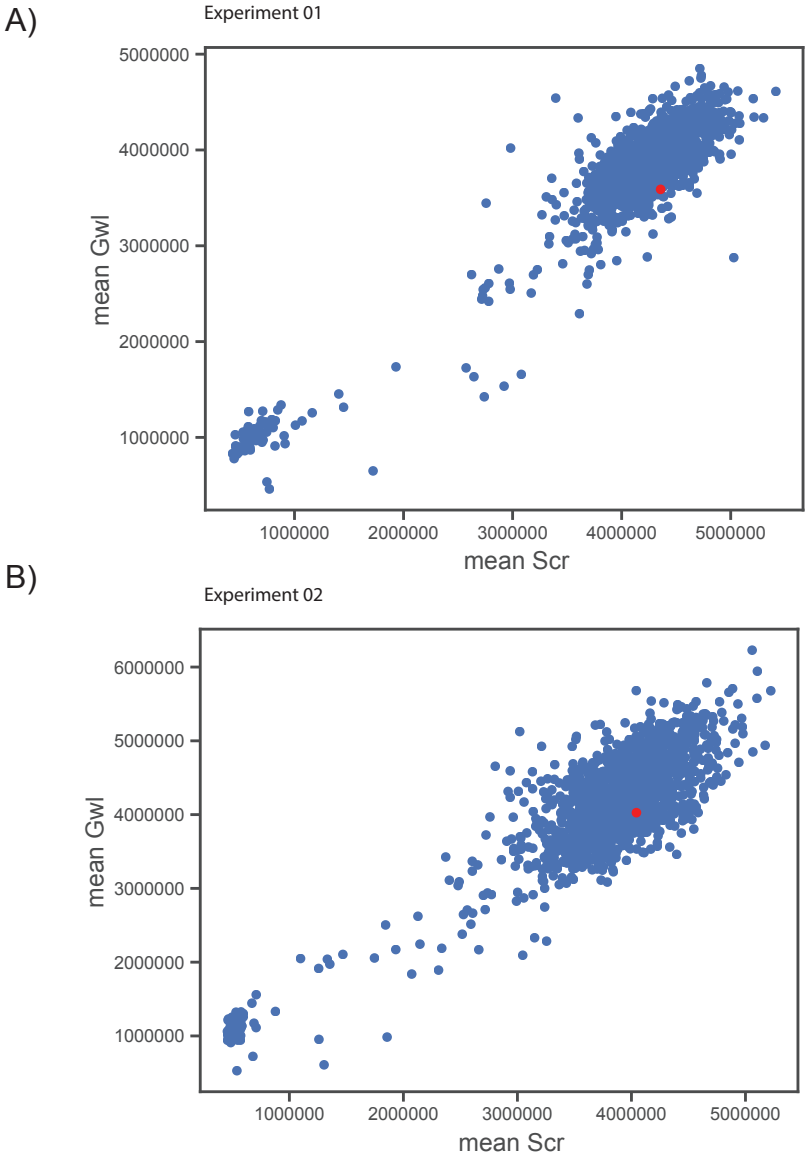

Figure 4.2 Results from two independent siRNA screens using MDA-MB-231 shScr and shGWL cells A) and B) represent two biological replicates of the screen. The viability of the GWL shRNA cells are on the y-axis, and the viability of the Scr shRNA cells are on the x-axis. Data points that are over to the bottom right quarter of the graph means that the siRNA had a more adverse effect on the shGWLcells compared to the control. The red dot in each plot represents the siRNA against CDK4.

Conversely, this also means that data points towards the top left corner of the graph means that a synthetic resistant effect was produced between the corresponding siRNA and GWL depletion.

The data from the siRNA screen was also analysed by dividing the results into pools of either ‘synthetic resistant’ or ‘synthetic sensitive’ hits and plotting their corresponding Drug Effect scores. The Drug Effect is a statistical analysis of the data that does not evaluate how large the effect is, but rather how confident one can be that the observed effect is real. Drug Effect corrected is the Drug Effect of the shScr cell line subtracted from the shGWL cell line to get the net effect of GWL knockdown compared to the control. So, the larger the corrected Drug Effect, the more confidence in the effect there can be. The synthetic sensitive hits and their corresponding Drug Effect scores are plotted in **Figure 4.3**, and a table showing the protein functions of these synthetic sensitive hits is shown in **Table 4.1**. As shown in **Table 4.1**, the majority of the genes that show synthetic sensitivity with GWL are involved in DNA replication or repair, cell cycle control and proliferative signalling pathways including CDK4. The siCDK4 may not be the most lethal siRNA to use in combination with GWL depletion, but this result was consistent across the two replicates and was not very toxic to the control shScr cells (**Fig. 4.2**). It must also be noted that some negative control siRNA oligonucleotides appeared as synthetic sensitive hits in **Fig. 4.3**. This is why the results cannot be taken at face value and must be evaluated with further experiments.

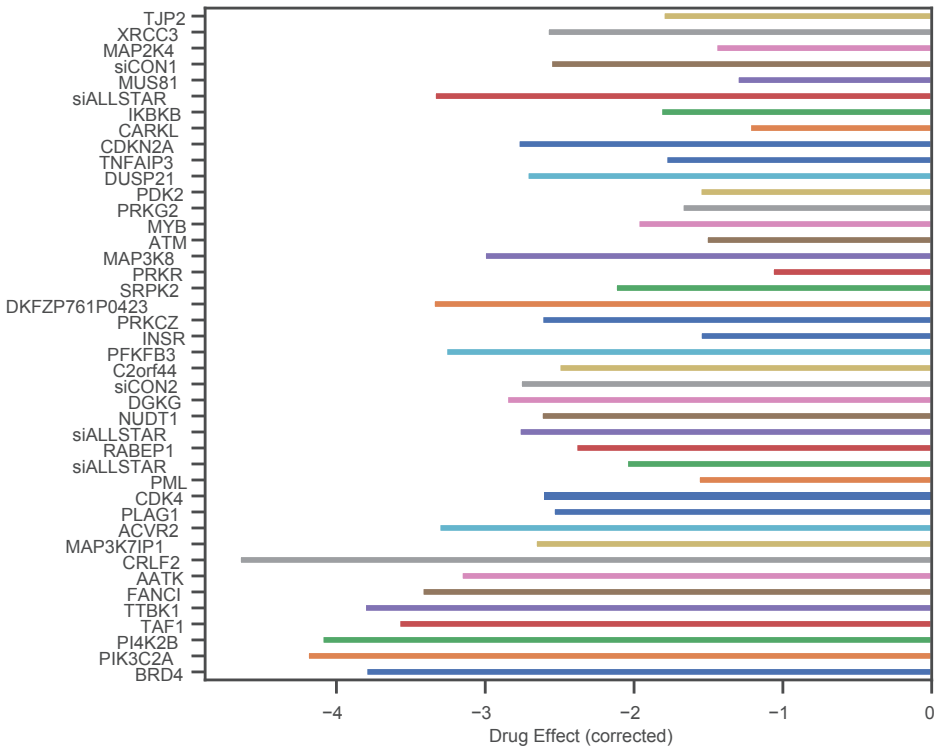

Figure 4.3 Synthetic sensitive hits with GWL found in the siRNA screen Drug Effect is a statistical analysis of the data that does not evaluate how large the effect is, but rather how confident one can be that the observed effect is real. Drug Effect corrected is the Drug Effect of the shScr cell line subtracted from the shGWL cell line to get the net effect of GWL knockdown compared to the control. So the more negative the corrected Drug Effect, the more confidence in the effect there can be.

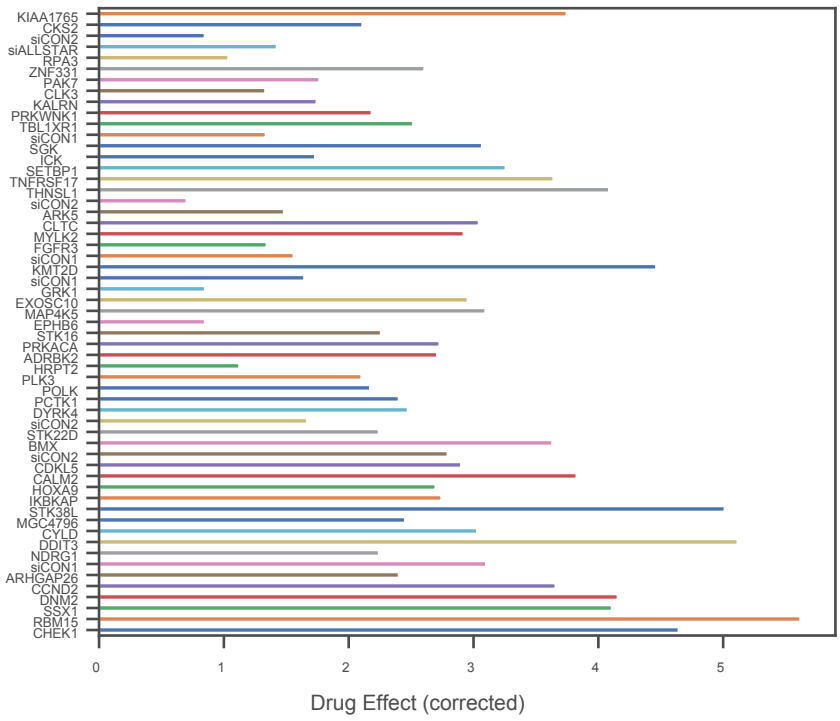

Figure 4.4 Synthetic resistant hits with GWL found in the siRNA screen This data is plotted in the manner shown in Fig. 4.3, but with the hits that produced a survival effect. The Drug Effect is a statistical analysis of the data that does not evaluate how large the effect is, but rather how confident one can be that the observed effect is real. Drug Effect corrected is the Drug Effect of the shScr cell line subtracted from the shGWL cell line to get the net effect of GWL knockdown compared to the control. So the larger the corrected Drug Effect, the more confidence in the effect there can be.

4.3 siRNA screen hits that exhibit synthetic resistance with Greatwall kinase depletion

In the same format as the synthetic sensitive results above, the synthetic resistant hits were also analysed. These genes, when simultaneously knocked down with GWL, exhibited an increase in cell viability compared to the Scr shRNA cells. The synthetic resistant hits and their corresponding Drug Effect scores are plotted in **Figure 4.4**, and a table showing the protein functions of these synthetic sensitive hits is shown in **Table 4.2**. Mirroring the results shown in **Table 4.1**, the majority of the genes that show synthetic resistance with GWL are also involved in DNA replication or repair, cell cycle control and proliferative signalling pathways (**Table 4.2**). Interestingly, the G1/S checkpoint protein CHEK1 is flagged as a synthetic resistant siRNA hit (**Fig. 4.4 and Table 4.2**). This makes sense, because if a cell with depleted GWL suffers DNA damage and chromosomal instability from a mismanaged mitosis caused by unrestricted PP2A-B55 phosphatase activity, then a simultaneous absence of CHEK1 could help push these cells through the DNA damage checkpoint during the subsequent G1/S phase.

Gene Name	Protein Name	Function	
XRCC3	DNA Repair Protein XRCC3	Homologous recombination repair	DNA repair, gene expression, nuclear localisation
MUS81	Crossover junction endonuclease MUS81	DNA repair, HR, meiosis	
MYB	MYB Proto-Oncogene, Transcription Factor	Transcription regulator; oncogene	
NUDT1	Nudix Hydrolase 1	Preventing incorporation of oxidized nucleoside triphosphates into DNA/RNA	
PML	Promyelocytic leukemia protein	Formation of PML nuclear bodies; tumour suppressor	
PLAG1	Pleiomorphic Adenoma Gene 1 Zinc Finger	Transcription factor; overexpression increases cell proliferation	
FANCI	Fanconi Anemia Complementation Group I	DNA repair	
TAF1	TATA-Box Binding Protein Associated Factor 1	Part of a transcription factor complex	
BRD4	Bromodomain Containing 4	Associates with acetylated chromatin; provides epigenetic memory for postmitotic G1 gene transcription	
TJP2	Tight Junction Protein 2	Tight junctions	Cytoskeleton, cell motility, intracellular transport
DKFZP761P0423	PEAK1 related, kinase-activating pseudokinase 1	Cell migration, motility and shape regulation	
RABEP1	Rab GTPase-binding effector protein 1	Endocytic membrane fusion; membrane trafficking of recycling endosomes	
TTBK1	Tau Tubulin Kinase 1	Regulates phosphorylation of tau protein, which associates with microtubule assemblies	
CDKN2A	Cyclin dependent kinase inhibitor 2A	Cell cycle; p16 and p14 are gene products	Cell cycle
ATM	Ataxia Telangiectasia Mutated kinase	PI3/PI4-kinase family; cell cycle checkpoint	
SRPK2	Serine/Arginine-Rich Protein-Specific Kinase 2	Upregulates cyclin D1 and cyclin A1 expression	
PRKCZ	Protein kinase C zeta type	PKC family; cell proliferation pathways	
CDK4	Cyclin dependent kinase 4	Cell cycle G1 phase progression; phosphorylates Rb	
MAP2K4	mitogen-activated protein kinase kinase 4	MAPK and SAP/JNK pathways	Proliferative signalling pathways
MAP3K8	Mitogen-Activated Protein Kinase Kinase Kinase 8	Cytoplasm; can activate MAP kinase and JNK kinase pathways	
ACVR2	Activin A Receptor Type 2A	Mediates the functions of activins, part of the transforming growth factor-beta (TGF-beta) superfamily	
MAP3K7IP1	Mitogen-activated protein kinase kinase kinase 7-interacting protein 1	Regulator of the MAP kinase kinase kinase MAP3K7/TAK1	
PI4K2B	Phosphatidylinositol 4-Kinase Type 2 Beta	Contributes to overall PI4-kinase activity; metabolism	
PIK3C2A	Phosphatidylinositol-4-Phosphate 3-Kinase Catalytic Subunit Type 2 Alpha	Part of the phosphoinositide 3-kinase (PI3K) family	
PRKG2	Protein kinase cGMP-dependent 2	Binds to and inhibits several Tyrosine Kinase Receptors	Anti-proliferative signalling pathways
IKBKB	Inhibitor Of Nuclear Factor Kappa B Kinase Subunit Beta	NF-kappa-B pathway	Immune response
TNFAIP3	Tumor Necrosis Factor Alpha Induced Protein 3	ubiquitin ligase and deubiquitinase activities; inflammation	
PRKR	Protein kinase R/eukaryotic translation initiation factor 2-alpha kinase 2	Immune response to viruses	
CRLF2	Cytokine Receptor Like Factor 2	Type I cytokine receptor family; activate STAT3, STAT5, and JAK2 pathways	
AATK	Apoptosis Associated Tyrosine Kinase	Induced during apoptosis	
CARKL	Sedoheptulokinase	Glucose metabolism	Metabolism
PDK2	Pyruvate dehydrogenase kinase 2	Increases conversion of pyruvate to lactate in cytosol	
INSR	Insulin receptor	Insulin signalling pathway; glucose and carbohydrate metabolism	
PFKFB3	6-phosphofructo-2-kinase/fructose-2,6-biphosphatase 3	Glucose metabolism and cell cycle progression; Cdk1 regulator	
DGKG	Diacylglycerol Kinase Gamma	Lipid metabolism; possibly cell cycle regulation	
C2orf44	WD Repeat And Coiled Coil Containing	Uncharacterised	
DUSP21	Dual specificity phosphatase 21	Found in cytoplasm and nucleus	

Table 4.1 A summary of the functions of the synthetic sensitive hits of the siRNA screen Each gene found as a synthetic sensitive hit in the siRNA screen alongside GWL depletion has next to it it's full protein name and a brief description of its function. These hits were then categorised into broad themes according to their function within the cell, and tabulated together.

Gene Name	Protein Name	Function	
KIAA1765	Serine/threonine-protein kinase DCLK3	Nuclear Ser/Thr kinase	
RPA3	Replication protein A 14 kDa subunit	DNA replication and DDR	
ZNF331	Zinc finger protein 331	Transcriptional regulation	
CLK3	Dual specificity protein kinase CLK3	Spliceosome	
TBL1XR1	Transducin beta like 1 X-linked receptor 1	Transcriptional regulation	
SETBP1	SET binding protein 1	DNA replication	DNA repair, gene expression, nuclear localisation
KMT2D	Lysine-specific methyltransferase 2D	Histone methyltransferase	
EXOSC10	Exosome component 10	RNA processing and degradation	
HRPT2	Cell Division Cycle 73	Transcriptional and post-transcriptional regulation	
POLK	DNA polymerase kappa	Translesion DNA synthesis	
HOXA9	Homeobox protein A9	Transcription factor	
MGC4796	Serine/threonine kinase 40	Regulates NF-k-B and p53-mediated transcription	
DDIT3	DNA Damage Inducible Transcript 3	Transcription factor	
SSX1	SSX family member 1	Transcriptional regulation	
RBM15	RNA binding protein 15	RNA methylation	
PAK7 or PAK5	p21 (RAC1) activated kinase 5	Cytoskeleton and cell proliferation	
KALRN	Kalirin	Cytoskeleton	
PRKWNK1	WNK lysine deficient protein kinase 1	Sodium and choloride ion transport	
ICK	Intestinal cell kinase	Ciliogenesis; intestinal epithelia proliferation	Cytoskeleton, cell motility, intracellular transport
ARK5	NUAK family SNF1-like kinase 1	Cell adhesion, senescence, cell proliferation	
CLTC	Clathrin heavy chain 1	Intracellular transport	
EPHB6	Ephrin type-B receptor 6	Cell adhesion and migration	
PCTK1	Cyclin dependent kinase 16	Intracellular transport; exocytosis	
CALM2	Calmodulin 2	Centrosome cycle; cytokinesis	
CYLD	CYLD Lysine 63 Deubiquitinase	Cytoskeleton	
ARHGAP26	Rho GTPase activating protein 26	Extracellular matrix; cytoskeleton	
DNM2	Dynamin 2	Endocytosis; cytoskeleton	
CKS2	CDC28 protein kinase regulatory subunit 2	Cell cycle; binds to Cdks	
PLK3	Polo-like kinase 3	Cell cycle; cell stress response	
STK38L	Serine/threonine-protein kinase 38-like	Cell cycle; apoptosis	Cell cycle
CCND2	Cyclin D2	Cell cycle; binds to Cdk4 or Cdk6	
CHEK1	Checkpoint kinase 1	Checkpoint mediated cell cycle arrest	
STK16	Serine/threonine-protein kinase 16	Cell membrane associated kinase	Proliferative signalling pathways
ADRBK2	G protein-coupled receptor kinase	Cell signalling	
DYRK4	Dual Specificity Tyrosine Phosphorylation Regulated Kinase 4	Cell differentiation and proliferation	
BMX	BMX non-receptor tyrosine kinase	Cell proliferation	
CDKL5	Cyclin-dependent kinase-like 5	Nerve cell growth, division and migration	
MYLK2	Myosin light chain kinase 2	Skeletal muscle specific	Tissue specific signalling
FGFR3	Fibroblast growth factor receptor 3	Bone development and maintenance	
GRK1	G protein-coupled receptor kinase 1/Rhodopsin kinase	Phototransduction	
STK22D	Testis specific serine kinase 1B	Spermiogenesis	
SGK	Serum/Glucocorticoid Regulated Kinase 1	Cell stress response; ion transport	
TNFRSF17	Tumour Necrosis Factor receptor superfamily member 17	B-cell development; autoimmune response	Immune response
MAP4K5	Mitogen-activated protein kinase kinase kinase kinase 5	Cellular stress response	
IKBKAP	Elongator Complex Protein 1	Proinflammatory signalling	
NDRG1	Protein NDRG1	Cellular stress response	
THNSL1	Threonine synthase-like 1	Binds pyridoxal phosphate	Metabolism
PRKACA	cAMP-dependent protein kinase catalytic subunit alpha	Glucose metabolism, cell division	

Table 4.2 A summary of the functions of the synthetic resistant hits of the siRNA screen Each gene found as a synthetic resistant hit in the siRNA screen alongside GWL depletion has next to it it's full protein name and a brief description of its function. These hits were then categorised into broad themes according to their function within the cell, and tabulated together.

4.4 Gene Ontology analysis to look for gene category statistical overrepresentation

The next question to ask is if the lists of synthetic sensitive and resistant candidate genes obtained from the siRNA screen are all there by chance, or if there is overrepresentation or enrichment for particular categories of genes according to their roles in the cell. An analysis was run on these two sets of hits using the PANTHER Gene List Analysis tool (Mi et al. 2013) (www.pantherdb.org) and selecting the 'statistical overrepresentation test' option.

PANTHER GO-Slim Biological Process	Client Text Box Input (expected)	Client Text Box Input (fold Enrichment)	Client Text Box Input (raw P-value)	Normalised (enriched divided by expected)
Regulation of cell cycle (GO:0051726)	0.33	12.23	0.00033500	37.06060606
Response to stress (GO:0006950)	1.15	5.23	0.00092800	4.547826087
Intracellular signal transduction (GO:0035556)	1.88	4.78	0.00007970	2.542553191
Phosphate-containing compound metabolic process (GO:0006796)	2.8	4.64	0.00000177	1.657142857

Table 4.3 Statistical Overrepresentation outputs of the synthetic sensitive hits from the siRNA screen

PANTHER GO-Slim Biological Process	**Client Text Box Input (expected)**	Client Text Box Input (fold Enrichment)	Client Text Box Input (raw P-value)	Normalised (enriched divided by expected)
Regulation of cell cycle (GO:0051726)	0.41	12.3	0.00005870	30
MAPK cascade (GO:0000165)	0.74	8.07	0.00010100	10.90540541
Regulation of catalytic activity (GO:0050790)	0.78	7.65	0.00013500	9.807692308
Phosphate-containing compound metabolic process (GO:0006796)	3.49	4.88	0.00000002	1.398280802

Table 4.4 Statistical Overrepresentation outputs of the synthetic resistant hits from the siRNA screen

The output from the analysis gives an 'expected' value for how many genes from particular categories should appear at random, as well as the 'fold enrichment'. To normalise the data, I divided the enriched value by the expected value, and the results of the synthetic sensitivity overrepresentation test are shown in **Table 4.3** and those for the synthetic resistant hits are shown in **Table 4.4**. Whilst the analysis gives some very generic gene categories that are not that informative, in both lists of hits they were found to be significantly enriched for genes involved in cell cycle control. Graphs summarising the enrichment folds of the categories of genes in the hit lists according to the PANTHER Gene Annotation database are shown in **Figure 4.5**.

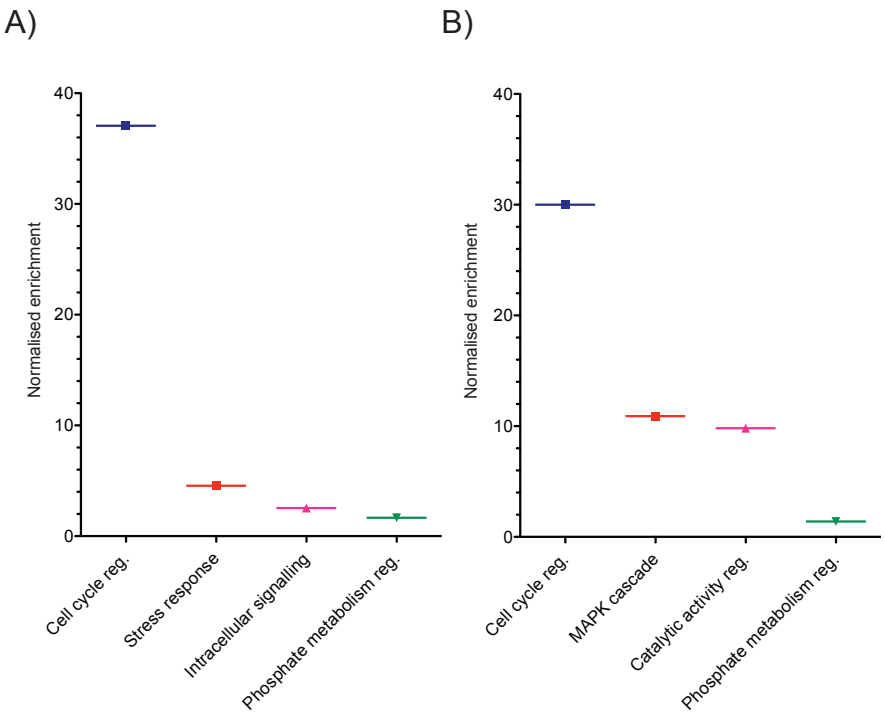

Figure 4.5 Normalised fold enrichment of the gene classification hits from the PANTHER GO Statistical Overrepresentation test A graphical summary of the data shown in Tables 4.1 and 4.2. A) Gene classifications that are overrepresented in the synthetic sensitive hits B) Gene classifications that are overrepresented in the synthetic resistant hits.

These graphs show how many more times cell cycle proteins appear as synthetic sensitive or resistant hits in the siRNA screen with GWL depletion.

4.5 Conclusions and discussion

It is important to bear in mind that siRNA screens, like all other screening approaches, are susceptible to false positives with one of the most important being off-target effects (OTEs) (Echeverri et al. 2006; Sigoillot & King 2011). With this in mind, the Lord lab performed a parallel screen with GWL shRNA MDA-MB-231 cells and a panel of drugs targeting proteins known to be important for cancer cell signalling. The CDK4/6 inhibitor Palbociclib was a hit in this drug screen as well as siCDK4 in the siRNA screen. A bioinformatics analysis of the siRNA screen hits found that they were significantly enriched for cell cycle genes, which strengthens the case for any hits that are involved in the cell cycle, as this means it is highly likely they have not appeared as hits by chance or as false positives. Thus, CDK4 was chosen as the most interesting candidate for further validation and investigation because this is a novel finding, pertains to the interesting links explained earlier regarding the non-mitotic functions of GWL (Charrasse et al. 2017), and there are already successful CDK4/6 inhibitors in clinical use.

Chapter 5. Confirming the synthetic sensitivity of Greatwall kinase and CDK4

5.1 Introduction

The observations described in the previous chapter raise the possibility that GWL depleted cancer cells display reduced proliferation rates not because of mitotic effects, but due to problems in S phase. As discussed previously, these could be due to earlier chromosome mis-segregation causing aneuploidy and stress. However, they could also reflect roles for GWL outside its canonical function as a mitotic kinase. Indeed, while work on this thesis was in progress the Castro lab published a study suggesting that GWL dependent inhibition of PP2A-B55 could be important for S phase progression via the stabilisation of Treslin, an important member of the complex that is associated with the replication fork (Charrasse et al. 2017).

We decided to follow this question up genetically and investigate synthetic sensitive interactions of the kinase using a siRNA depletion and small molecule drug screen, which was discussed in **Chapter 4**. This chapter will explore the experimental validation of one of the most convincing synthetic sensitive candidates from the screens – CDK4.

5.2 Confirming the synthetic sensitivity between Greatwall kinase and CDK4

One of the most convincing and interesting synthetic sensitive results from this screen was CDK4. We were especially confident in this result because CDK4

was identified as a hit in both the siRNA and drug screens. Both the biological implications and the therapeutic potential of this genetic interaction warranted further efforts to explore this finding further. From a mechanistic point of view this is an intriguing result because CDK4 is active in G1/S phase, in contrast to GWL's peak activity in mitotic entry. This suggests a novel, additional role for GWL outside of mitosis. Secondly, the CDK4/6 inhibitors Palbociclib (IBRANCE®) and Ribociclib (Kisqali®) are in clinical use for breast cancer patients in the UK and US (Iacobucci 2017; Kmietowicz 2017; Finn et al. 2016; Hortobagyi et al. 2016), therefore any synergy between GWL and CDK4/6 will be clinically relevant. As mentioned in **Chapter 1 – Introduction**, certain types of TNBC cell have been shown to be resistant to CDK4/6 inhibition (Asghar et al. 2017) but also a synergistic reaction between PI3K and CDK4/6 inhibitors exists in PIK3CA-mutant cells. There is an on-going therapeutic trial that is assessing the effectiveness of CDK4/6 inhibition in combination with PI3K inhibition, in patients with *PIK3CA*-mutant TNBC (Asghar et al. 2017). This opens up the possibility of using CDK4/6 inhibitors in certain types of TNBC cells when there is a synergistic relationship between CDK4/6 and another protein, as well as a biomarker to indicate this sensitivity. This makes the discovery of a kind of synergy between GWL and CDK4/6 particularly exciting, as this could have clinical relevance. **Figure 5.1** shows the summary of the results from the siRNA and drug screens that highlighted CDK4 as a hit. In both screens, targeting CDK4 with siRNA (**Fig. 5.1A**) or Palbociclib (**Fig. 5.1B**) caused significant reductions in cell viability when GWL was also knocked down.

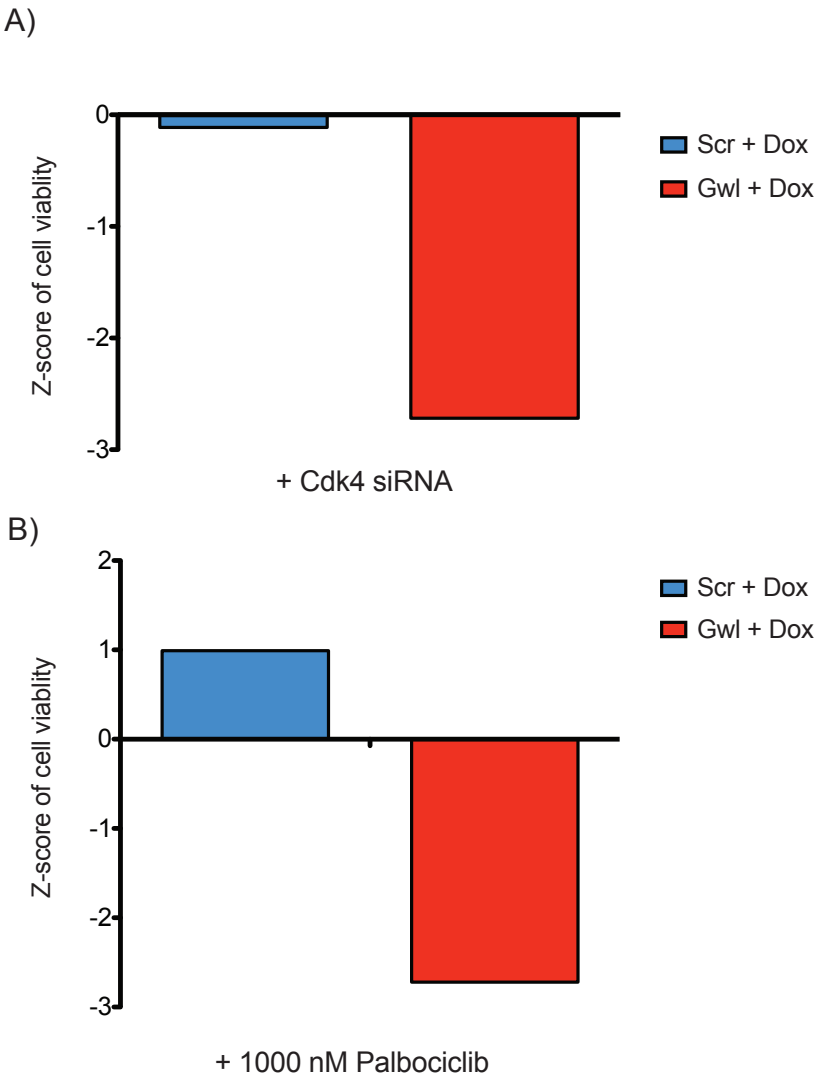

Figure 5.1 Summary of high-throughput siRNA and drug screens that identified CDK4 as a synthetic lethality hit with GWL Scr and GWL shRNA MDA-MB-231 cell lines were tested with either a DMSO control or Dox treatment, and with or without an additional siRNA or an anti-cancer drug. Each treatment was carried out with three technical replicates (three 96-well plate wells) and then the entire experiment was carried out a second time to give a total of two biological replicates. The plotted Z-scores as a measure of cell viability by MTT assay, are the mean of the two repeats. A) with Cdk4 siRNA B) with 1000 nM Cdk4/6 inhibitor Palbociclib.

In pharmacology the terms synergistic and additive have distinct, precise definitions. Synergy is the interaction of biological structures or substances that together, produce an overall effect that is greater than the sum of the individual effects. An additive effect is when two substances used in combination produce a total effect that is the same as the sum of the individual effects. In the remaining Results chapters – **Chapters 5** and **6**, I refer to the effects seen when both GWL and CDK4 are inhibited as either a 'synergy', 'synthetic lethal' or 'synthetic sensitive' effect. Whilst clear deleterious effects on cell viability and the cell cycle profiles can be seen in these treated cells, I cannot say for certain at this stage that it is truly a synergistic relationship as defined in the pharmacological literature (Foucquier & Guedj 2015; Chou 2006). This is expanded upon further in the **Chapter 7** discussion.

5.3 Using siRNA and small molecule libraries to screen for synthetic sensitivity in MDA-MB-231 Greatwall shRNA cells

The next step was to validate this synergy experimentally. Reflecting the structure of Chapter 3, I started by analysing the effect of depleting both GWL and CDK4/6 with colony formation assays. I carried out colony formation assays in MDA-MB-231 shGWL cells with a range of concentrations of Ribociclib (also known as Lee011 by the supplier, so Ribociclib is labelled as Lee011 in figures) (**Figure 5.2**) and Palbociclib (**Figure 5.3**), with and without Dox. As shown by **Figs 5.2** and **5.3**, the synthetic sensitivity between GWL and CDK4 appears to be present in these cells. I wanted to find a concentration of the CDK4/6 inhibitors that wouldn't significantly affect the cell viability when used alone but could show synergy when used alongside GWL knockdown.

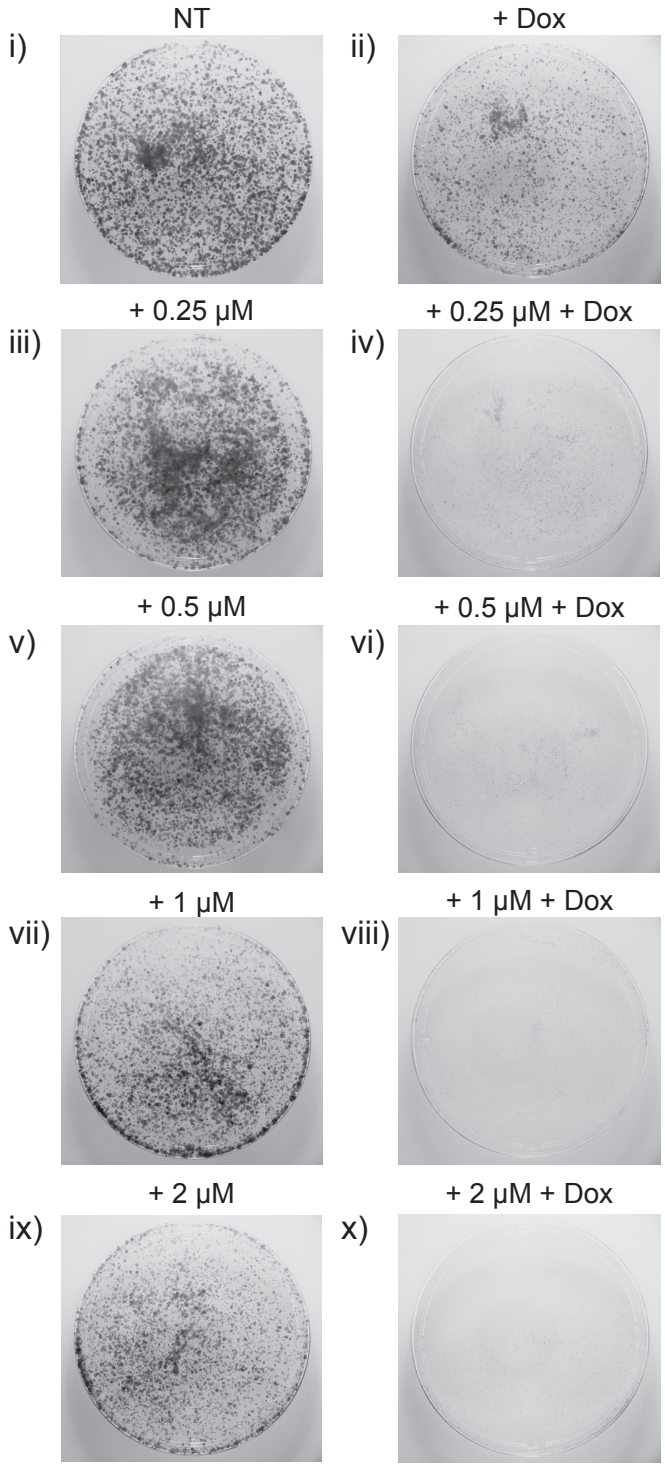

Figure 5.2 A range of Ribociclib/Lee011 doses to determine optimal synthetic lethality with GWL 20,000 MDA-MB-231 shGWL cells were plated onto 10 cm dishes, treated with the indicated treatments and allowed to grow for 7-8 days before staining with Crystal Violet solution. N=3

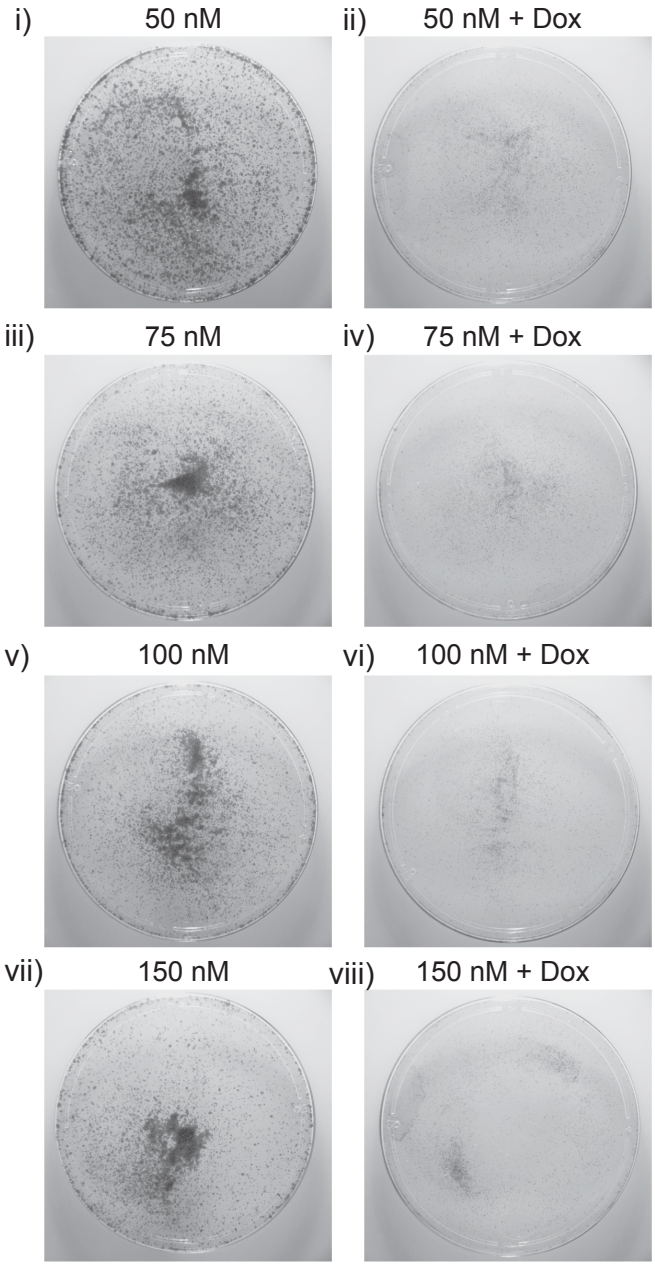

Figure 5.3 A range of Palbociclib doses to determine optimal synthetic lethality with GWL 20,000 MDA-MB-231 shGwl cells were plated onto 10 cm dishes, treated with the indicated treatments and allowed to grow for 7-8 days before staining with Crystal Violet solution. N=3

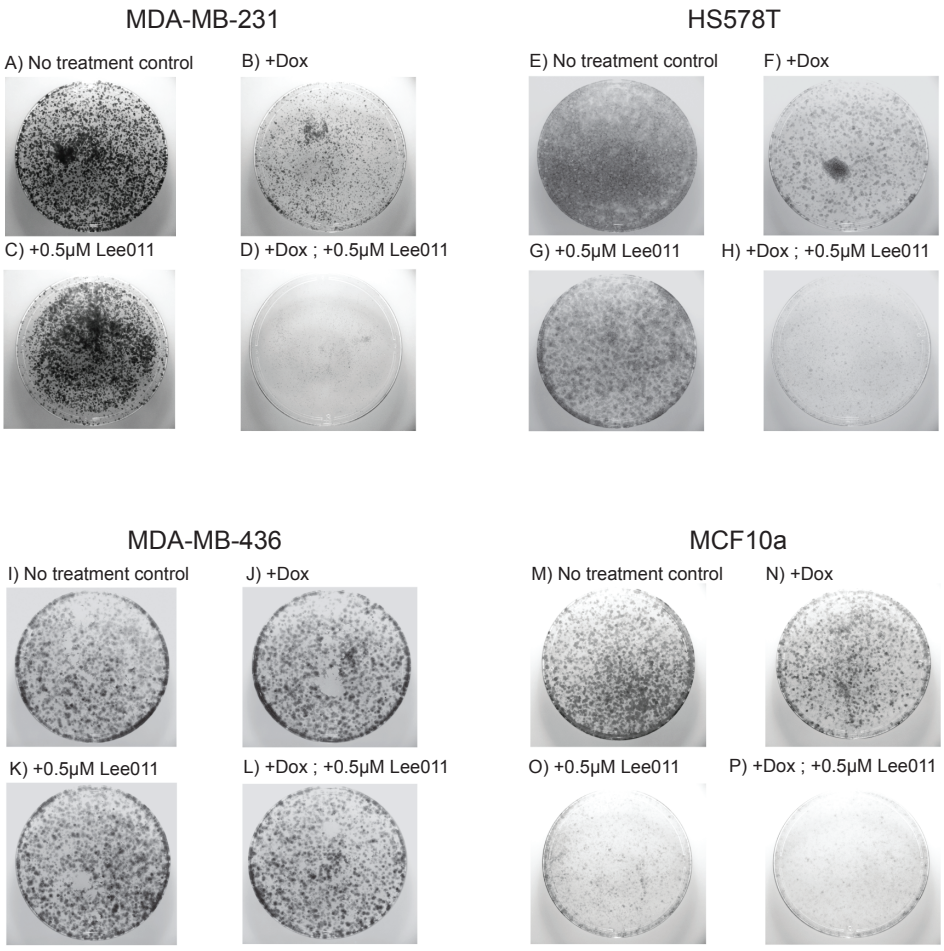

Figure 5.4 The sensitivity of a panel of breast cell lines to simultaneous GWL depletion and CDK4/6 inhibition Representative images of this experiment: 20,000 live cells were plated onto each 10 cm dish, the appropriate treatment added and grown for 7-8 days prior to staining with 0.05% Crystal Violet solution. N=3

I found that 0.5 μM Ribociclib/Lee011 and 50 nM Palbociclib were the best concentrations to achieve this effect, so an additional set of colony assay experiments was carried out using Ribociclib/Lee011 at 0.5 μM using four cell lines (MDA-MB-231, HS578T, MDA-MB-436 and MCF10a). The results are shown in **Figure 5.4**. Each experiment was carried out three separate times and the plates photographed, but the colonies were not counted. These colony assays look different to those in Chapter 3 because instead of using a feeder layer, plating 1000 cells and growing the cells over the course of two weeks; the plates in **Fig. 5.4** were plated with 20,000 cells and grown for 7-8 days.

It is clear that the MDA-MB-231 and HS578T cells (**Fig. 5.4A** to **H**) are very sensitive to the simultaneous depletion of GWL and inhibition of CDK4/6. The MDA-MB-436 cells, like with the just GWL knockdown treatment described in Chapter 3, are not sensitive to GWL knockdown nor the double treatment of GWL depletion and CDK4/6 inhibition.

The 436 cells also show no sensitivity to the 0.5 μM dose of Ribociclib/Lee011 (**Fig. 5.4K**), when the other three cell lines show a degree of sensitivity to this treatment. It is logical that MDA-MB-436 cells are resistant to CDK4/6 inhibition because, unlike MDA-MB-231 and HS578T cells, they lack the Retinoblastoma (Rb) protein (Robinson et al. 2013). The MCF10a cells also show GWL and CDK4/6 synthetic lethality, and are the most sensitive to the single Ribociclib/Lee011 treatment out of the cell lines tested (**Fig 5.4M** to **P**), while MDA-MB-231 and HS578T display resistance to CDK4/6 inhibition, which is typical of many TNBC cells (Asghar et al. 2017).

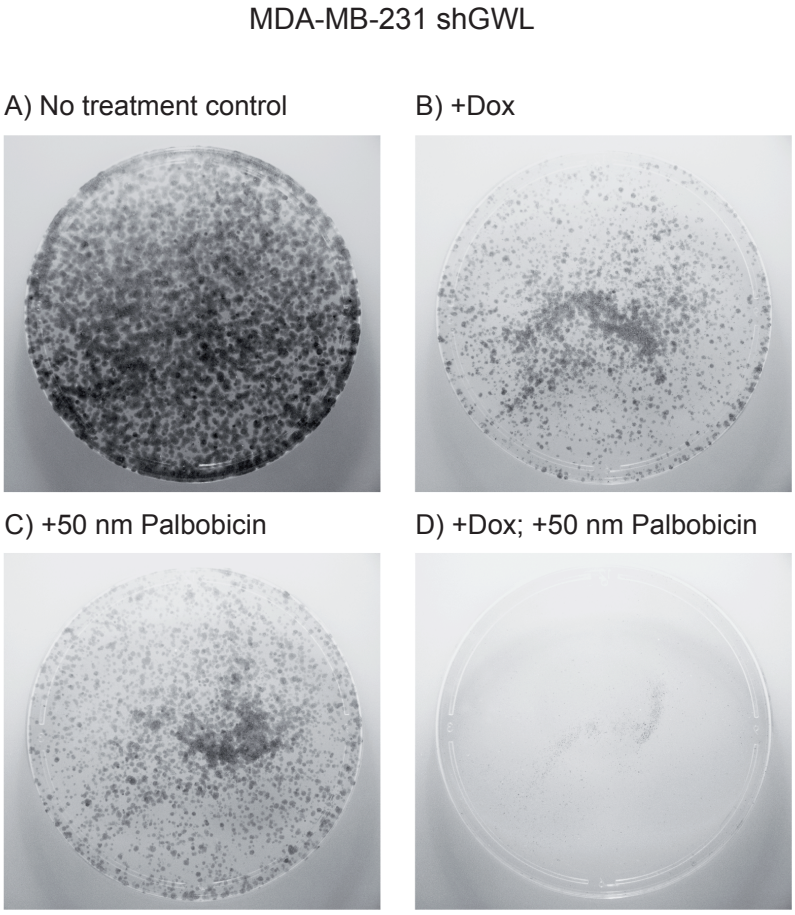

Figure 5.5 Treatment with the CDK4/6 inhibitor Palbociclib shows synthetic lethality with GWL knockdown in MDA-MB-231 cells 20,000 live cells were plated onto each 10 cm dish, the appropriate treatment added and grown for 7-8 days prior to staining with 0.05% Crystal Violet solution. Represenative images of N=3.

I then tested the GWL-CDK4 synergy once more using the other clinically approved CDK4/6 inhibitor – Palbociclib. **Figure 5.5** shows that whilst Palbociclib seems to be more effective than Ribociclib/Lee011 on MDA-MB-231 cells because of the lower doses used, the synergistic effect between CDK4/6 inhibition and GWL knockdown is still apparent at 50 nM.

Recurring problems when using RNAi technologies are off-target effects. So far, all results have been produced with a single shRNA and could be due to the depletion of other factors rather than loss of GWL. To check that the effect of GWL knockdown on cell proliferation as well as the GWL-CDK4 synergy are reliable and not a product of shRNA off-target effects, I replicated the colony assay experiment shown in **Fig 5.4** but with Dox-inducible CRISPR-GWL MDA-MB-231 cells, and a Scr control (Álvarez-Fernández, Sanz-Flores, Sanz-Castillo, Salazar-Roa, Partida, Zapatero-Solana, Ali, Manchado, Lowe, VanArsdale, Shields, Caldas, Quintela-Fandino & Malumbres 2018b). These cell lines were generously gifted from Marcos Malumbres and have also been published in the following study (Álvarez-Fernández, Sanz-Flores, Sanz-Castillo, Salazar-Roa, Partida, Zapatero-Solana, Ali, Manchado, Lowe, VanArsdale, Shields, Caldas, Quintela-Fandino & Malumbres 2018b). The immunoblot to verify the GWL knockdown in this inducible CRISPR-GWL line is shown in **Figure 5.6**. The results of the colony assays to verify the reliability of the GWL knockdown phenotype and the GWL-CDK4 synthetic lethality are shown in **Figure 5.7**.

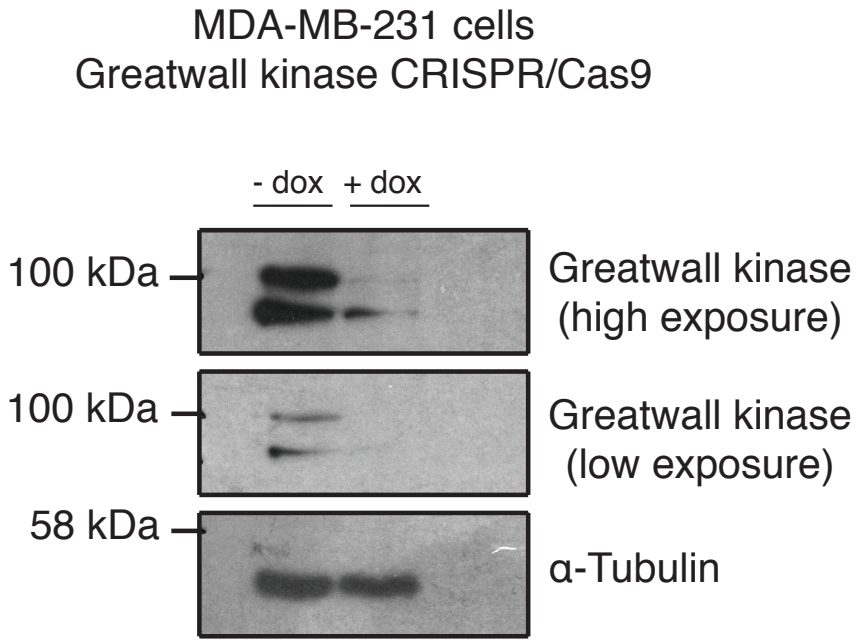

Figure 5.6 Immunoblot to verify the Greatwall kinase knockout using the MDA-MB-231 inducible CRISPR-Cas9 GWL cell line The stable and reversible CRISPR mechanism was induced by adding 2 µg/mL Doxycycline and incubating cells for 5 days before harvesting cell lysate. GWL expression levels were detected using an anti-MASTL antibody, and an anti-α-Tubulin antibody was used as a loading control.

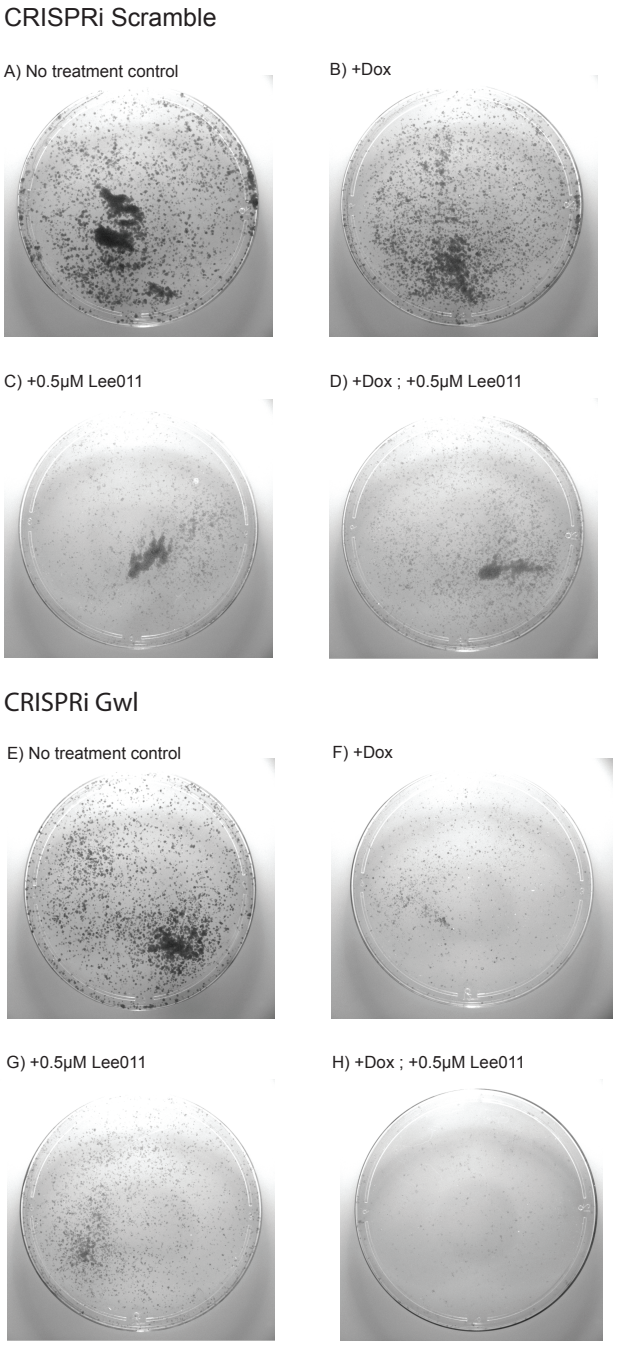

Figure 5.7 Confirming synergy between GWL and CDK4 using an inducible CRISPR-Cas9 MDA-MB-231 cell line 20,000 live cells were plated onto each 10 cm dish, the appropriate treatment added and grown for 7-8 days prior to staining with 0.05 % Crystal Violet solution. N=2.

Similar to the shRNA depletion, the induced GWL knockout causes a significant reduction in colony formation to these Cas9 expressing MDA-MB-231 cells (**Fig. 5.7F**), and these cell lines are also sensitive to just the CDK4/6 inhibition treatment alone (**Fig 5.7C** and **G**). However, there is a clear synergistic effect when both GWL and CDK4/6 are targeted that almost completely wipes out colonies. This effect is specific for the GWL gRNA and does not occur in the control CRISPR-Scr line (**Fig 5.7D** and **H**).

5.4 The synergy between Greatwall kinase and CDK4 results in a depletion of S phase cells

In order to further characterise the synergy between GWL and CDK4, I evaluated the effect of the double treatment of GWL knockdown and CDK4/6 inhibition on the cell cycle phase populations using pulse EdU labelling and Propium Iodide (PI) staining followed by FACS analysis. A representative example of a set of FACS plots for this experiment is shown in **Figure 5.8A**. Using the BD CSampler™ Analysis Software, values for how many cells are in which cell cycle stage can be obtained by gating around the appropriate sections of the plots. However, for a range of reasons including sub-G1 cells, polyploidy cells, and cell fragments, not every cell that passes through the FACS analysis falls neatly into G1, S or G2/M phase. This means the percentages of the cell cycle stages do not add up to 100%, and thus would prevent meaningful comparisons across different experiments.

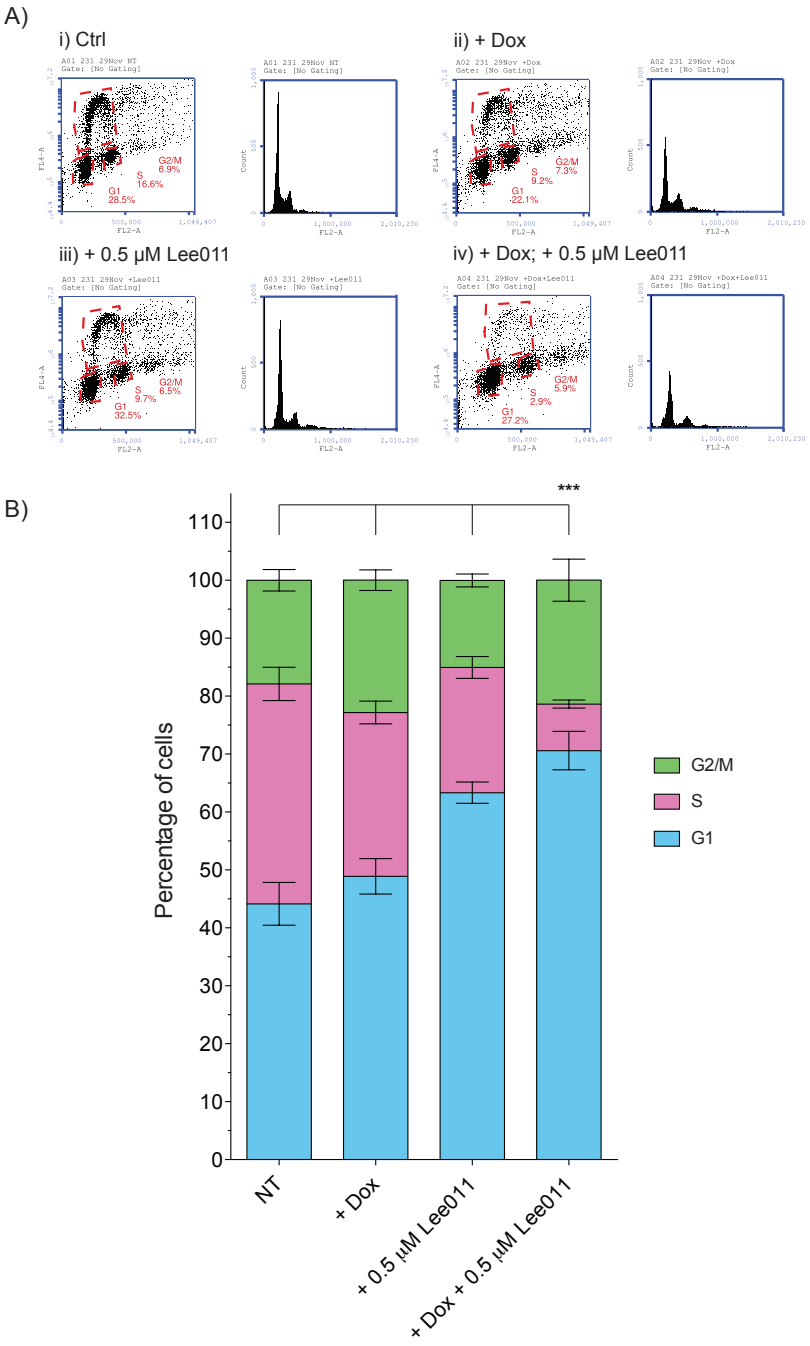

Figure 5.8 Simultaneous knockdown of GWL and CDK4/6 inhibition causes a dramatic loss in the S-phase cell population MDA-MB-231 shGWL cells treated with 2 μM Dox for 5 days. In the final 24 hours, some cells were also treated with 0.5 μM Ribociclib/Lee011. A) Representative FACS plot B) Means of N=4 experiments normalised. Unpaired t-test used to compare individual conditions to the NT control group.

To normalise this data, the total of the gated percentages of G1, S and G2/M cells became the new ‘100%’. Then, each gated percentage of each cell cycle phase was normalised to this value. This normalised data is plotted in **Figure 5.8B**. GWL depletion causes a mild increase in the G2 population, while both CDK4 inhibition and GWL depletion causes a mild decrease of S phase cells and increase in G1 population. Strikingly, after double treatment (ie CDK4 inhibition and GWL depletion) the S phase population drops by a further 50% compared to the single treatments resulting in less than 10 % of the overall cell population. Using the GraphPad Prism software, I performed unpaired t-tests comparing the S phase population of each treatment against the S phase population of the double treatment + Dox + Lee011 condition. All three of these tests showed $p < 0.001$ which is represented by the three stars on the graph in **Fig. 5.8 B**.

To further analyse the differences between the S phase populations compared to the control, I used the Shared Control function in the Estimation Statistics tool to analyse just the different S phase counts (Ho et al. 2018). The results of this analysis are shown in **Figure 5.9**. This method of plotting the data allows for the mean differences and their confidence intervals to be easily compared. Because there are multiple groups or treatments in this experiment, the side-by-side plotting allows the visual comparison of effect sizes. The bold, vertical line representing the 95% Confidence Interval of the + Dox and + Lee011 treatment lies outside those of both the single treatments against GWL and CDK4/6 (**Fig. 5.9)**.

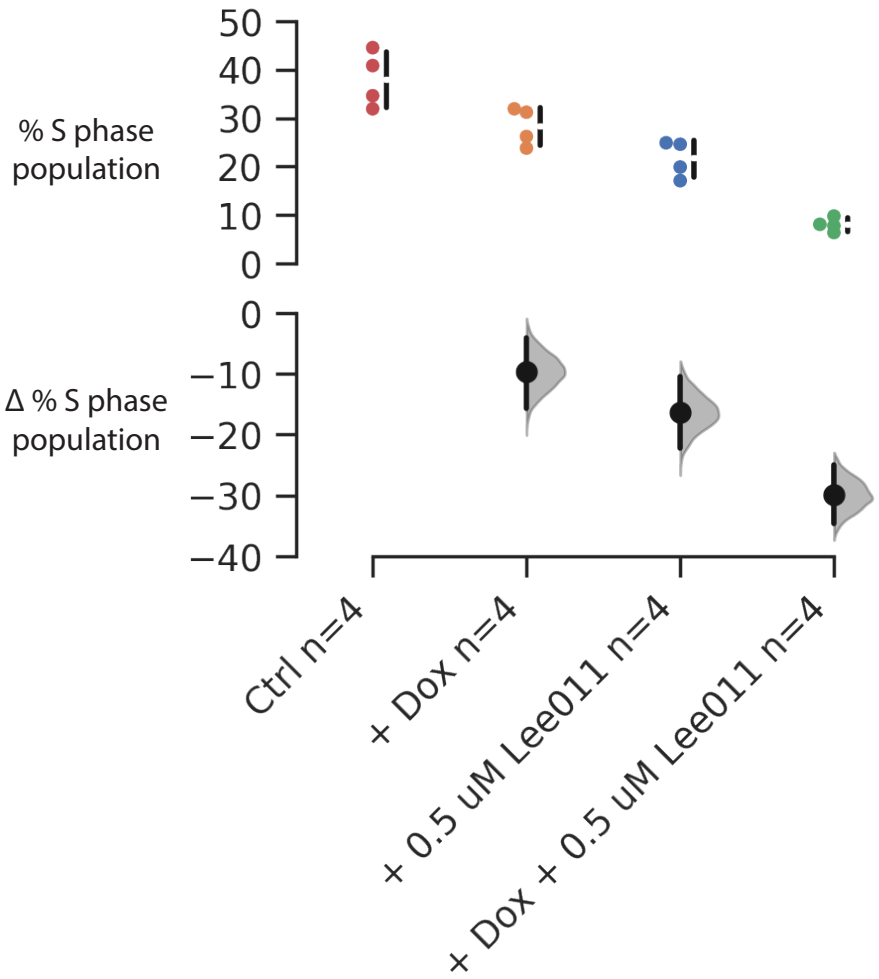

Figure 5.9 Shared Control analysis to evaluate the differences in S-phase populations in MDA-MB-231 shGWL cells treated with GWL knockdown and CDK4/6 inhibitor Using the Estimation Statistics tool (Ho et al. 2018) a swarm plot of just the S-phase populations from the data shown in **Fig. 5.8B**.

The experiment shown in **Fig. 5.8** was repeated, but with MDA-MB-436 cells and Ribociclib/Lee011, MDA-MB-231 inducible CRISPR-GWL cells and Ribociclib/Lee011, and finally with MDA-MB-231 shGWL cell and Palbobicin. The data of the MDA-MB-436 experiment is shown in **Figure 5.10**, where again a representative set of FACS plots (**Fig. 5.10A**) is shown as well as the normalised data across the biological replicates (**Fig. 5.10B**). Not only do the individual treatments of either GWL knockdown or CDK4/6 inhibition not have any noticeable effect on the cell cycle populations, but the double treatment also shows no significant effect. This experiment was repeated three times so the S phase populations between the non-treatment control group and the + Dox; + Lee011 group were tested with an unpaired t-test in GraphPad Prism and no significant difference was found.

This experiment format was repeated again but instead using the inducible CRISPR-GWL MDA-MB-231 cell line. This data is shown in **Figure 5.11** and the experiment was repeated only twice so this result lacks statistical analysis. The same effect is seen, with the S phase population decreasing in the condition of the double treatment, however the SEM error bars on the boundaries of the G1 and the S phase cells are large. The G2/M population of this set of cells in the + Dox; + Ribociclib/Lee011 group has also increased more compared to that seen in the shGWL cells in **Fig. 5.8**. Ideally this experiment needs more biological replicates to make the data more reliable.

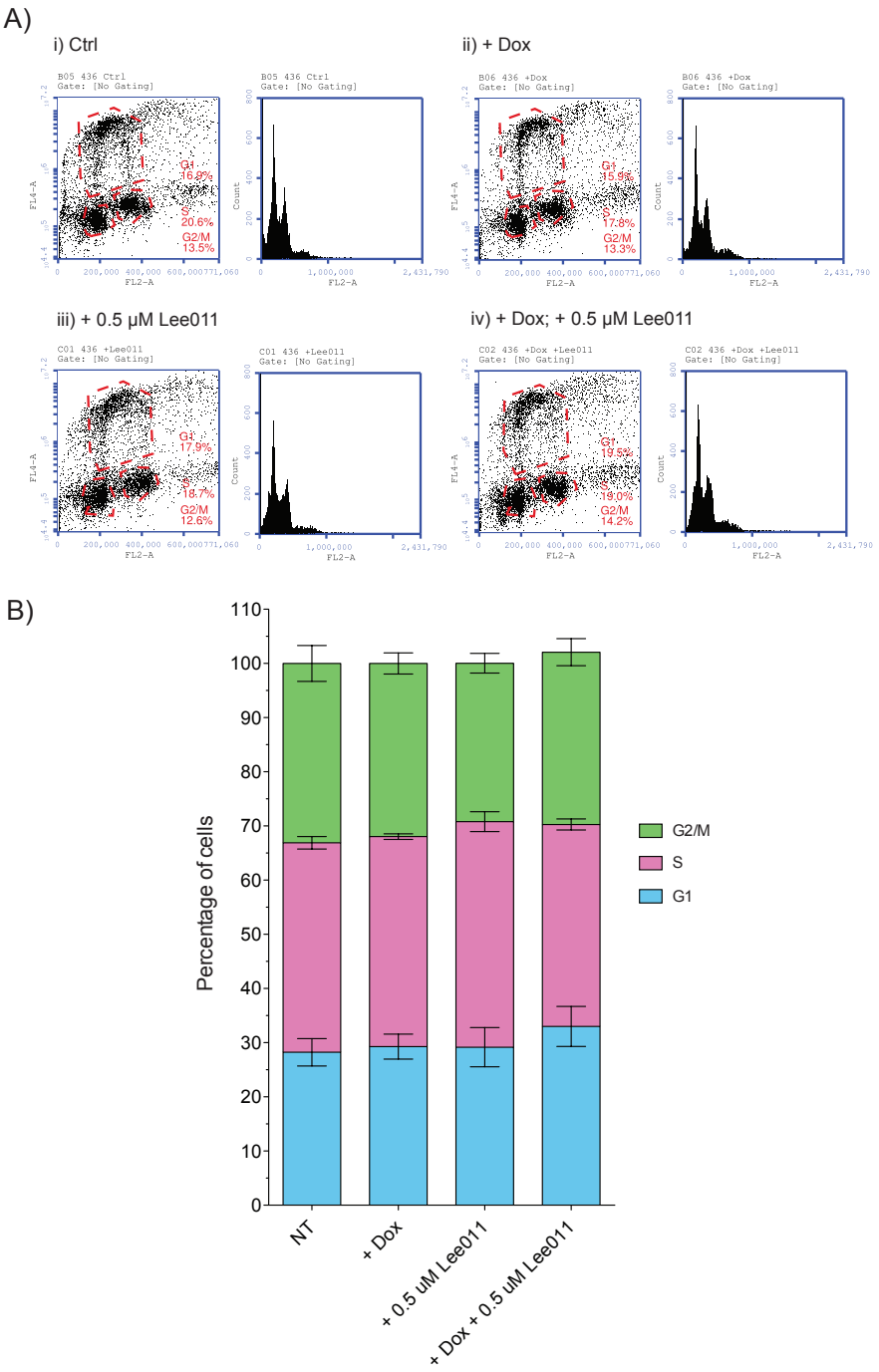

Figure 5.10 MDA-MB-436 cells are resistant to simultaneous knock-down of Greatwall kinase and CDK4/6 inhibition MDA-MB-436 shGWL-cells treated with 2 µM Dox for 5 days. In the final 24 hours, some cells were also treated with 0.5 µM Ribociclib/Lee011. A) Representative FACS plot B) Means of N=3 experiments normalised. Unpaired t-test used to compare individual conditions to the NT control group.

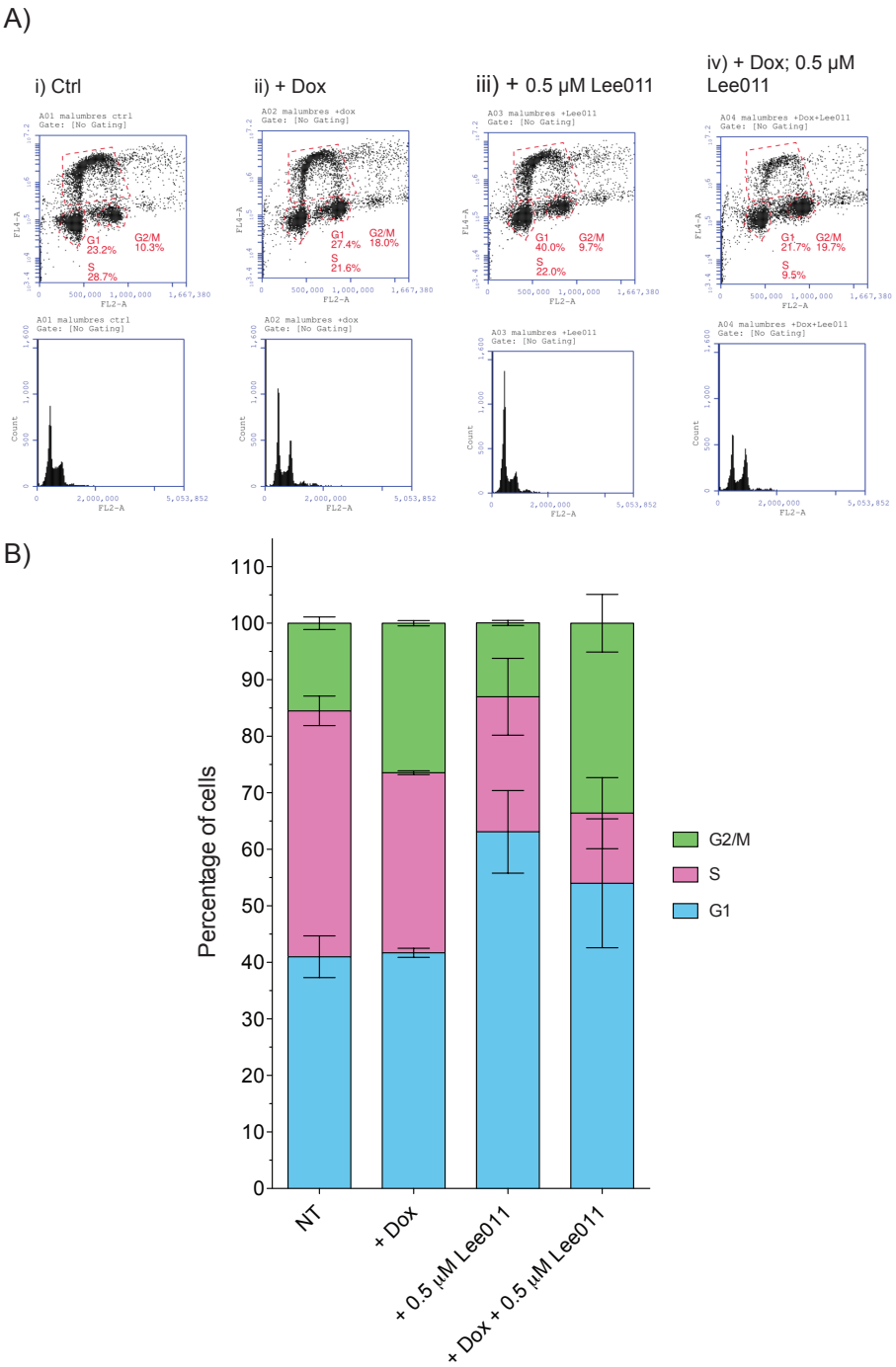

Figure 5.11 MDA-MB-231 CRISPR-GWL cells are sensitive to simultaneous knockdown of Greatwall kinase and CDK4/6 inhibition MDA-MB-231 CRISPR-GWL cells treated with 2 µM Dox for 5 days. In the final 24 hours, some cells were also treated with 0.5 µM Ribociclib/Lee011. A) Representative FACS plot B) Means of N=2 experiments normalised.

In addition, the experiment shown in **Fig. 5.8** with the shGWL MDA-MB-231 cells was repeated but this time with 50 nM Palbociclib used as the method of CDK4/6 inhibition. This data is shown in **Figure 5.12**, and also this experiment was repeated twice so lacks statistical analysis. The data here is however consistent across the two samples so the error bars are very small. 50 nM Palbobicin treatment alone is quite deleterious to these cells, and the S phase population shrinks dramatically and the G1 population increases. However, in the double treatment including GWL knockdown, the S phase population decreases further slightly.

To further investigate the fate of MDA-MB-231 cells lacking both GWL and CDK/6 activity, we used live cell imaging. MDA-MB-231 shGWL cells were seeded onto a 2-chamber imaging plate, 48 hours prior to commencement of imaging. One chamber had just 0.5 μM Ribociclib/Lee011 added to it five hours before imaging began. The second chamber of cells received this treatment too plus the 2 μg/mL Dox dose immediately after seeding, so these cells had 48 hours of Dox exposure before imaging began. When analysing the resulting movies, one daughter cell from each division was tracked. If no further divisions are indicated following mitosis, then this means that neither daughter cell underwent a subsequent division. Moreover, this method allows us to determine, if the double treatment causes depletion cells by cell death, or simply cell cycle arrests. The analysis is shown in **Figure 5.13**.

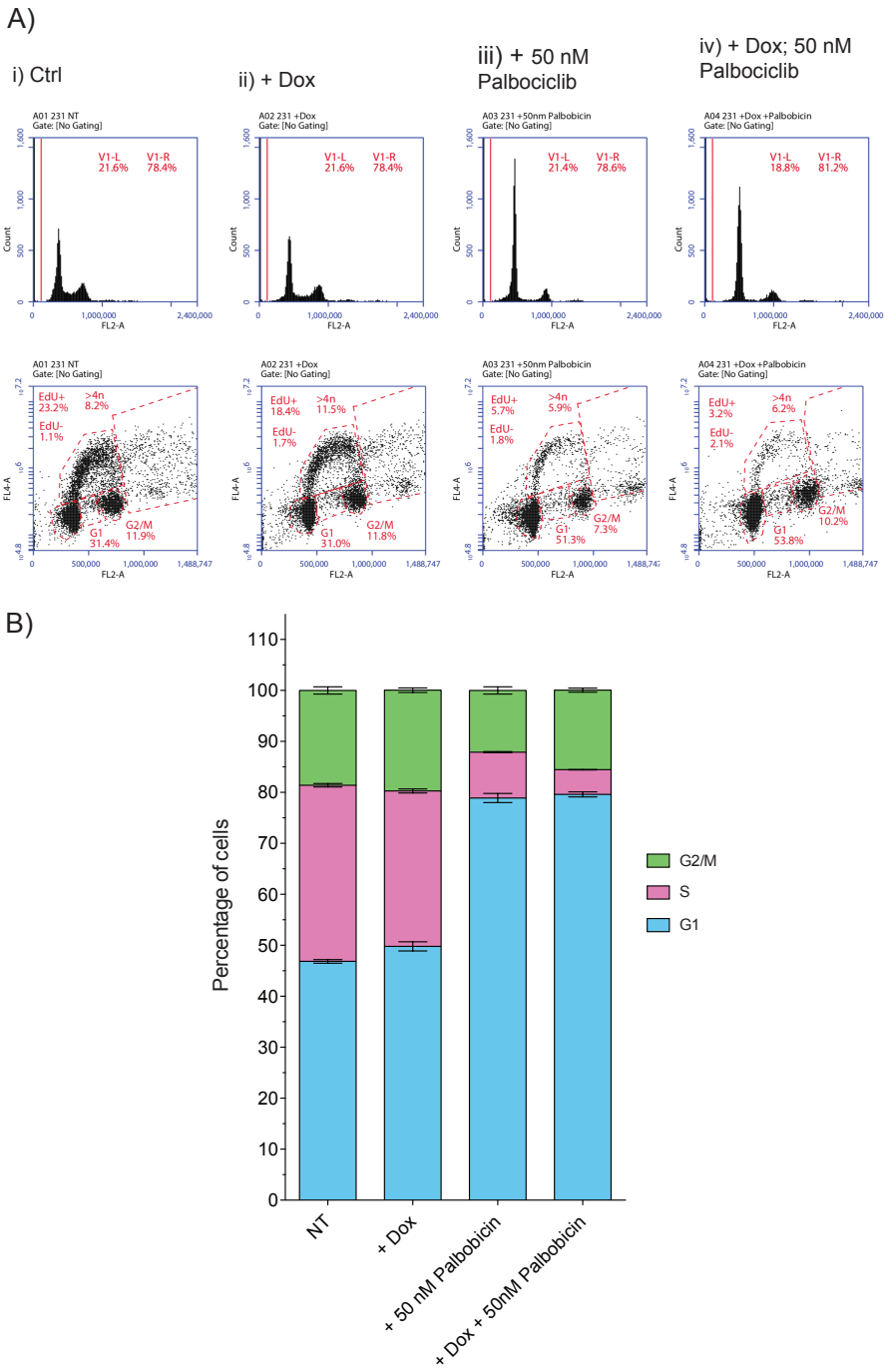

Figure 5.12 CDK4/6 inhibitor Palbociclib has a synergistic effect with GWL knockdown in MDA-MB-231 shGWL cells MDA-MB-231 shGWL cells treated with 2 μM Dox for 5 days. In the final 24 hours, some cells were also treated with 50 nM Palbociclib. A) Representative FACS plot B) Means of N=2 experiments normalised.

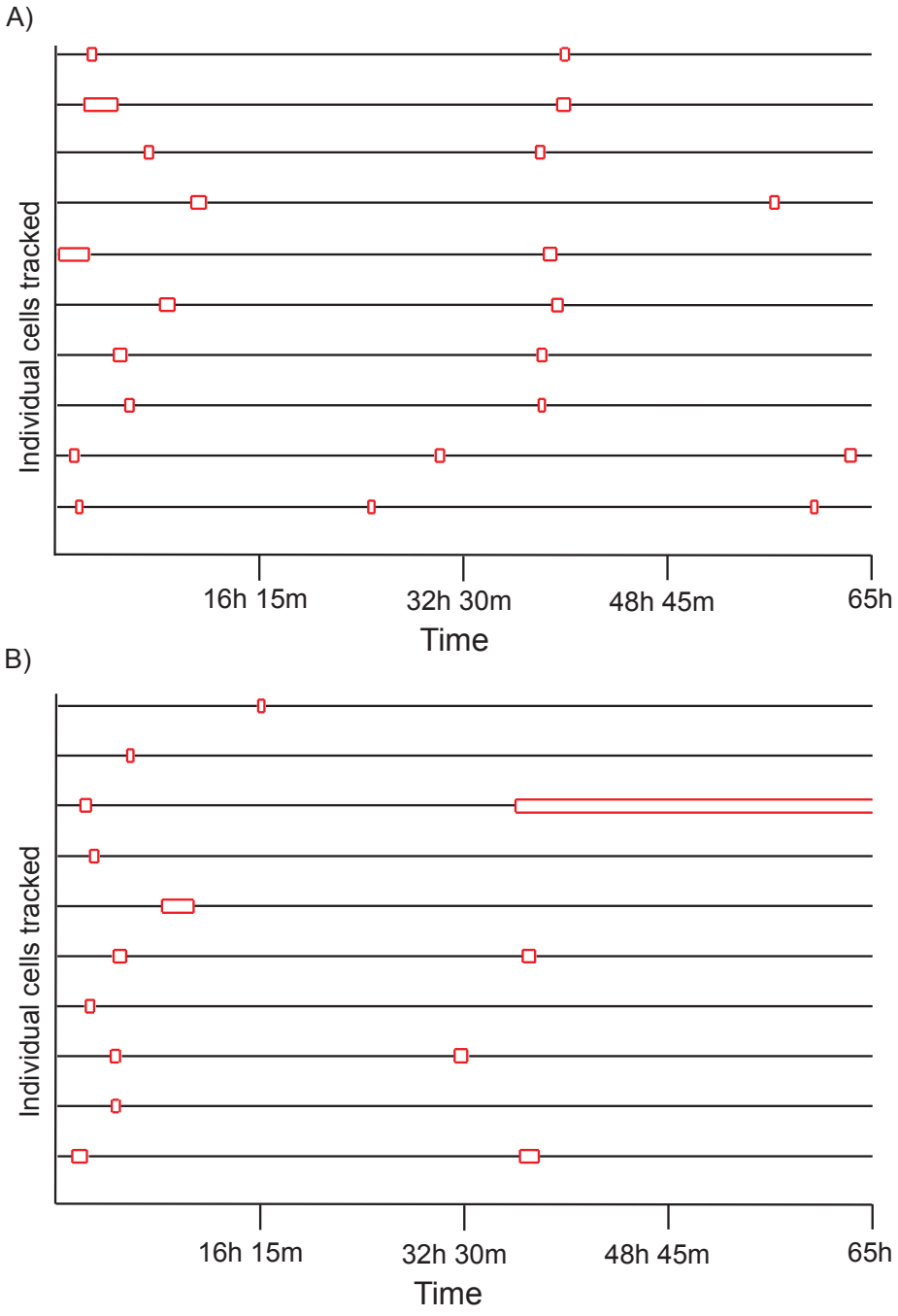

Figure 5.13 Treating MDA-MB-231 shGWL cells with both CDK4/6i and GWL knockdown inhibits cell proliferation Cells were plated onto a 2-well imaging chamber 48 hours prior to filming. A) On day of filming, cells treated with 0.5 μM Lee011/Ribociclib only B) Cells treated with 2 μM Dox at time of plating 48 hours before filming and 0.5 μM Lee011/Ribociclib on day of filming. The horizontal red lines represent how long the cells stay in a rounded, mitotic state, and one daughter cell was tracked after each mitosis.

In **Fig. 5.13A** the 0.5 μM dose of CDK4/6 inhibitor Ribociclib/Lee011 the observed cells all divided twice or three times during imaging. In the cells that received both Dox and Lee011 treatments, in **Fig. 5.13B**, there is a reduction in cell proliferation compared to the singular Lee011 treatment. In the cells treated with both Dox and Lee011, seven out of the ten cells tracked only completed one round of mitosis, including one that failed to exit after entering mitosis. These cells were approaching full shRNA-mediated GWL knockdown during filming in addition to the CDK4/6 treatment. However, this result mirrors the one seen in **Fig. 3.9**, which was filming the cells with just GWL knockdown treatment so no new information pertaining to the mechanism of the effect of the CDK4/6 inhibition in combination with GWL knockdown is gained here. This result suggests that when certain breast cancer cells with depleted GWL either exit the cell cycle, undergo arrest in G1 phase, or enter a G1-like state, rather than dying due to a programmed cell death pathway. However, this experiment would be much improved with a no treatment control to compare with the effect of the single CDK4/6 inhibitor treatment. Looking at **Fig. 5.13A** alone, without the no treatment control for this experiment it isn't known if just the CDK4/6 inhibitor perturbs the cell cycle. Further investigation into the possible mechanism behind the GWL and CDK4 synergy will be explored in the next chapter.

5.5 Conclusions and discussion

The work done in this chapter has verified that targeting GWL and CDK4 simultaneously causes synthetic lethality in the Triple Negative breast cancer cell line MDA-MB-231. When looking at **Figs. 5.8**, **5.11**, and **5.12**, these results

clearly demonstrate that there is a genetic relationship between G1 kinase CDK4 and mitotic kinase GWL that is causing an increase in G1 cells and a reduction in S phase cells to occur. It was also found that using a different method of GWL knockdown, with the inducible CRISPR-GWL cell line, replicated the results of the shRNA induced GWL knockdown method: showing both growth inhibition in MDA-MB-231 cells, as well as synthetic lethality when combining GWL depletion with CDK4 inhibition. Combining the results from the live cell imaging experiments and the FACS analysis suggest that the cells are indeed arresting in G1 or exiting the cell cycle following co-depletion of both kinases. Intriguingly, GWL depletion alone already delays interphase progression in these cells (see **Fig 3.8**) and reduces the S phase population, but these effects are greatly exacerbated by simultaneous CDK4 inhibition. It is important to note that the synthetic lethal phenotype is not seen in the RB negative cell line MDA-MB-436.

Taken together, these findings point to a novel role of GWL in early G1. This could be the result of GWL/ENSA depletion on Treslin that was recently described by Anna Castro and colleagues (Charrasse et al. 2017). If this were the case, however, we would not expect to see such specific phenotypes of GWL depletion on RB wild-type (WT) cells (MDA-MB-231), and no effects in the RB mutated cell line (MDA-MB-436). Taken together this suggest that the synergy between CDK4 and GWL does, indeed, occur at the level of RB inhibition, but further work comparing larger panels of cell lines will be necessary to substantiate this claim.

What the experiments in this chapter have not been able to fully quantify is the difference between the G1 phase cells that are still actively progressing through the cell cycle, and the G1 phase cells that are arrested in this phase. Some experiments with some G1 specific markers may help to clarify this. For example, time course immunoblots tracking the cell cycle status of the culture over several days and blotting for multiple G1 arrest markers such as Cdt1, p53, p21, p27 and p16. Since cell cycle pathways are often perturbed in cancerous cells it would be better to analyse a range of markers in order to make an informed observation. In addition, the fluorescent marker mVenus p27K$^-$ is able to label quiescent cells so this experiment could be done via IF microscopy (Oki et al. 2014).

In conclusion, the data in this chapter has validated the synthetic lethality identified in the screen carried out by our collaborators in the ICR and strengthens the rationale for the theory that GWL is linked to other phases of the cell cycle (Charrasse et al. 2017; Peng et al. 2010). To our knowledge, the observation that knocking down GWL as well as inhibition of CDK4/6 significantly reduces the S phase population whilst increasing the G1 phase population is original to this thesis.

Our discovery of synthetic lethality between GWL and CDK4 is relevant for both clinical and basic research purposes. Not only could this synthetic lethality be potentially beneficial from a treatment regimen standpoint, but also with further research could lead to the discovery of non-mitotic roles of GWL which would increase our understanding of cell cycle control.

The next step in this project is to try to elucidate the mechanism of this novel phenotype. The active cyclin D-CDK4 complex is able to add an inhibitory phosphorylation to the RB protein. This relieves the RB-mediated inhibition of the transcription factor E2F, which commits the cell to progression into S phase and through the cell cycle. It has been found that inhibition of CDK4 is sufficient to induce senescence (Lessard et al. 2018), so it makes sense that inhibition of RB phosphorylation via CDK4/6 inhibition in combination with knockdown of pro-mitotic GWL decreases cell proliferation. It is also known that the downstream target of GWL, the phosphatase PP2A-B55, is a tumour suppressor that is often mutated or inactivated in cancer, including breast tumours (Álvarez-Fernández, Sanz-Flores, Sanz-Castillo, Salazar-Roa, Partida, Zapatero-Solana, Ali, Manchado, Lowe, VanArsdale, Shields, Caldas, Quintela-Fandino & Malumbres 2018b; Perrotti & Neviani 2013; Janssens et al. 2005). It is possible that PP2A-B55 could also be responsible for inhibiting the activation of CDK7/CAK, CDK4 and/or inhibiting the phosphorylation of Rb. So, with PP2A-B55 being a known tumour suppressor, it could be the case that, in the context of a cancer cell with a high DNA damage load, GWL can act as a suppressor of the tumour suppressor PP2A-B55, thus linking GWL to CDK4 via its regulation of PP2A-B55.

Chapter 6. Investigation into the mechanism of the synergy between Greatwall kinase and CDK4

6.1 Introduction

In this chapter I report results that were inspired by the findings of the previous chapters (**Chapters 4 and 5**), which found a synergistic relationship between GWL and CDK4 in TNBC cells. The next logical step is to work out a mechanism for this relationship. In this chapter I enquire whether the synergy is dependent on either the downstream target of GWL, the phosphatase PP2A-B55 or two of GWL's currently known substrates and inhibitors of PP2A-B55: ENSA and ARPP19.

The major function of GWL is the inhibition of PP2A-B55 during mitosis. Likewise, GWL inactivation in telophase is required for the re-activation of PP2A–B55α and δ complexes during mitotic exit (Manchado et al. 2010; Hégarat et al. 2014; Mochida et al. 2009; Castilho et al. 2009). If GWL is knocked down, then this means PP2A-B55 remains active throughout mitosis. Premature PP2A-B55 activity in GWL depleted cells could be linked to the G1/S transition by dephosphorylating RB, Cdc25 and/or dephosphorylating a CAK of CDK4, and thus inhibiting a cell from progressing past G1-phase. It is already known that PP2A-B55 dephosphorylates and inactivates Cdc25 at mitotic exit (Mochida et al. 2009; Forester et al. 2007; E. S. Johnson & Kornbluth 2012), but the role of Cdc25 in G1 phase is not well established. It has been proposed that a different subunit of the PP2A holoenzyme family, PP2A-B" also known as PR72, is capable of dephosphorylating RB (Wlodarchak & Xing 2016) as well as the PP2A-B55α complex (Jayadeva et al. 2010). PP1 is also capable of partially

dephosphorylating and deactivating GWL during mitotic exit (Rogers et al. 2016), and is able to dephosphorylate RB (Kolupaeva & Janssens 2012; Kurimchak & Graña 2012; Hirschi et al. 2010; Wlodarchak & Xing 2016). Overall, the current consensus seems to be that PP1 is responsible for the complete dephosphorylation of RB after mitosis, whereas PP2A can be active throughout the cell cycle, dephosphorylating RB and p107/130 in response to various conditions (Kolupaeva & Janssens 2012; Kurimchak & Graña 2012; Wlodarchak & Xing 2016). Moreover, deregulated GWL would predominantly cause raised PP2A/B55 levels in late anaphase/early telophase, rather than in early G1, at a time when PP2A-B55 is already active. A synergy between GWL and CDK4 via PP2A-B55 would thus suggest that GWL function continues to be important beyond mitosis. This does not correlate with current models of GWL activation by mitotic CDK1, but agrees with the recent findings on S-phase functions of the GWL/ENSA pathway (Charrasse et al. 2017).

Overall, a precise knowledge of the basic mechanism of the CDK4/GWL genetic interaction will be important both for our understanding of cell cycle control and for potential further clinical development of this synthetic lethality.

6.2 The GWL-CDK4 synergy is not reversed by co-depletion of PP2A/B55

The results described in the previous chapter could be regarded as controversial. So far, no other GWL substrates have been described and all phenotypes of GWL have been attributed to its phosphorylation of ENSA/ARPP19. However, GWL could have other substrates that have been

missed in previous screens or could also act in a kinase independent fashion. Nevertheless, GWL could still be impacting on PP2A-B55.

A way to test PP2A involvement in the synergy between GWL and CDK4 would be to carry out double treatment targeting CDK4 and GWL and also PP2A-B55 to see, if this rescues the S-phase population. Thus, I carried out siRNA knockdowns of the PP2A-B55α and δ subunits alongside shRNA-mediated knockdown of GWL and CDK4/6 inhibition. MDA-MB-231 shGWL cells were plated in cell culture and Dox added to knockdown GWL. 48 hours later, cells would be transfected with siCtrl or siB55α and siB55δ. Then 48 hours after siRNA transfection and 24 hours before cell harvesting, the 0.5 μM dose of Lee011/Ribociclib was added. This means that the cells were exposed to GWL shRNA for a total of 5 days, which is sufficient to deplete GWL (as shown in **Chapter 3**) and immunoblotting analysis showed a complete depletion of PP2A-B55 α and δ after 72 hours of siRNA exposure. The immunoblots confirming the knockdown of GWL and PP2A-B55 α and δ are shown in **Figure 6.1**.

Alongside the cells plated for the immunoblots, additional cells were plated and treated with the same protocol and were analysed by FACS with PI and EdU staining. On the day of cell harvesting, five days after plating, the cells were pulse labelled with 10 μM EdU for 1 hour before fixing and processing for FACS. The experiment was repeated three times in total, and the cell cycle phase population percentages were normalised as described in **Chapter 4**. A representative FACS plot, as well as the normalised cell cycle phase populations for the three replicates are shown in **Figure 6.2**.

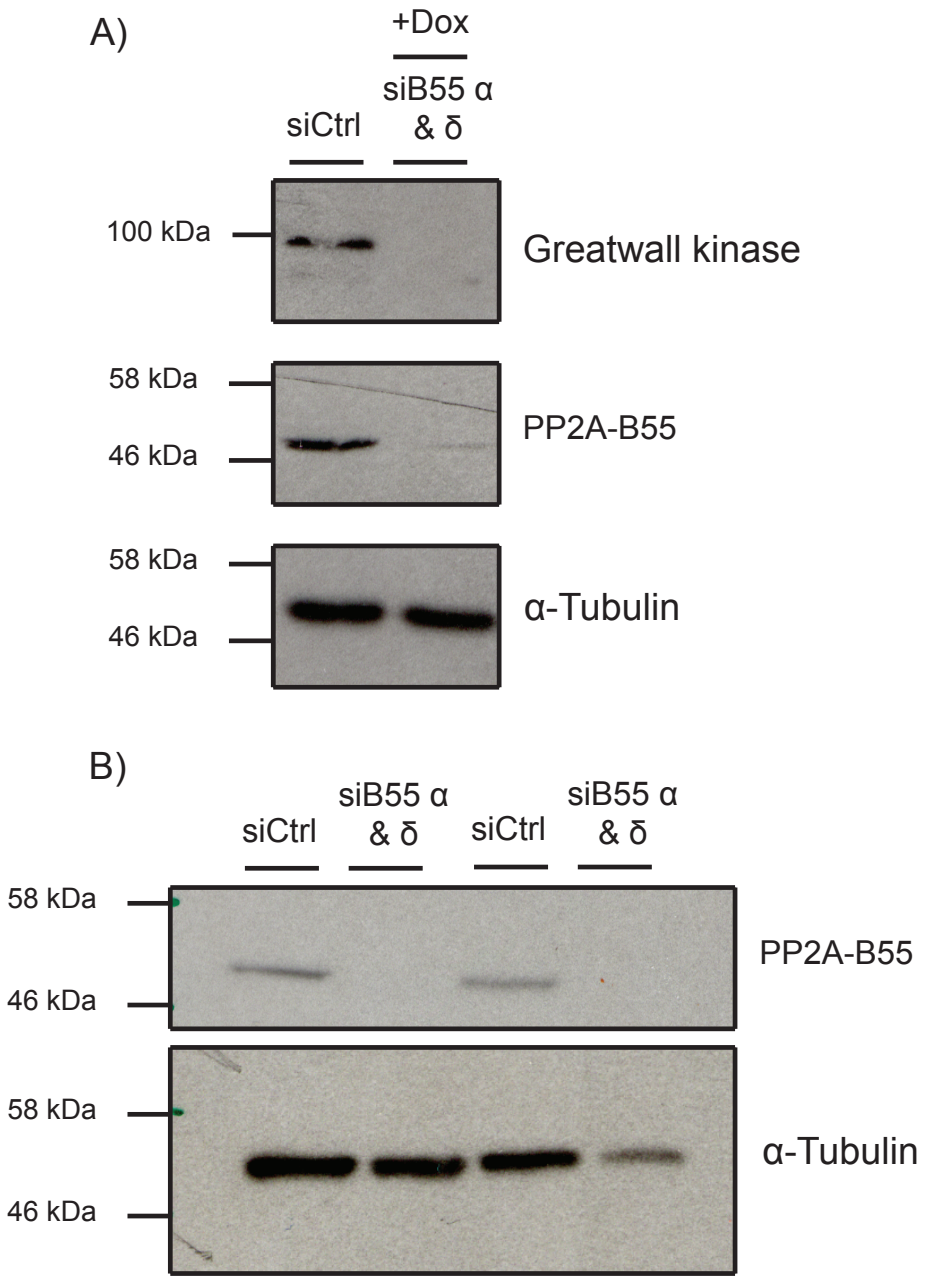

Figure 6.1 Immunoblot to show the knockdown of GWL and PP2A-B55 shGWL induced for a total of 5 days and siPP2A-B55α & δ induced for a total of three days prior to cell harvesting. A) Immunoblot of the first biological replicate showing how GWL and PP2A-B55 can successfully be knocked down simultaneously B) Immunoblot of PP2A-B55 of the second and third biological replicates.

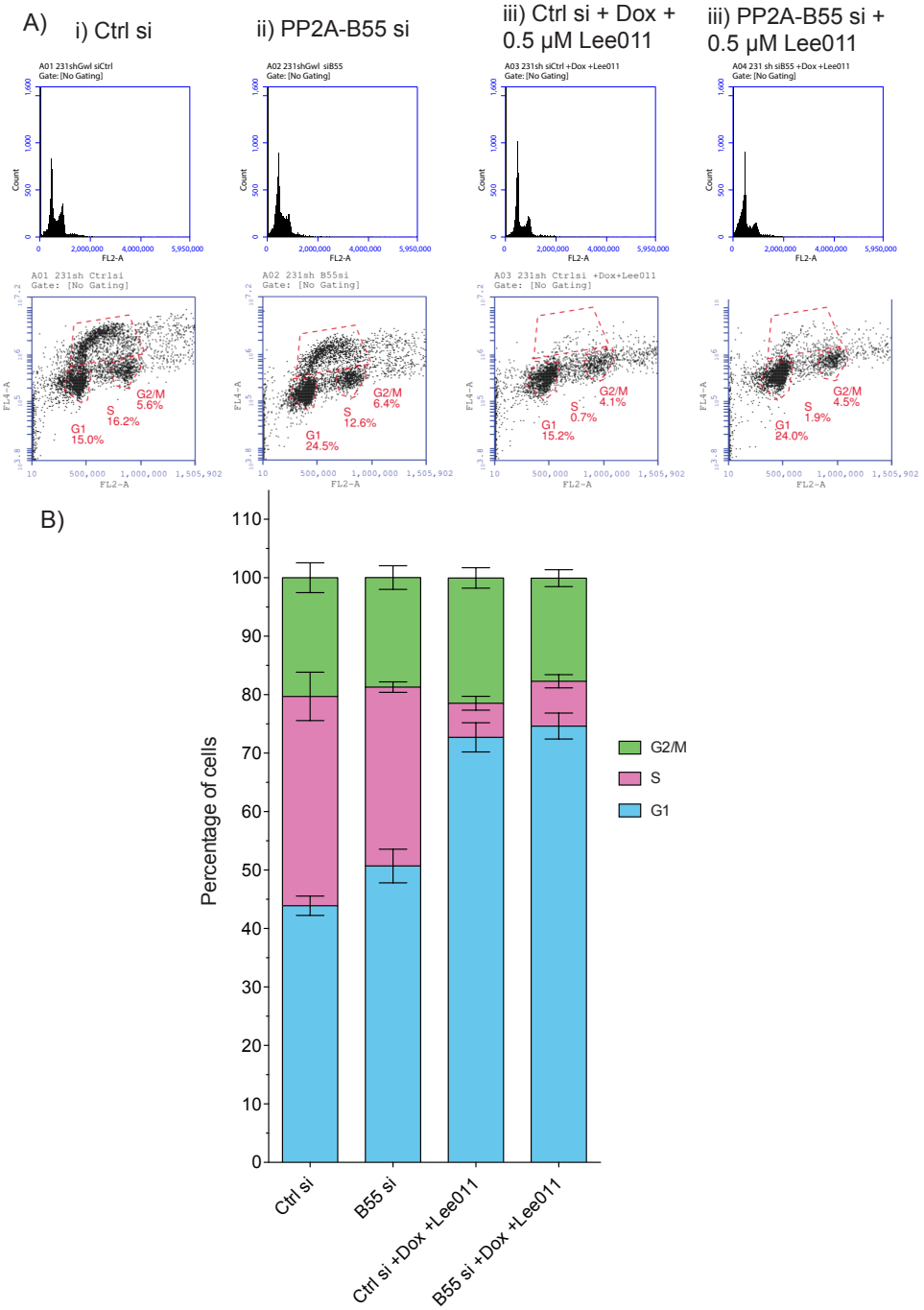

Fig. 6.2 Knockdown of PP2A-B55α and δ does not rescue MDA-MB-231 cells from the Greatwall kinase and Cdk4/6 synergistic effect on the G1- and S-phase population MDA-MB-231 shGwl cells treated with 2 µM Dox for 5 days and the indicated siRNA for 72 hours. In the final 24 hours, some cells were also treated with 0.5 µM Ribociclib/Lee011. A) Representative FACS plot B) Means of N=3 experiments normalised. Unpaired t-tests found no significant differences between the cell cycle populations of the Ctrl si +Dox +Lee011 and the B55α and δ si +Dox +Lee011 groups.

In **Fig. 6.2**, the phenotype in which the G1 population increases and the S population is significantly decreased that was shown in **Chapter 4** is replicated in the Ctrl siRNA + Dox + Lee011 cells. When cells are also treated with siB55 α and δ, the S-phase population is only marginally increased, and these changes are not statistically significant according to an unpaired t-test (GraphPad Prism analysis).

6.3 The Greatwall-CDK4 synergy is recapitulated by ENSA/ARPP depletion

To implicate PP2A inhibition in the CDK4 synergy we tested, we would see a similar synergy following depletion of the GWL substrates ENSA and ARPP19 with siRNA. MDA-MB-231 cells were transfected with siCtrl or both siENSA and siARPP19 for a total of 72 hours. In the final 24 hours before cell harvesting, the 0.5 μM dose of Lee011/Ribociclib was added. I did not treat the cells with Dox as this would have knocked down GWL upstream of ENSA/ARPP19 and the GWL-CDK4 synergy phenotype would be seen instead. The immunoblots showing the knockdown of ENSA across the three biological replicates are shown in **Figure 6.3**. A representative FACS plot for this experiment and the normalised cell cycle phase populations for the three replicates are shown in **Figure 6.4**. ENSA/ARPP19 depletion had only minor effects on the cell cycle profile of MDA-MB-231 cells resulting in a small increase in G2/M cells. Moreover, combined inhibition of CDK4 and ENSA/ARPP19 depletion did not show a significant decrease in the S-phase population, as previously observed in GWL depleted cells. This result suggests that GWL does not act in this particular pathway via its canonical substrates ENSA/ARPP19.

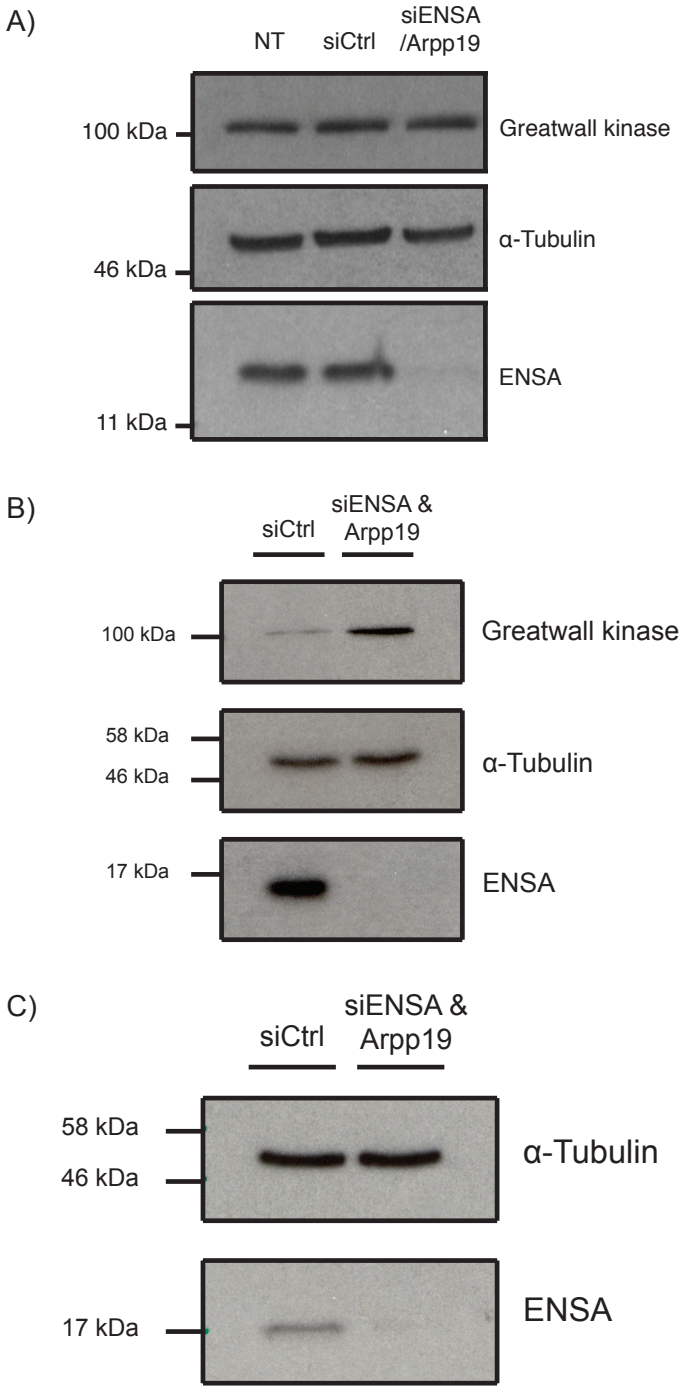

Figure 6.3 Immunoblot to show the knockdown of ENSA shGWL induced for a total of 5 days and siENSA and siArpp19 induced for a total of three days prior to cell harvesting. A) Immunoblot of the first biological replicate showing how ENSA can successfully be knocked down B) Immunoblot of the second replicate C) Immunoblot of the third replicate.

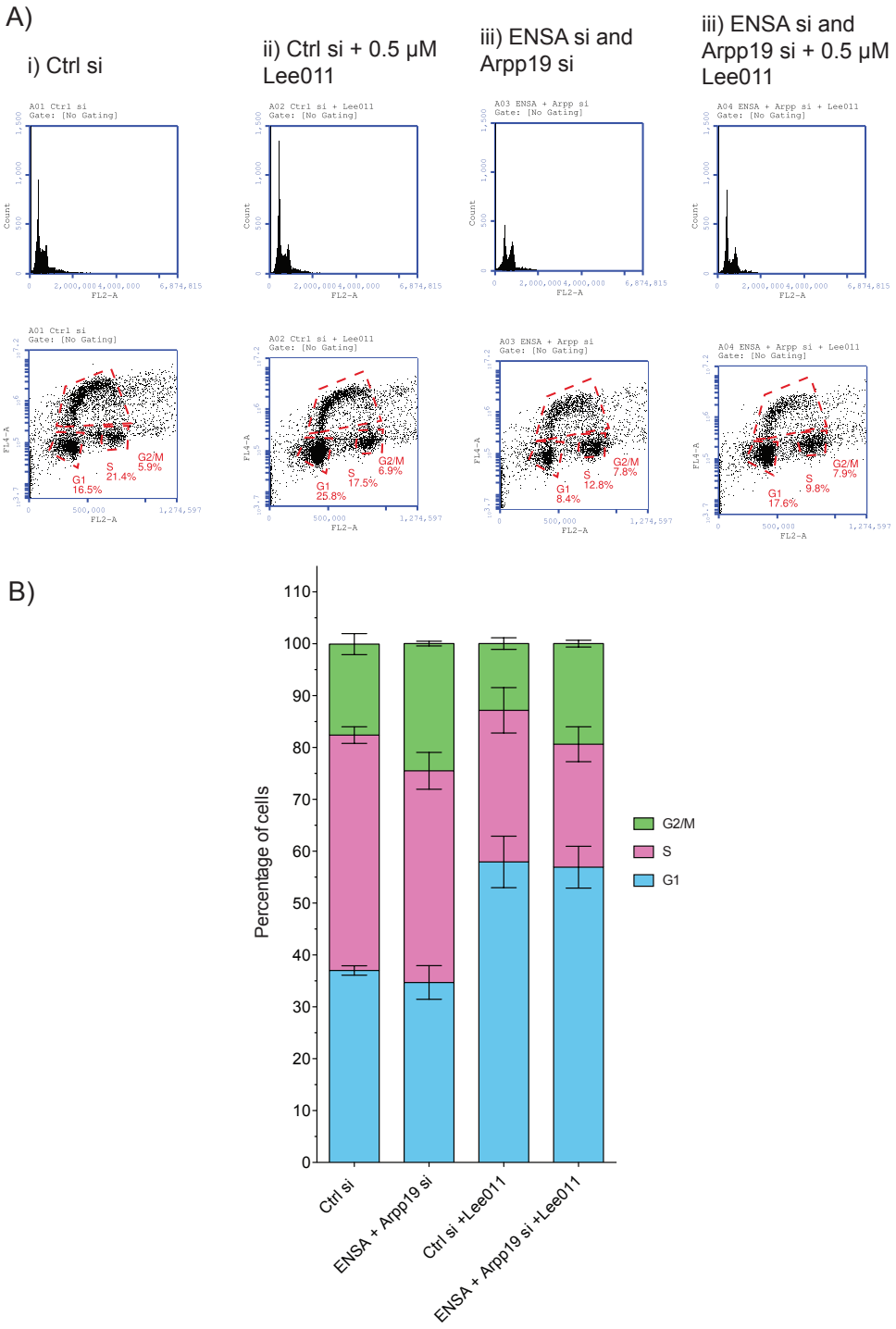

Figure 6.4 Greatwall kinase/CDK4 synergy is not reversed by co-depletion of ENSA and Arpp19 siENSA and siArpp19 induced for a total of three days, and 24 hours treatement with 0.5 μM Ribociclib/Lee011 prior to cell harvesting. A) Representative FACS plot B) Means of N=3 experiments normalised.

This hints at an ENSA and ARPP19 independent function of GWL that pertains to the G1/S phase transition.

6.4 Greatwall and CDK4 act in parallel on CDK2 activity in interphase cells

To further investigate the mechanism of GWL and CDK4 synergy on S-phase progression we employed a single cell assay for CDK2 activity. This is based on work from the Meyer lab (Spencer et al. 2013) that reported a CDK2 probe based on cellular localisation. This fluorescent fusion protein is found in the cytoplasm when CDK2 activity is high, and in the nucleus when it is low. The ratio of nuclear and cytoplasmic signal is thus a direct read-out for CDK2 kinase activity.

We obtained a lentiviral expression plasmid containing the DHB-Venus fusion protein from Sabrina Spencer and exchanged the Venus FP with mCherry to visualise the probe in our GFP expression shRNA cells. Stable cell lines were generated and incubated for 3 days with Dox to deplete GWL. We then added 0.5 μM Lee01 and imaged the cells for 25 hours using the Operetta high-throughput microscope. **Figure 6.5A** shows that GWL depletion alone has a significant effect on CDK2 activation following cytokinesis. However, the effect of CDK4 inhibition alone is more pronounced and comparable to the double treatment. It appears that there is an upward trend in CDK2 in activity in the CDK4 inhibited cells which is not present in the double treatment cells than in the later time points (around 10-14 hours post cytokinesis). However, this does not appear to be highly significant. Later time points may reveal a more

dramatic effect of the double treatment on CDK2 reactivation, compared to CDK4 inhibition on its own.

There was, however a striking difference in the cells lacking both GWL and CDK4 activity. In **Figure 6.5B**, the levels of CDK2 activity are judged by eye and an example of this qualitative classification is shown in **Figure 6.5C**. The medium CDK2 activity is when there is no discernible difference in fluorescence between inside and outside the nucleus. High CDK2 activity is when the cytoplasm shows high fluorescence and there is no fluorescence in the nucleus. Low CDK2 activity is when the nucleus clearly shows higher fluorescence than the cytoplasm. Cells with high CDK2 activity were either undergoing mitosis and reverting to G1 or maintaining the CDK2-high state throughout the experiment. In the double inhibited cells, however, every single CDK2-high cell that we observed reverted to a CDK2-low state within 5-10 hours after CDK4 inhibition (**Fig 6.5B**).

These data suggest that GWL and CDK4 collaborate to maintain a high CDK2 activity throughout interphase. The mechanism of this interaction remains to be determined but is likely to involve RB phosphorylation. Indeed, previous work (K. E. Knudsen et al. 2000) has found that RB dephosphorylation in S-phase can cause a cell cycle exit, and that this frequently occurs in response to DNA damaging agents.

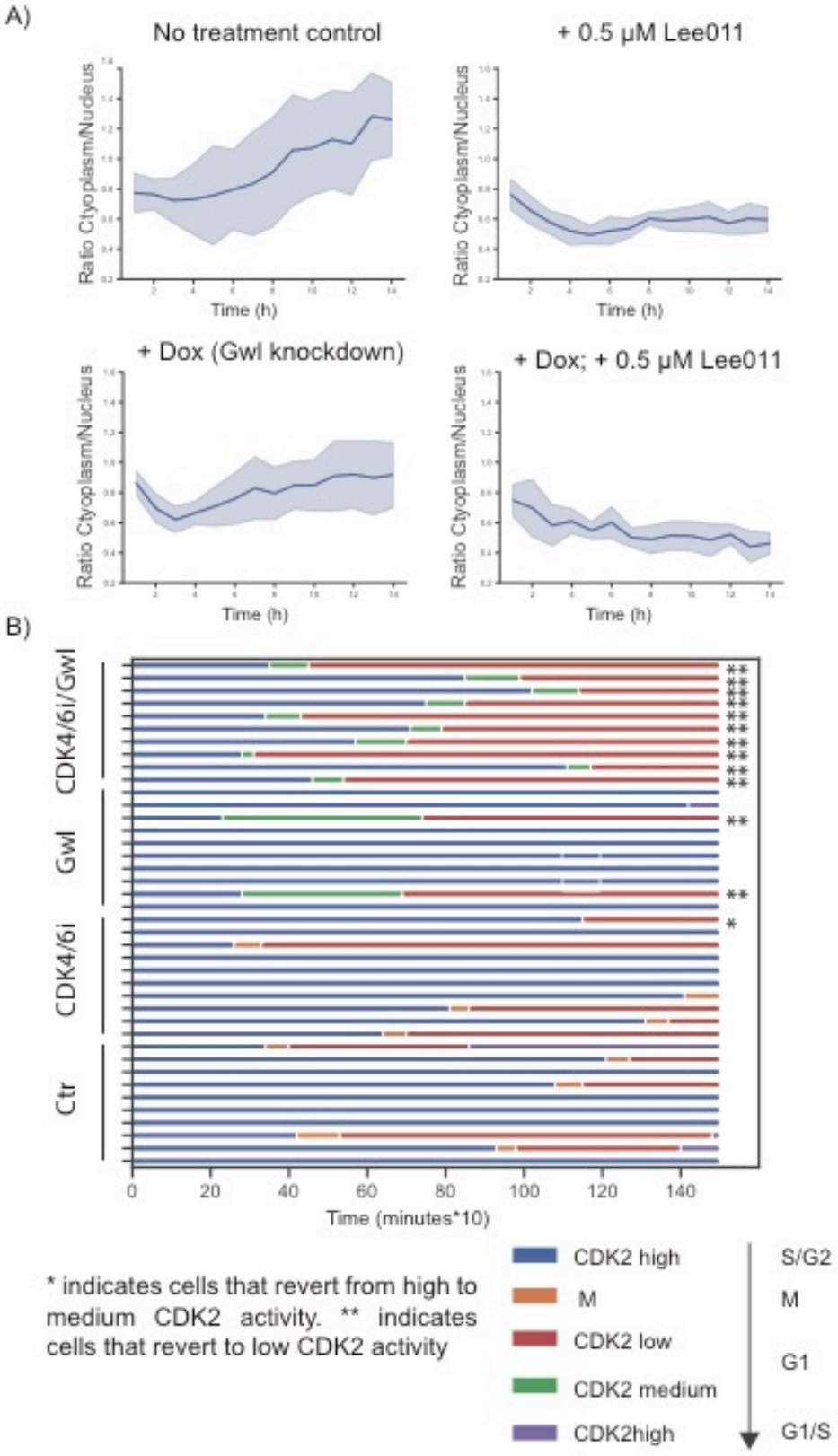
A)
No treatment control
+ 0.5 μM Lee011
+ Dox (Gwl knockdown)
+ Dox; + 0.5 μM Lee011
Ratio Ctyoplasm/Nucleus
Time (h)
B)
CDK4/6i/Gwl
Gwl
CDK4/6i
Ctr
Time (minutes*10)
* indicates cells that revert from high to medium CDK2 activity. ** indicates cells that revert to low CDK2 activity
CDK2 high
M
CDK2 low
CDK2 medium
CDK2high
S/G2
M
G1
G1/S

C)

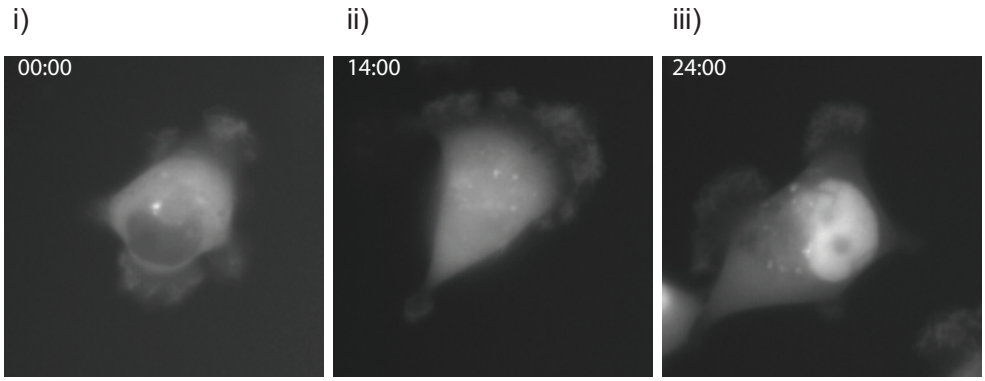

Figure 6.5 Effects of GWL depletion and/or CDK4/6 inhibition on CDK2 activity

A) CDK2 activity was quantified by measuring the ratio of mean cytoplasmic/mean nuclear fluorescent intensity of the DHB-mCherry probe. Each cell was followed in hourly intervals with the first timepoint co-inciding with cytokinesis.

B) Qualitative analysis of CDK2 activity in cells that showed high activity (cytoplasmic probe localistion at the onset of the experiment.

* indicates cells that revert from high to medium CDK2 activity.

** indicates cells that revert to low CDK2 activity.

C) Example of a Greatwall depleted cell following CDK4 inhibition that reverts to a CDK2-low state without intermittent mitosis. i) High CDK2 activity is when the cytoplasm shows high fluorescence and there is no fluorescence in the nucleus. ii) The medium CDK2 activity is when there is no discernable difference in fluorescence between inside and outside the nucleus. iii) Low CDK2 activity is when the nucleus clearly shows higher fluorescence than the cytoplasm.

6.5 Conclusions and discussion

This chapter attempted to elucidate the mechanism underpinning the synthetic lethality between GWL and CDK4 that has been observed in the TNBC cell line, MDA-MB-231. The most obvious first candidate would be that this mechanism is mediated by PP2A-B55. This theory being that if PP2A were responsible for inhibiting the activation of CDK4 and/or inhibiting the phosphorylation of RB, then GWL would be linked to CDK4 via its indirect regulation of PP2A-B55. However, when we knocked down the α and δ subunits of PP2A-B55, there was no rescue of the S phase population, indicating that another protein was keeping the cells in a G1-like state of arrest. Because GWL influences PP2A-B55 activity via it's known substrates, ENSA and ARPP19, if the knockdown of these proteins in combination with the CDK4/6 inhibition ameliorated the S phase population, then this would indicate that the BEG pathway (PP2A-B55α/ENSA/GWL) is involved.

Overall, the work in this chapter challenges the idea that GWL exclusively works in mitosis via its substrates ENSA and ARPP19 to inhibit PP2A-B55. Our findings point to an ENSA/ARPP19 independent role of the kinase in G1 and S-phase in concert with CDK4. Given that these effects have been observed in RB positive cells and previous chapters showed the RB negative cell MDA-MB-436 cells resistant to this treatment, it is likely that RB is the ultimate target of this pathway. Although, GWL could act on other aspects of CDK2 activity, such as Y15 dephosphorylation, or CKI stability. However, these effects should also be observable in RB negative cells.

GWL could be directly involved in RB phosphorylation, or act via regulating RB phosphatases. It is also possible that this new function does not depend on the GWL kinase activity but involves a kinase independent mechanism. Further work will be required to uncover how precisely CDK4 and GWL support each other to maintain CDK2 activity.

Chapter 7. General discussion and future directions

The work presented here has focused on searching for a weakness in the armour of TNBC cells by examining the role of the mitotic kinase GWL. The use of a stable, Dox-inducible shRNA-mediated knockdown system allowed for flexible investigation of GWL depletion phenotypes in TNBC cells. Using this system, we found that GWL knockdown reduces cell proliferation, causes a reduction in the number of actively cycling cells (as shown by a reduction in the S phase population), and causes cells to exit the cell cycle and enter either senescence or quiescence, or commit apoptosis, probably following mitotic catastrophe. This data is largely in agreement with other works regarding GWL knockdown phenotypes (Álvarez-Fernández et al. 2013). However, we were surprised to find that the major consequence of loss of GWL in these cells appeared to be on the replicating cell population, and not on the progression through mitosis, which would have been the expected result. Another interesting part of our work, supported by the recent study from the Malumbres lab (Álvarez-Fernández, Sanz-Flores, Sanz-Castillo, Salazar-Roa, Partida, Zapatero-Solana, Ali, Manchado, Lowe, VanArsdale, Shields, Caldas, Quintela-Fandino & Malumbres 2018b) is the different responses to GWL depletion in various cell types. To date, no GWL knockout cell line that is viable has been reported and it is likely that small amounts of the kinase are absolutely critical for mitotic function. However, cancer cells often have highly elevated levels of this protein and a subset of these cells has become very sensitive to perturbations of GWL activity. Clearly, we do not necessarily see a correlation between high expression and sensitivity (compare for example, the GWL levels

observed in MDA-MB-231 and MDA-MB-436 cells). This makes it difficult to conclude on a presumptive 'tumour driver' function of GWL, and other biomarkers are urgently needed to predict sensitivity to GWL inhibition.

The observed S phase defects described in **Chapter 3** are a reduced number of EdU positive (S phase) cells as well as a reduction in the total mean EdU intensity, which indicates a reduced number of firing DNA replication forks. This is in contradiction with the study that found that total knockdown of GWL caused cells to arrest in G2, and partial knockdown caused arrest in prometaphase (summarised in **Table 1.1**) (Burgess et al. 2010). Though that study by the Castro group was carried out in HeLa (cervical cancer) cells, which may behave differently to breast cancer cell lines. A more careful analysis of this phenotype will be necessary to conclude on the exact effects of GWL on the replication machinery. However, the Castro study already provides a potential mechanism by suggesting Treslin stability as a potential target (Charrasse et al. 2017). Further work on this subject will require means to specifically inhibit GWL in interphase to rule out knock-on effects from segregation errors in the previous mitosis. Specific inhibitors of GWL would be useful, but combination of cell synchronisation and depletion may also be a potential way forward to further address this phenotype. A factor that is confounding efforts to synthesise selective and powerful GWL inhibitor molecules is the fact that no X-ray structures of full-length GWL are available. Although the amino acid sequence of GWL is highly related to the N- and C-terminal kinase lobes of the MAST kinases (microtubule-associated serine/threonine kinase; MAST1, 2, 3 and 4) and other AGC kinases, GWL has

an unusual ~500 amino acid insertion between the DFG and APE motifs of the activation segment connecting the N- and C-terminal lobes - a feature which so far has prevented full-length crystallography of the protein (Blake-Hodek et al. 2012; Ocasio et al. 2016). Given the lack of mechanistic insight in the observed S-phase defects in GWL depleted cells, we chose a genetic approach to further investigate this phenotype. This, a major part of this work was dedicated to finding and validating a synthetic lethality hit in combination with GWL depletion. This thesis shows for the first time a synthetic sensitivity relationship between the cell cycle kinases GWL and CDK4. This interaction was initially discovered in a siRNA and drug screen, and then validated in a panel of breast cells using shGWL and in MDA-MB-231 cells with inducible CRISPR-Cas9 GWL knockout.

Synthetic lethality is a well-established concept and should be based on careful quantification. Synergism can be defined as an effect that is more than additive, whereas antagonism is an effect that is less than additive (Chou 2006; Foucquier & Guedj 2015). The colony formation assays and EdU incorporation assays that I performed are not suitable to perform this type of classification, but just suggest an overall trend of synergy. As shown by the results in **Chapter 5**, GWL depletion has a noticeable deleterious effect on a cell type, and a low dose of CDK4/6 inhibitor alone (0.5 μM Ribociclib/Lee011 or 50 nM Palbociclib) has minimal effect. However in combination they have an effect that is greater than that of GWL depletion alone, so this effect could be described as enhancement or potentiation (Chou 2006). The observed effect could indeed be truly synergistic, but a different experimental set up would be needed to

determine if this is the case. Whilst the synthetic sensitivity observed in **Chapter 5** is very clear, as a next step, clonogenic assays should be designed with the Loewe or Bliss scoring systems in mind to assess the size of the effect caused by this combination treatment with GWL depletion and CDK4/6 inhibition. There are software packages available to calculate such scores, such as CompuSyn for the Loewe model (Chou 2006). Asghar and colleagues used the sulforhodamine B (SRB) cell viability assay and the Bliss addition score system to quantify at which doses and in which cell lines a CDK4/6 inhibitor and a PI3K inhibitor were acting in synergy (Asghar et al. 2017).

It is striking that the observed effects of GWL and CDK4 are exclusive to an RB-positive TNBC cell line, while not observed in an RB-negative cell line. This suggests that ultimately the effects of GWL on progression from G1 to S-phase are likely to occur on the level of RB phosphorylation. Initially we hypothesised that GWL could participate in this pathway via ENSA/ARPP19 dependent inhibition of PP2A-B55, for example by reducing the RB phosphatase activity. However, the results presented in **Chapter 6** points to the surprising conclusion that the function of GWL does not rely on its canonical downstream target. Efficient depletion of ENSA/ARPP19 does not synergise with CDK4 inhibition, and PP2A-B55 subunit α and δ depletion does not prevent this synergy. It is thus tempting to speculate that GWL acts either via a novel substrate, or in a kinase independent manner in concert with CDK4.

The final experiments of this thesis further substantiate our findings on a new GWL function in the G1/S phase of the cell cycle. We observe a clear effect of

GWL depletion on CDK2 reactivation in G1 phase. Moreover, cells that have already high CDK2 activity and are in late G1 or S phase revert back to a low CDK2 state after double kinase inhibition. A similar reversion of S phase was previously observed following RB dephosphorylation (K. E. Knudsen et al. 2000). It could be speculated that GWL is required in cells that are RB positive and suffer from high replication stress to support CDK4 in maintaining RB phosphorylation and allow S phase progression. This is a testable hypothesis, and the further work that is required will be carried out by the Hochegger lab to further investigate this mechanism. Spencer and colleagues demonstrated that the bifurcation of cell fate into either a more proliferative or resting state after mitogen starvation is determined by the CDK inhibitor p21 (Spencer et al. 2013). They used time-lapse microscopy, followed by fixed-cell immunostaining and a jitter-correction computer script to trace individual fixed, antibody-stained cells back to their corresponding live filmed cells. They found that high levels of p21 were responsible for causing a cell to enter the $CDK2^{low}$ state after mitosis (Spencer et al. 2013). A similar strategy could be used to work out what state the breast cancer cell lines enter after being treated with single and double treatments of GWL knockdown and CDK4/6 inhibitor by filming and immunostaining the cells for RB phosphorylation and p21. This could be done using the method outlined above (Spencer et al. 2013) or with flow cytometry if tracing individually back to each live cell was not deemed necessary. Cells could be fixed at various time points and then have their RB phosphorylation levels and/or p21 levels analysed with one of these methods. For example, antibodies (including fluorescent conjugates) to detect RB phosphorylation at Serine 807/811 are available, and so could be used in flow cytometry and

immunoblotting experiments to see if double treatment of GWL depletion and CDK4/6 inhibition causes a reduction in this RB phosphorylation. Including conditions with and without serum starvation could also be interesting. I would predict that since the majority of cells treated with both GWL shRNA and CDK4/6 inhibitor showed a low ratio of Cytoplasm/Nuclear DHB-mCherry probe, these cells would show hypo-phosphorylated RB, high p21 levels, and would not progress into S phase.

The flow cytometry experiments in **Chapters 5** and **6** show a large accumulation of cells that are apparently in G1 phase. This could be due to cell cycle arrest at G1, or perhaps exhaustion of S/G2/M phase cells due to cell death, and any remaining G1 cells might be still technically be cycling. In addition, because many previous studies of GWL depletion in human cells report mitotic defects (**Table 1.1**), as well as some observed cell death in the live cell imaging (**Figures 3.9** and **3.10**) some further experiments should be done to clearly determine if any of the observed phenotypes in this thesis are due to a mitotic arrest or mitotic catastrophe. Whilst classifying the cells by DNA content using PI staining in the flow cytometry experiments should distinguish between G1 and M cells, there is the possibility that many mitotic cells were lost. An issue with the flow cytometry experiments in this thesis is that the cell culture medium, which may have contained many dead and mitotic cells, was discarded during cell harvesting and fixation. To be more certain on the mitotic status of cells treated with both GWL shRNA and CDK4/6 inhibitor, some more live cell imaging and flow cytometry experiments should be done. Live cell imaging with fluorogenic cytoskeletal and DNA markers suitable for live cell

microscopy should be performed, such as SiR-tubulin and SiR-DNA. The microtubules, the doubled centrosomes and chromosomes behave very distinctively and uniquely during mitosis, and so mitotic phenotypes following synthetic sensitivity should be visible, if present. Another method would be to analyse cyclin levels using flow cytometry, whilst also using PI staining for DNA content (Pozarowski & Darzynkiewicz 2004). As shown in **Figure 1.1**, Cyclin D1 is expressed by some G1 cells as well as some cells entering and progressing through S phase, and most G2/M cells are Cyclin D1 negative. Cells express Cyclin A as they enter S phase, and maximally by G2 cells whereas mitotic cells (post-prometaphase) are Cyclin A negative. Cyclin B is expressed by late S cells, which peaks in G2/M. Mitotic cells should also not be expressing Cyclin E. Thus, staining cells for at least Cyclin B1 to detect mitotic cells, as well as one other to find some G1 cells such as Cyclin D1 (Pozarowski & Darzynkiewicz 2004), whilst using treatments to deplete GWL and CDK4, should provide some resolution as to where in the cell cycle the affected cells are.

In addition, experiments should be carried out for G1 arrest markers. The experiments of **Chapters 5** and **6** ideally should be repeated and expanded as described below, including harvesting the original cell culture medium to analyse the cells within, which could include dead and mitotic cells. However, there is no singular marker for G1 arrest, and the cell cycle pathways are often disrupted in cancer cells and so a range of markers should be analysed. As mentioned in **Chapter 5**, time course immunoblots tracking the cell cycle status of the culture over several days could be performed. Then these immunoblots could be probed for multiple G1 arrest markers such as Cdt1, p53, p21, p27

and p16. Experiments probing for senescent cells could be done, such as a β-galactosidase assay. Also, the fluorescent marker mVenus p27K$^-$ is able to label quiescent cells so this experiment could be done via IF microscopy (Oki et al. 2014).

The inhibitors of CDK4 in clinical use also inhibit CDK6. It could be worth carrying out experiments comparing GWL depletion with siCDK6 and siCDK4 to see if there is any preferential effect between these two CDK enzymes.

The synergy between GWL and CDK4 that is described in this thesis could one day have a significant clinical impact. It remains to be seen, if GWL inhibition will have an effect on cells that have acquired resistance to CDK4 inhibition. If the mechanism of resistance is loss of RB, then it is very unlikely that a beneficial therapeutic effect will emerge. However, RB independent mechanisms of CDK4 resistance, such as Cyclin E and E2F over-expression are frequently observed in cancer (E. S. Knudsen & Witkiewicz 2017) and so could be susceptible to combined GWL and CDK4 treatment. Until specific inhibitors of GWL are discovered, it might be beneficial to test the efficacy of PP2A activator drugs in combination with CDK4/6 inhibitors. A PP2A activating drug is almost the reflection of a GWL inhibitor, by promoting the phosphatase activity rather than shutting off its inhibition by GWL. FTY720 (also known as Fingolimod or Gilenya) is a PP2A activating drug in clinical use as an immunosuppressant for multiple sclerosis patients (Oaks et al. 2013), is gaining interest as a potential cancer therapeutic (Cristóbal et al. 2016) as well as PP2A activating compounds in general as an anti-cancer strategy. This is due to the

known tumour suppressing effects of this phosphatase (C. M. O'Connor et al. 2018; Janssens et al. 2005). Further work on acquired resistance will be necessary to gain more confidence in the therapeutic applicability of the findings presented here. The next steps to interrogate the clinical potential of targeting GWL and CDK4 simultaneously would be to evaluate tumour killing ability and toxicity in *in vivo* studies. MDA-MB-231 cells are commonly used in xenografts, so shRNA-containing cell lines could be grafted into mouse models, and appropriate doses of Dox and Palbociclib given to see if this causes tumour reduction. Measuring the effects of GWL depletion and CDK4 inhibition in 3D tumour models would also be beneficial, as cancer cells behave differently and in a more clinically relevant fashion in 3D. 3D cell cultures create an environment that is closer to *in vivo* than 2D cultures, and so the cells may behave and communicate differently. For example, there could be hypoxic cells in the centre of a 3D culture or organoid. Once GWL inhibitors are available, *in vivo* studies with patient-derived xenografts (PDX) should be tested in immunocompetent mice using combination treatments of GWL and CDK4/6 inhibitors as this would provide toxicity data on the drug treatments, how the mammalian immune system reacts to the treatment, and patient-derived cells are more clinically relevant than cell lines. There is pre-clinical research that suggests CDK4/6 inhibition is beneficial for stimulating anti-tumour immune responses (Deng et al. 2018).

The work presented here tells us that there is much more to be learned about the formerly elusive GWL from the perspectives of both basic and translational biology. Whilst the precise basis for the relationship between GWL and CDK4 remains unknown, this thesis lays the foundation for more exciting discoveries.

A)

Plate	Well	GeneID	GeneID	Collection nu	SC DMSO	SC DOX	GWL DMSO	GWL DOX	SC DE	GWL DE
11	O07	canertinib(pan-ErbBi)(1000nM)	1000nM	ND	-1.442046	-1.8544	-0.930362	-1.643359	-0.363218	-2.066817
12	E13	Lenvatinib(VEGFi)(500nM)	500nM	ND	0.5463485	0.3452834	2.3333891	1.4795056	-0.573577	-2.074239
12	E14	Lenvatinib(VEGFi)(50nM)	50nM	ND	0.5134561	0.7560015	1.4569857	0.6258048	0.6771188	-2.114179
12	J16	PF-03758309(PAKi)(1nM)	1nM	ND	0.2693871	0.1314399	0.3593729	-0.427399	-0.28611	-2.119918
12	G21	XAV-939(TNKSi/Wnti)(500nM)	500nM	ND	-1.666875	-1.39673	0.4856427	-0.312582	1.631063	-2.136843
12	H05	vinorelbine(anti-mitotic)(5nM)	5nM	ND	-0.09963	0.3853391	1.1500528	0.3178415	1.5999589	-2.153061
12	F08	lestaurtinib(1mM)(JAK2/FLT3/TrkAi)(0.2nM)	1000nM	ND	0.1447602	0.5111677	0.6811063	-0.159133	1.1709298	-2.230354
12	B09	olaparib(PARP1/2i)(5nM)	5nM	ND	1.0104216	0.749997	0.8610143	-0.001772	-0.925817	-2.271729
12	B02	NEG	NEG	NEG	-0.979885	-0.864815	-0.431139	-1.262573	0.9221631	-2.336491
11	D12	gemcitabine.HCl(DNArepinhib)(1nM)	1nM	ND	0.226314	0.3827192	0.2242885	-0.644459	0.5523201	-2.362987
11	K03	DMX_1783(TNKSiinhibitor)(1000nM)	1000nM	ND	-1.793894	-1.827943	-0.827391	-1.662268	0.8335923	-2.392546
11	A06	5-FU(anti-metabolite)(50nM)	50nM	ND	1.4387118	1.3443694	1.8035975	0.8355609	-0.634789	-2.452819
12	A11	KU60019(ATMi)(1000nM)	1000nM	ND	-1.520988	-1.254037	-0.291171	-1.211302	1.5634762	-2.565904
12	G09	BIBW2992(EGFR/HER2i)(500nM)	500nM	ND	-2.448082	-1.351694	0.711074	-0.262334	4.2501069	-2.595937
12	E03	PD-0332991(CDK4/6i)(1000nM)	1000nM	ND	-1.278774	-1.182262	0.5305731	-0.480041	0.9906102	-2.720248
12	E10	lestaurtinib(1mM)(JAK2/FLT3/TrkAi)(10nM)	10nM	ND	0.7051088	1.485595	1.9257157	0.8320623	2.1006368	-2.786658
12	E20	AZ4547(FGFRi)(100nM)	100nM	ND	0.4748981	0.086934	2.0271792	0.9043014	-1.066199	-2.85575
12	F12	Lenvatinib(VEGFi)(1nM)	1nM	ND	1.1716193	1.1636919	1.1632414	0.0370929	-0.286304	-2.966217
11	F05	BMN-673(PARPi)(5nM)	5nM	ND	0.3862484	0.3112953	-0.789711	-1.877171	-0.157389	-3.088207
12	F17	PF-332991(CDK4/6i)(5nM)	5nM	ND	0.4082319	0.1266435	0.7175019	-0.435509	-0.742647	-3.092989
11	B10	Sotrastaurin/AEB071(PKCi)(0.5nM)	0.5nM	ND	1.0432658	1.2253646	1.6940685	0.3647754	0.2954053	-3.466968
12	I03	sorafenib(inhibitsRAF,PDGF,VEGF1&2)(1000nM)	1000nM	ND	0.7693564	0.9634793	2.5958677	0.9903248	0.4391165	-4.126803
11	I18	MLN-4924(NEDDi)(50nM)	50nM	ND	1.2997556	1.9144143	3.0655441	0.269879	1.3988818	-7.370332
11	F03	BMN-673(PARPi)(10nM)	10nM	ND	-0.030245	-0.151101	-2.175958	-2.842715	-0.11792	-2.084849
11	G06	Flavopiridol(CDKi)(50nM)	50nM	ND	-1.688806	-2.172382	-1.660859	-2.423279	-0.462646	-2.289541
11	M03	MDV-3100(CRPCi)(1000nM)	1000nM	ND	-3.502861	-4.5179	-4.708064	-5.35084	-1.215541	-2.315578
11	I06	decitabine(DNAmeth)(50nM)	50nM	ND	0.8735419	0.3901952	-1.386466	-2.229046	-1.492611	-2.479515
11	G17	methotrexate(500nM)	500nM	ND	-0.787797	0.1306586	-1.285992	-2.404446	3.0859707	-3.232358
11	M19	KU0057788(DNA-Pki)(1000nM)	1000nM	ND	-2.208364	-2.569809	-2.000693	-3.215043	0.0870174	-3.58204
12	E17	PF-332991(CDK4/6i)(500nM)	500nM	ND	-4.628571	-5.232655	-3.415589	-4.610091	0.3836032	-3.693094
12	E16	PF-332991(CDK4/6i)(100nM)	100nM	ND	-2.55921	-2.441982	-0.692464	-2.022698	1.5634031	-3.749685
12	H03	vinorelbine(anti-mitotic)(10nM)	10nM	ND	-3.248655	-1.522974	-1.211947	-2.663917	6.3275393	-4.148075
12	M05	salinomycin(microtubulepoison)(500nM)	500nM	ND	-5.396891	-2.957345	-2.624382	-4.044916	9.1829357	-4.22672
12	E09	lestaurtinib(1mM)(JAK2/FLT3/TrkAi)(100nM)	100nM	ND	-1.131196	-1.271725	-1.750295	-3.230007	0.270019	-4.288153
12	E15	PF-332991(CDK4/6i)(1000nM)	1000nM	ND	-4.690565	-5.381184	-4.417272	-5.975221	0.1671445	-4.818027
11	E11	crizotonib(ALKi)(1000nM)	1000nM	ND	-7.696137	-8.962741	-3.711268	-5.442284	-0.230708	-5.214854
11	M09	DMX_2320(IKKeinhibitor)(500nM)	500nM	ND	-3.785225	-2.540198	-1.078609	-2.992513	5.2025517	-5.412764
11	M13	2-methoxyestradiol(anti-angiogenesis)(500nM)	500nM	ND	-8.853153	-4.905661	-4.282975	-6.065434	14.779544	-5.42454
11	E13	crizotonib(ALKi)(500nM)	500nM	ND	-5.566222	-3.612868	-2.38994	-4.370513	7.8947905	-5.751463
12	M16	PF-03814735(Aurora)(100nM)	100nM	ND	-3.583774	-4.247776	-3.04835	-5.050834	-0.203772	-5.889472
11	I16	MLN-4924(NEDDi)(100nM)	100nM	ND	-1.169543	-1.088177	-0.371952	-3.955301	0.9044247	-9.957016

B)

Plate	Well	GeneID	GeneID	Collection	SC DMSO	SC DOX	GWL DMSO	GWL DOX	SC DE	GWL DE
11	N13	2-methoxyestradiol(anti-angiogenesis)(5nM)	5nM	ND	0.3861084	0.3686708	-0.600839	0.3743684	0.0031088	2.651048
11	G11	ABT-737(Bcl2i)(1000nM)	1000nM	ND	1.2847477	1.2211398	0.9212217	1.7245956	-0.487128	2.3534249
11	B15	AG-14699(PfizerPARPi)(10nM)	10nM	ND	0.9986351	0.9564976	0.1772355	1.2453253	-0.312158	2.999814
12	E19	AZ4547(FGFRi)(1000nM)	1000nM	ND	0.8718027	0.4819973	0.1019843	0.8933792	-1.230975	2.2240678
12	F20	AZ4547(FGFRi)(1nM)	1nM	ND	0.7656151	0.9424719	0.3047333	1.2725334	0.3924572	2.7368062
12	O14	bleomycinsulfate(DNAbreaks)(50nM)	50nM	ND	-1.517495	-1.977102	-1.634752	-0.792638	-0.464685	2.1608007
11	D03	carboplatin(DNAalkylation)(10nM)	10nM	ND	0.8981875	1.0386809	0.3720867	1.1171332	0.237698	2.1273064
11	K04	DMX_1783(TNKSiinhibitor)(100nM)	100nM	ND	0.7266872	0.1594251	0.0851296	0.8830479	-1.667629	2.2401702
11	N10	DMX_2320(IKKeinhibitor)(0.5nM)	0.5nM	ND	0.0041504	-0.257665	-0.817503	0.0160516	-0.524962	2.2330003
11	H08	erlotinib(EGFRi)(1nM)	1nM	ND	1.2121573	1.2443168	0.7715178	1.5170829	-0.190785	2.1756255
12	B22	GDC-0449(SMOi)(0.5nM)	0.5nM	ND	-0.558081	-0.692718	-0.94759	-0.017508	0.0559415	2.4852773
11	D20	lapatinib(Her2i)(1nM)	1nM	ND	1.4770752	0.7364677	1.2242331	1.9163977	-2.452996	2.0807515
12	C14	MK0752(NOTCHi)(50nM)	50nM	ND	0.930685	1.2961586	0.8029288	1.4915378	0.8522166	2.0214473
11	F20	MK2206(AKTi)(1nM)	1nM	ND	1.665473	1.067483	1.0099652	1.8157033	-2.130936	2.3703938
11	K13	MSC2358705A(DNA-Pki,Merck)(500nM)	500nM	ND	0.8198876	0.693989	0.1340273	0.8558926	-0.473918	2.0351137
11	H20	resveratrol(NSAID)(1nM)	1nM	ND	1.3541537	1.5238663	1.3197288	1.9895362	0.135811	2.0299927
11	B22	RO-3306(CDK1i,2mM)(0.2nM)	0.5nM	ND	0.0058477	0.382937	-0.385898	0.5323516	1.2565993	2.5184055
11	O06	Sapacitabine(CNDAC)(50nM)	50nM	ND	-0.1513	-1.179448	-3.324039	-1.974744	-2.600147	3.3682786
11	K16	SAR-20106(CHK1,Sutton)(100nM)	100nM	ND	0.9839389	1.0807118	0.2576823	1.0488551	0.0812481	2.2417266
12	H06	vinorelbine(anti-mitotic)(0.5nM)	0.5nM	ND	0.3741508	0.8285472	0.3416587	1.2239753	1.3241142	2.5042059
12	L05	voronostat(classI&IIHDACi)(5nM)	5nM	ND	0.228547	0.4308431	-1.296841	-0.350013	0.679436	2.4906992
11	L20	YM155(Survivin-suppressant)(1nM)	1nM	ND	0.0527527	-0.679546	-3.608679	-2.298792	-1.85694	3.2256441

Appendix 1: Raw data from a small molecule drug screen using a panel of drugs on MDA-MB-231 shScr and shGWL cells treated with Dox. Drug names and their targets are listed in column headed 'GeneID' A) Drugs which displayed synthetic sensitivity with GWL. The CDK4/6 inhibitor Palbociclib is highlighted in yellow. B) Drugs which displayed synthetic resistance with GWL.

References

Abraham, R.T., 2001. Cell cycle checkpoint signaling through the ATM and ATR kinases. *Genes & Development*, 15(17), pp.2177–2196.

Alberts, A.J. et al., 2002. *Molecular Biology of the Cell* 5 ed., New York & London: Garland Publishing Inc.

Albiges, L. et al., 2014. Chk1 as a new therapeutic target in triple-negative breast cancer. *The Breast*, 23(3), pp.250–258.

Antoni, L. et al., 2007. CHK2 kinase: cancer susceptibility and cancer therapy – two sides of the same coin? *Nature Reviews Cancer*, 7(12), pp.925–936.

Aono, S. et al., 2018. The fission yeast Greatwall–Endosulfine pathway is required for proper quiescence/G 0phase entry and maintenance. *Genes to Cells*, 24(2), pp.172–186.

Araki, H., 2010. Cyclin-dependent kinase-dependent initiation of chromosomal DNA replication. *Current Opinion in Cell Biology*, 22(6), pp.766–771.

Archambault, V. et al., 2007. Mutations in Drosophila Greatwall/Scant Reveal Its Roles in Mitosis and Meiosis and Interdependence with Polo Kinase. *PLoS genetics*, 3(11), p.e200.

Arnold, A. & Papanikolaou, A., 2005. Cyclin D1 in Breast Cancer Pathogenesis. *JCO*, 23(18), pp.4215–4224.

Asghar, U. et al., 2015. The history and future of targeting cyclin-dependent kinases in cancer therapy. *Nature Reviews Drug Discovery*, 14, pp.130 EP –.

Asghar, U.S. et al., 2017. Single-Cell Dynamics Determines Response to CDK4/6 Inhibition in Triple-Negative Breast Cancer. *Clinical cancer research : an official journal of the American Association for Cancer Research*, 23(18), pp.5561–5572.

Ashworth, A. & Lord, C.J., 2018. Synthetic lethal therapies for cancer: what's next after PARP inhibitors? *Nature Reviews Clinical Oncology*, 15(9), pp.564–576.

Álvarez-Fernández, M. et al., 2013. Greatwall is essential to prevent mitotic collapse after nuclear envelope breakdown in mammals. *Proceedings of the National Academy of Sciences of the United States of America*, 110(43), pp.17374–17379.

Álvarez-Fernández, M., Sanz-Flores, M., Sanz-Castillo, B., Salazar-Roa, M., Partida, D., Zapatero-Solana, E., Ali, H.R., Manchado, E., Lowe, S., VanArsdale, T., Shields, D., Caldas, C., Quintela-Fandino, M. & Malumbres, M., 2018a. Therapeutic relevance of the PP2A-B55 inhibitory kinase MASTL/Greatwall in breast cancer. *Cell Death & Differentiation*, 25(5), pp.828–840.

Álvarez-Fernández, M., Sanz-Flores, M., Sanz-Castillo, B., Salazar-Roa, M., Partida, D., Zapatero-Solana, E., Ali, H.R., Manchado, E., Lowe, S., VanArsdale, T., Shields, D., Caldas, C., Quintela-Fandino, M. & Malumbres, M., 2018b. Therapeutic relevance of the PP2A-B55 inhibitory kinase MASTL/Greatwall in breast cancer. *Cell Death & Differentiation*, 25(5), pp.828–840.

Bandara, L.R. et al., 1991. Cyclin A and the retinoblastoma gene product complex with a common transcription factor. *Nature*, 352(6332), pp.249–251.

Barberis, M., Spiesser, T.W. & Klipp, E., 2010. Replication Origins and Timing of Temporal Replication in Budding Yeast: How to Solve the Conundrum? *Current Genomics*, 11(3), pp.199–211.

Barnum, K.J. & O'Connell, M.J., 2014. Cell Cycle Regulation by Checkpoints. *Methods in molecular biology (Clifton, N.J.)*, 1170, pp.29–40.

Barr, F.A., Elliott, P.R. & Gruneberg, U., 2011. Protein phosphatases and the regulation of mitosis. *Journal of Cell Science*, 124(14), pp.2323–2334.

Barrière, C. et al., 2007. Mice thrive without Cdk4 and Cdk2. *Molecular Oncology*, 1(1), pp.72–83.

Bartek, J. & Lukas, J., 2003. Chk1 and Chk2 kinases in checkpoint control and cancer. *Cancer Cell*, 3(5), pp.421–429.

Baughn, L.B. et al., 2006. A Novel Orally Active Small Molecule Potently Induces G 1Arrest in Primary Myeloma Cells and Prevents Tumor Growth by Specific Inhibition of Cyclin-Dependent Kinase 4/6. *Cancer Res.*, 66(15), pp.7661–7667.

Beauséjour, C.M. et al., 2003. Reversal of human cellular senescence: roles of the p53 and p16 pathways. *EMBO J.*, 22(16), pp.4212–4222.

Beijersbergen, R.L., Wessels, L.F.A. & Bernards, R., 2017. Synthetic Lethality in Cancer Therapeutics. *Annu. Rev. Cancer Biol.*, 1(1), pp.141–161.

Bell, S.P. & Dutta, A., 2002. DNA Replication in Eukaryotic Cells. *Annu. Rev. Biochem.*, 71(1), pp.333–374.

Berthet, C. et al., 2003. Cdk2 Knockout Mice Are Viable. *Current Biology*, 13(20), pp.1775–1785.

Bertoli, C., Skotheim, J.M. & de Bruin, R.A.M., 2013. Control of cell cycle transcription during G1 and S phases. *Nature Reviews Molecular Cell Biology*, 14, pp.518 EP –.

Besson, A. et al., 2007. Discovery of an oncogenic activity in p27(Kip1) that causes stem cell expansion and a multiple tumor phenotype. *Genes & Development*, 21(14), pp.1731–1746.

Bharadwaj, R. & Yu, H., 2004. The spindle checkpoint, aneuploidy and cancer. *Oncogene*, 23(11), pp.2016–2027.

Bianchini, G. et al., 2016. Triple-negative breast cancer: challenges and opportunities of a heterogeneous disease. *Nature Reviews Clinical Oncology*, 13(11), pp.674–690.

Bisschops, M.M.M. et al., 2014. To divide or not to divide: A key role of Rim15 in calorie-restricted yeast cultures. *Biochimica et Biophysica Acta (BBA) - Molecular Cell Research*, 1843(5), pp.1020–1030.

Blagosklonny, M.V., 2004. Analysis of FDA Approved Anticancer Drugs Reveals the Future of Cancer Therapy. *Cell Cycle*, 3(8), pp.1033–1040.

Blake-Hodek, K.A. et al., 2012. Determinants for Activation of the Atypical AGC Kinase Greatwall during M Phase Entry. *Molecular and Cellular Biology*, 32(8), pp.1337–1353.

Bollen, M., Gerlich, D.W. & Lesage, B., 2009. Mitotic phosphatases: from entry guards to exit guides. *Trends in cell biology*, 19(10), pp.531–541.

Bolognese, F. et al., 1999. The cyclin B2 promoter depends on NF-Y, a trimer whose CCAAT-binding activity is cell-cycle regulated. *Oncogene*, 18, pp.1845 EP –.

Bomont, P. et al., 2005. Unstable microtubule capture at kinetochores depleted of the centromere-associated protein CENP-F. *EMBO J.*, 24(22), pp.3927–3939.

Bousset, K. & Diffley, J.F., 1998. The Cdc7 protein kinase is required for origin firing during S phase. *Genes & Development*, 12(4), pp.480–490.

Boutros, R., Lobjois, V. & Ducommun, B., 2007. CDC25 phosphatases in cancer cells: key players? Good targets? *Nature Reviews Cancer*, 7(7), pp.495–507.

Brandeis, M. et al., 1998. Cyclin B2-null mice develop normally and are fertile whereas cyclin B1-null mice die in utero. *Proceedings of the National Academy of Sciences*, 95(8), pp.4344–4349.

Brito, D.A., Yang, Z. & Rieder, C.L., 2008. Microtubules do not promote mitotic slippage when the spindle assembly checkpoint cannot be satisfied. *The Journal of Cell Biology*, 182(4), pp.623–629.

Brown, A.J., Jones, T. & Shuttleworth, J., 1994. Expression and activity of p40MO15, the catalytic subunit of cdk-activating kinase, during Xenopus oogenesis and embryogenesis. *Molecular Biology of the Cell*, 5(8), pp.921–932.

Brown, E.J. & Baltimore, D., 2003. Essential and dispensable roles of ATR in cell cycle arrest and genome maintenance. *Genes & Development*, 17(5), pp.615–628.

Burgess, A. et al., 2010. Loss of human Greatwall results in G2 arrest and multiple mitotic defects due to deregulation of the cyclin B-Cdc2/PP2A balance. pp.1–6.

Campisi, J. et al., 1982. Restriction point control of cell growth by a labile protein: evidence for increased stability in transformed cells. *Proceedings of the National Academy of Sciences of the United States of America*, 79(2), pp.436–440.

Cao, L. et al., 2016. Chronological Lifespan in Yeast Is Dependent on the Accumulation of Storage Carbohydrates Mediated by Yak1, Mck1 and Rim15 Kinases. *PLoS genetics*, 12(12), pp.e1006458–e1006458.

Cappell, S.D. et al., 2016. Irreversible APCCdh1 Inactivation Underlies the Point of No Return for Cell-Cycle Entry. *Cell*, 166(1), pp.167–180.

Carter, S.L. et al., 2006. A signature of chromosomal instability inferred from gene expression profiles predicts clinical outcome in multiple human cancers. *Nature Genetics*, 38(9), pp.1043–1048.

Castilho, P.V. et al., 2009. The M Phase Kinase Greatwall (Gwl) Promotes Inactivation of PP2A/B55. pp.1–13.

Charrasse, S. et al., 2017. Ensa controls S-phase length by modulating Treslin levels. *Nature Communications*, 8, p.206.

Chavez, K.J., Garimella, S.V. & Lipkowitz, S., 2010. Triple Negative Breast Cancer Cell Lines: One Tool in the Search for Better Treatment of Triple Negative Breast Cancer. *Breast disease*, 32(1-2), pp.35–48.

Chen, H., Liu, H. & Qing, G., 2018. Targeting oncogenic Myc as a strategy for cancer treatment. *Signal Transduction and Targeted Therapy*, 3(1), p.5.

Cheung, T.H. & Rando, T.A., 2013. Molecular regulation of stem cell quiescence. *Nature Reviews Molecular Cell Biology*, 14(6), pp.10.1038/nrm3591–340.

Chica, N. et al., 2016. Nutritional Control of Cell Size by the Greatwall-Endosulfine-PP2A·B55 Pathway. *Current Biology*, 26(3), pp.319–330.

Chinnam, M. & Goodrich, D.W., 2011. RB1, development, and cancer. *Current topics in developmental biology*, 94, pp.129–169.

Choi, Y.J. et al., 2012. The Requirement for Cyclin D Function in Tumor Maintenance. *Cancer Cell*, 22(4), pp.438–451.

Chou, T.C., 2006. Theoretical basis, experimental design, and computerized simulation of synergism and antagonism in drug combination studies. *Pharmacological Reviews*, 58(3), pp.621–681.

Ciccia, A. & Elledge, S.J., 2010. The DNA Damage Response: Making it safe to play with knives. *Molecular Cell*, 40(2), pp.179–204.

Coudreuse, D. & Nurse, P., 2010. Driving the cell cycle with a minimal CDK control network. *Nature*, 468(7327), pp.1074–1079.

Cristóbal, I. et al., 2016. Potential anti-tumor effects of FTY720 associated with PP2A activation: a brief review. *Current Medical Research and Opinion*, 32(6), pp.1137–1141.

Cross, F.R., Buchler, N.E. & Skotheim, J.M., 2011. Evolution of networks and sequences in eukaryotic cell cycle control. *Philosophical Transactions of the Royal Society B: Biological Sciences*, 366(1584), pp.3532–3544.

Cundell, M.J. et al., 2013. The BEG (PP2A-B55/ENSA/Greatwall) Pathway Ensures Cytokinesis follows Chromosome Separation. *Molecular Cell*, 52(3), pp.393–405.

D'Adda Di Fagagna, F. et al., 2003. A DNA damage checkpoint response in telomere-initiated senescence. *Nature*, 426(6963), pp.194–198.

De Wulf, P., Montani, F. & Visintin, R., 2009. Protein phosphatases take the mitotic stage. *Current Opinion in Cell Biology*, 21(6), pp.806–815.

DeMichele, A. et al., 2015. CDK 4/6 Inhibitor Palbociclib (PD0332991) in Rb+ Advanced Breast Cancer: Phase II Activity, Safety, and Predictive Biomarker Assessment. *Clinical cancer research : an official journal of the American Association for Cancer Research*, 21(5), pp.995–1001.

Deng, J. et al., 2018. CDK4/6 Inhibition Augments Antitumor Immunity by Enhancing T-cell Activation. *Cancer Discovery*, 8(2), pp.216–233.

Dent, R. et al., 2007. Triple-Negative Breast Cancer: Clinical Features and Patterns of Recurrence. *Clinical cancer research : an official journal of the American Association for Cancer Research*, 13(15), pp.4429–4434.

Dephoure, N. et al., 2008. A quantitative atlas of mitotic phosphorylation. pp.1–6.

DePinto, W. et al., 2006. In vitro and in vivo activity of R547: a potent and selective cyclin-dependent kinase inhibitor currently in phase I clinical trials. *Molecular Cancer Therapeutics*, 5(11), pp.2644–2658.

Di Fiore, R. et al., 2013. RB1 in cancer: Different mechanisms of RB1 inactivation and alterations of pRb pathway in tumorigenesis. *Journal of Cellular Physiology*, 228(8), pp.1676–1687.

Diffley, J.F.X., 2004. Regulation of Early Events in Chromosome Replication. *Current Biology*, 14(18), pp.R778–R786.

Diril, M.K. et al., 2016. Loss of the Greatwall Kinase Weakens the Spindle Assembly Checkpoint R. S. Hawley, ed. *PLoS genetics*, 12(9), p.e1006310.

Do, K. et al., 2015. Phase I Study of Single-Agent AZD1775 (MK-1775), a Wee1 Kinase Inhibitor, in Patients With Refractory Solid Tumors. *JCO*, 33(30), pp.3409–3415.

Do, K., Doroshow, J.H. & Kummar, S., 2013. Wee1 kinase as a target for cancer therapy. *Cell Cycle*, 12(19), pp.3159–3164.

Domingo-Sananes, M.R. et al., 2011. Switches and latches: a biochemical tug-of-war between the kinases and phosphatases that control mitosis. *Philosophical Transactions of the Royal Society B: Biological Sciences*, 366(1584), pp.3584–3594.

Donnelly, M.L.L. et al., 2001. Analysis of the aphthovirus 2A/2B polyprotein 'cleavage' mechanism indicates not a proteolytic reaction, but a novel translational effect: a putative ribosomal 'skip'. *Journal of General Virology*, 82(5), pp.1013–1025.

Dorée, M. & Hunt, T., 2002. From Cdc2 to Cdk1: when did the cell cycle kinase join its cyclin partner? *J. Cell Sci.*, 115(12), p.2461.

Draetta, G. et al., 1987. Identification of p34 and p13, human homologs of the cell cycle regulators of fission yeast encoded by cdc2+ and suc1. *Cell*, 50(2), pp.319–325.

Duronio, R.J. & Xiong, Y., 2013. Signaling pathways that control cell proliferation. *Cold Spring Harbor Perspectives in Biology*, 5(3), pp.a008904–a008904.

Echeverri, C.J. et al., 2006. Minimizing the risk of reporting false positives in large-scale RNAi screens. *Nature Methods*, 3, pp.777 EP –.

Elledge, S.J., 1996. Cell Cycle Checkpoints: Preventing an Identity Crisis. *Science*, 274(5293), pp.1664–1672.

Evans, T. et al., 1983. Cyclin: A protein specified by maternal mRNA in sea urchin eggs that is destroyed at each cleavage division. *Cell*, 33(2), pp.389–396.

Evers, B., Helleday, T. & Jonkers, J., 2010. Targeting homologous recombination repair defects in cancer. *Trends in Pharmacological Sciences*, 31(8), pp.372–380.

Farmer, H. et al., 2005. Targeting the DNA repair defect in BRCA mutant cells as a therapeutic strategy. *Nature*, 434, pp.917 EP –.

Feinberg, A.P. & Tycko, B., 2004. The history of cancer epigenetics. *Nature Reviews Cancer*, 4(2), pp.143–153.

Ferrer, J.-L. et al., 2006. Structural Basis for the Modulation of CDK-Dependent/Independent Activity of Cyclin D1. *Cell cycle (Georgetown, Tex.)*, 5(23), pp.2760–2768.

Fesquet, D. et al., 1993. The MO15 gene encodes the catalytic subunit of a protein kinase that activates cdc2 and other cyclin-dependent kinases (CDKs) through phosphorylation of Thr161 and its homologues. *EMBO J.*, 12(8), pp.3111–3121.

Finn, R.S. et al., 2016. Palbociclib and Letrozole in Advanced Breast Cancer. *N Engl J Med*, 375(20), pp.1925–1936.

Finn, R.S. et al., 2009. PD 0332991, a selective cyclin D kinase 4/6 inhibitor, preferentially inhibits proliferation of luminal estrogen receptor-positive human breast cancer cell lines in vitro. *Breast Cancer Research*, 11(5), pp.R77–R77.

Finn, R.S. et al., 2015. The cyclin-dependent kinase 4/6 inhibitor palbociclib in combination with letrozole versus letrozole alone as first-line treatment of oestrogen receptor-positive, HER2-negative, advanced breast cancer (PALOMA-1/TRIO-18): a randomised phase 2 study. *The lancet oncology*, 16(1), pp.25–35.

Fisher, R.P. & Morgan, D.O., 1994. A novel cyclin associates with M015/CDK7 to form the CDK-activating kinase. *Cell*, 78(4), pp.713–724.

Fokas, E. et al., 2014. Targeting ATR in DNA damage response and cancer therapeutics. *Cancer Treatment Reviews*, 40(1), pp.109–117.

Fong, P.C. et al., 2009. Inhibition of poly(ADP-ribose) polymerase in tumors from BRCA mutation carriers. *New England Journal of Medicine*, 361(2), pp.123–134.

Forester, C.M. et al., 2007. Control of mitotic exit by PP2A regulation of Cdc25C and Cdk1. *Proceedings of the National Academy of Sciences of the United States of America*, 104(50), pp.19867–19872.

Foucquier, J. & Guedj, M., 2015. Analysis of drug combinations: current methodological landscape. *Pharmacology Research & Perspectives*, 3(3), p.e00149.

Foulkes, W.D., Smith, I.E. & Reis-Filho, J.S., 2010. Triple-Negative Breast Cancer. *N Engl J Med*, 363(20), pp.1938–1948.

Fung, T.K. & Poon, R.Y.C., 2005. A roller coaster ride with the mitotic cyclins. *Cell Cycle and Development*, 16(3), pp.335–342.

Furukawa-Hibi, Y. et al., 2002. FOXO Forkhead Transcription Factors Induce G2-M Checkpoint in Response to Oxidative Stress. *Journal of Biological Chemistry*, 277(30), pp.26729–26732.

Gadi, V.K. & Davidson, N.E., 2017. Practical Approach to Triple-Negative Breast Cancer. *JOP*, 13(5), pp.293–300.

Garrett, M.D. & Collins, I., 2011. Anticancer therapy with checkpoint inhibitors: what, where and when? *Trends in Pharmacological Sciences*, 32(5), pp.308–316.

Gelbert, L.M. et al., 2014. Preclinical characterization of the CDK4/6 inhibitor LY2835219: in-vivo cell cycle-dependent/independent anti-tumor activities alone/in combination with gemcitabine. *Investigational New Drugs*, 32(5), pp.825–837.

Gharbi-Ayachi, A. et al., 2010. The Substrate of Greatwall Kinase, Arpp19, Controls Mitosis by Inhibiting Protein Phosphatase 2A. *Science*, 330(6011), pp.1673–1677.

Goel, S. et al., 2016. Overcoming Therapeutic Resistance in HER2-Positive Breast Cancers With CDK4/6 Inhibitors. *Cancer Cell*, 29(3), pp.255–269.

Goldar, A., Marsolier-Kergoat, M.-C. & Hyrien, O., 2009. Universal Temporal Profile of Replication Origin Activation in Eukaryotes J. Bähler, ed. *PLoS One*, 4(6), p.e5899.

Gong, D. & Ferrell, J.E., 2010. The Roles of Cyclin A2, B1, and B2 in Early and Late Mitotic Events D. J. Lew, ed. *Molecular Biology of the Cell*, 21(18), pp.3149–3161.

Grandori, C. et al., 2000. The Myc/Max/Mad Network and the Transcriptional Control of Cell Behavior. *Annu. Rev. Cell Dev. Biol.*, 16(1), pp.653–699.

Gu, Y., Rosenblatt, J. & Morgan, D.O., 1992. Cell cycle regulation of CDK2 activity by phosphorylation of Thr160 and Tyr15. *EMBO J.*, 11(11), pp.3995–4005.

Haffty, B.G. et al., 2006. Locoregional Relapse and Distant Metastasis in Conservatively Managed Triple Negative Early-Stage Breast Cancer. *JCO*, 24(36), pp.5652–5657.

Hagting, A. et al., 1999. Translocation of cyclin B1 to the nucleus at prophase requires a phosphorylation-dependent nuclear import signal. *Current Biology*, 9(13), pp.680–689.

Hanahan, D. & Weinberg, R.A., 2011. Hallmarks of Cancer: The Next Generation. *Cell*, 144(5), pp.646–674.

Harbour, J.W. & Dean, D.C., 2000. The Rb/E2F pathway: expanding roles and emerging paradigms. *Genes Dev.*, 14, pp.2393–2409.

Hartwell, L. & Weinert, T., 1989. Checkpoints: controls that ensure the order of cell cycle events. *Science*, 246(4930), pp.629–634.

He, G. et al., 2005. Induction of p21 by p53 following DNA damage inhibits both Cdk4 and Cdk2 activities. *Oncogene*, 24, pp.2929 EP –.

Heijink, A.M., Krajewska, M. & van Vugt, M.A.T.M., 2013. The DNA damage response during mitosis. *Chromatin modifications*, 750(1), pp.45–55.

Heim, A., Konietzny, A. & Mayer, T.U., 2015. Protein phosphatase 1 is essential for Greatwall inactivation at mitotic exit. *EMBO Reports*, 16(11), pp.1501–1510.

Herrera-Abreu, M.T. et al., 2016. Early Adaptation and Acquired Resistance to CDK4/6 Inhibition in Estrogen Receptor–Positive Breast Cancer. *Cancer research*, 76(8), pp.2301–2313.

Herschkowitz, J.I. et al., 2008. The functional loss of the retinoblastoma tumour suppressor is a common event in basal-like and luminal B breast carcinomas. *Breast Cancer Research*, 10(5), pp.R75–R75.

Hégarat, N. et al., 2014. PP2A/B55 and Fcp1 regulate Greatwall and Ensa dephosphorylation during mitotic exit. G. P. Copenhaver, ed. *PLoS genetics*, 10(1), p.e1004004.

Hirschi, A. et al., 2010. An Overlapping Kinase and Phosphatase Docking Site Regulates Activity of the Retinoblastoma Protein. *Nature Structural & Molecular Biology*, 17(9), pp.1051–1057.

Ho, J. et al., 2018. Moving beyond P values: Everyday data analysis with estimation plots.

Hochegger, H., Takeda, S. & Hunt, T., 2008. Cyclin-dependent kinases and cell-cycle transitions: does one fit all? *Nature Reviews Molecular Cell Biology*, 9(11), pp.910–916.

Hortobagyi, G.N. et al., 2016. Ribociclib as First-Line Therapy for HR-Positive, Advanced Breast Cancer. *N Engl J Med*, 375(18), pp.1738–1748.

Howard, A. & Pelc, S.R., 1986. Synthesis of desoxyribonucleic acid in normal and irradiated cells and its relation to chromosome breakage. *International Journal of Radiation Biology and Related Studies in Physics, Chemistry and Medicine*, 49(2), pp.207–218.

Iacobucci, G., 2017. NICE recommends routine NHS funding for new breast cancer drugs. *BMJ*, 359, p.j5309.

Infante, A. et al., 2008. E2F2 represses cell cycle regulators to maintain quiescence. *Cell Cycle*, 7(24), pp.3915–3927.

Iorns, E. et al., 2009. Integrated Functional, Gene Expression and Genomic Analysis for the Identification of Cancer Targets T. Ouchi, ed. *PLoS One*, 4(4), p.e5120.

Jackman, M., Firth, M. & Pines, J., 1995. Human cyclins B1 and B2 are localized to strikingly different structures: B1 to microtubules, B2 primarily to the Golgi apparatus. *EMBO J.*, 14(8), pp.1646–1654.

Janssens, V., Goris, J. & Van Hoof, C., 2005. PP2A: the expected tumor suppressor. *Oncogenes and cell proliferation*, 15(1), pp.34–41.

Jares, P., Donaldson, A. & Blow, J., 2000. The Cdc7/Dbf4 protein kinase: target of the S phase checkpoint? *EMBO Reports*, 1(4), pp.319–322.

Jayadeva, G. et al., 2010. B55α PP2A Holoenzymes Modulate the Phosphorylation Status of the Retinoblastoma-related Protein p107 and Its Activation. *Journal of Biological Chemistry*, 285(39), pp.29863–29873.

Jazayeri, A. et al., 2005. ATM- and cell cycle-dependent regulation of ATR in response to DNA double-strand breaks. *Nature Cell Biology*, 8(1), pp.37–45.

Jeffrey, P.D. et al., 1995. Mechanism of CDK activation revealed by the structure of a cyclinA-CDK2 complex. *Nature*, 376(6538), pp.313–320.

Johnson, E.S. & Kornbluth, S., 2012. Phosphatases Driving Mitosis: Pushing the Gas and Lifting the Brakes. In S. Shenolikar, ed. *Protein Phosphorylation in Health and Disease*. Progress in Molecular Biology and Translational Science. Academic Press, pp. 327–341.

Johnson, H.J. et al., 2009. The in vivo inactivation of MASTL kinase results in thrombocytopenia. *Experimental hematology*, 37(8), pp.901–908.

Johnson, N. et al., 2009. Cdk1 Participates in BRCA1-Dependent S Phase Checkpoint Control in Response to DNA Damage. *Molecular Cell*, 35(3), pp.327–339.

Jones, S., 2004. An overview of the basic helix-loop-helix proteins. *Genome biology*, 5(6), pp.226–226.

Jordan, M.A. & Wilson, L., 2004. Microtubules as a target for anticancer drugs. *Nature Reviews Cancer*, 4(4), pp.253–265.

Kaldis, P. et al., 1998. Human and Yeast Cdk-activating Kinases (CAKs) Display Distinct Substrate Specificities T. Hunt, ed. *Molecular Biology of the Cell*, 9(9), pp.2545–2560.

Kalkat, M. et al., 2017. MYC Deregulation in Primary Human Cancers. *Genes*, 8(6), p.151.

Kang, C. et al., 2015. The DNA damage response induces inflammation and senescence by inhibiting autophagy of GATA4. *Science*, 349(6255), pp.aaa5612–aaa5612.

Kastan, M.B. & Bartek, J., 2004. Cell-cycle checkpoints and cancer. *Nature*, 432, pp.316 EP –.

Katula, K.S. et al., 1997. Cyclin-dependent kinase activation and S-phase induction of the cyclin B1 gene are linked through the CCAAT elements. *Cell Growth Differ.*, 8, pp.811–820.

Kim, M.-Y. et al., 2012. Bypassing the Greatwall-Endosulfine pathway: plasticity of a pivotal cell-cycle regulatory module in Drosophila melanogaster and Caenorhabditis elegans. *Genetics*, 191(4), pp.1181–1197.

Kitajima, T.S. et al., 2006. Shugoshin collaborates with protein phosphatase 2A to protect cohesin. *Nature*, 441(7089), pp.46–52.

Klein, M.E. et al., 2018. CDK4/6 Inhibitors: The Mechanism of Action May Not Be as Simple as Once Thought. *Cancer Cell*, 34(1), pp.9–20.

Kmietowicz, Z., 2017. Pfizer makes breast cancer drug free while NICE decides its future. *BMJ*, 357, p.j2225.

Knudsen, E.S. & Witkiewicz, A.K., 2017. The Strange Case of CDK4/6 Inhibitors: Mechanisms, Resistance, and Combination Strategies. *Trends in cancer*, 3(1), pp.39–55.

Knudsen, K.E. et al., 2000. RB-Dependent S-Phase Response to DNA Damage. *Molecular and Cellular Biology*, 20(20), pp.7751–7763.

Kolupaeva, V. & Janssens, V., 2012. PP1 and PP2A phosphatases - cooperating partners in modulating retinoblastoma protein activation. *FEBS Journal*, 280(2), pp.627–643.

Kovatcheva, M. et al., 2015. MDM2 turnover and expression of ATRX determine the choice between quiescence and senescence in response to CDK4 inhibition. *Oncotarget*, 6(10), pp.8226–8243.

Kubiczkova, L. et al., 2012. TGF-β – an excellent servant but a bad master. *Journal of Translational Medicine*, 10(1), p.183.

Kumagai, A. et al., 2010. Treslin Collaborates with TopBP1 in Triggering the Initiation of DNA Replication. *Cell*, 140(3), pp.349–359.

Kurimchak, A. & Graña, X., 2012. PP2A holoenzymes negatively and positively regulate cell cycle progression by dephosphorylating pocket proteins and multiple CDK substrates. *Gene*, 499(1), pp.1–7.

Lee, J.-H. & Paull, T.T., 2007. Activation and regulation of ATM kinase activity in response to DNA double-strand breaks. *Oncogene*, 26, pp.7741 EP –.

Lee, M.G. & Nurse, P., 1987. Complementation used to clone a human homologue of the fission yeast cell cycle control gene cdc2. *Nature*, 327(6117), pp.31–35.

Lemmens, B. et al., 2018. DNA Replication Determines Timing of Mitosis by Restricting CDK1 and PLK1 Activation. *Molecular Cell*, 71(1), pp.117–128.e3.

Lessard, F. et al., 2018. Senescence-associated ribosome biogenesis defects contributes to cell cycle arrest through the Rb pathway. *Nature Cell Biology*, 20(7), pp.789–799.

Lew, D.J., Dulić, V. & Reed, S.I., 1991. Isolation of three novel human cyclins by rescue of G1 cyclin (cln) function in yeast. *Cell*, 66(6), pp.1197–1206.

Li, J. et al., 2014. The anti-proliferative function of the TGF-β1 signaling pathway involves the repression of the oncogenic TBX2 by its homologue TBX3. *Journal of Biological Chemistry*, 289(51), pp.35633–35643.

Liao, D.J. et al., 2007. Perspectives on c-Myc, Cyclin D1, and Their Interaction in Cancer Formation, Progression, and Response to Chemotherapy. 13(2), pp.93–158.

Liedtke, C. et al., 2008. Response to Neoadjuvant Therapy and Long-Term Survival in Patients With Triple-Negative Breast Cancer. *JCO*, 26(8), pp.1275–1281.

Lindqvist, A. et al., 2007. Cyclin B1–Cdk1 Activation Continues after Centrosome Separation to Control Mitotic Progression D. Pellman, ed. *PLOS Biology*, 5(5), p.e123.

Lindqvist, A., Rodríguez-Bravo, V. & Medema, R.H., 2009. The decision to enter mitosis: feedback and redundancy in the mitotic entry network. *The Journal of Cell Biology*, 185(2), pp.193–202.

Loftus, K.M. et al., 2017. Mechanism for G2 phase-specific nuclear export of the kinetochore protein CENP-F. *Cell Cycle*, 16(15), pp.1414–1429.

Lolli, G. & Johnson, L.N., 2005. CAK—Cyclin-Dependent Activating Kinase: A Key Kinase in Cell Cycle Control and a Target for Drugs? *Cell Cycle*, 4(4), pp.565–570.

Lorca, T. & Castro, A., 2012. The Greatwall kinase: a new pathway in the control of the cell cycle. *Oncogene*, 32(5), pp.537–543.

Lord, C.J. & Ashworth, A., 2017. PARP inhibitors: Synthetic lethality in the clinic. *Science*, 355(6330), pp.1152–1158.

Lord, C.J. & Ashworth, A., 2012. The DNA damage response and cancer therapy. *Nature*, 481(7381), pp.287–294.

Lundberg, A.S. & Weinberg, R.A., 1998. Functional Inactivation of the Retinoblastoma Protein Requires Sequential Modification by at Least Two Distinct Cyclin-cdk Complexes. *Molecular and Cellular Biology*, 18(2), pp.753–761.

Malumbres, M., 2011. Physiological Relevance of Cell Cycle Kinases. *Physiological Reviews*, 91(3), pp.973–1007.

Malumbres, M. & Barbacid, M., 2009. Cell cycle, CDKs and cancer: a changing paradigm. *Nature Reviews Cancer*, 9(3), pp.153–166.

Malumbres, M. & Barbacid, M., 2005. Mammalian cyclin-dependent kinases. *Trends in Biochemical Sciences*, 30(11), pp.630–641.

Malumbres, M. & Barbacid, M., 2001. To cycle or not to cycle: a critical decision in cancer. *Nature Reviews Cancer*, 1(3), pp.222–231.

Manchado, E. et al., 2010. Targeting Mitotic Exit Leads to Tumor Regression In Vivo: Modulation by Cdk1, Mastl, and the PP2A/B55α,δ Phosphatase. *Cancer Cell*, 18(6), pp.641–654.

Manic, G. et al., 2015. Trial Watch: Targeting ATM–CHK2 and ATR–CHK1 pathways for anticancer therapy. *Molecular & Cellular Oncology*, 2(4), p.e1012976.

Manni, I. et al., 2001. NF-Y Mediates the Transcriptional Inhibition of thecyclin B1, cyclin B2, and cdc25CPromoters upon Induced G2 Arrest. *Journal of Biological Chemistry*, 276(8), pp.5570–5576.

Manning, G. et al., 2002. The protein kinase complement of the human genome. *Science*, 298(5600), pp.1912–1934.

Maréchal, A. & Zou, L., 2013. DNA Damage Sensing by the ATM and ATR Kinases. *Cold Spring Harbor Perspectives in Biology*, 5(9), p.a012716.

Marmé, F. & Schneeweiss, A., 2015. Targeted Therapies in Triple-Negative Breast Cancer. *Breast Care*, 10(3), pp.159–166.

Masai, H. & Arai, K.-I., 2002. Cdc7 kinase complex: A key regulator in the initiation of DNA replication. *Journal of Cellular Physiology*, 190(3), pp.287–296.

Masai, H. et al., 2000. Human Cdc7-related Kinase Complex: IN VITRO PHOSPHORYLATION OF MCM BY CONCERTED ACTIONS OF Cdks AND Cdc7 AND THAT OF A CRITICAL THREONINE RESIDUE OF Cdc7 BY Cdks. *Journal of Biological Chemistry*, 275(37), pp.29042–29052.

Masaki, T. et al., 2003. Cyclins and cyclin-dependent kinases: Comparative study of hepatocellular carcinoma versus cirrhosis. *Hepatology*, 37(3), pp.534–543.

Matheson, C.J., Backos, D.S. & Reigan, P., 2016. Targeting WEE1 Kinase in Cancer. *Trends in Pharmacological Sciences*, 37(10), pp.872–881.

Matsuoka, M. et al., 1994. Activation of cyclin-dependent kinase 4 (cdk4) by mouse MO15-associated kinase. *Molecular and Cellular Biology*, 14(11), pp.7265–7275.

Mazzarello, P., 1999. A unifying concept: the history of cell theory. *Nature Cell Biology*, 1(1), pp.E13–E15.

McNeely, S., Beckmann, R. & Bence Lin, A.K., 2014. CHEK again: Revisiting the development of CHK1 inhibitors for cancer therapy. *Pharmacology & Therapeutics*, 142(1), pp.1–10.

Mi, H. et al., 2013. Large-scale gene function analysis with the PANTHER classification system. *Nature Protocols*, 8, pp.1551 EP –.

Michaud, K. et al., 2010. Pharmacologic Inhibition of Cyclin-Dependent Kinases 4 and 6 Arrests the Growth of Glioblastoma Multiforme Intracranial Xenografts. *Cancer Res.*, 70(8), pp.3228–3238.

Miki, Y. et al., 1994. A strong candidate for the breast and ovarian cancer susceptibility gene BRCA1. *Science*, 266(5182), pp.66–71.

Minshull, J. et al., 1990. The A- and B-type cyclin associated cdc2 kinases in Xenopus turn on and off at different times in the cell cycle. *EMBO J.*, 9(9), pp.2865–2875.

Minshull, J. et al., 1989. The role of cyclin synthesis, modification and destruction in the control of cell division. *Journal of Cell Science*, 1989(Supplement 12), pp.77–97.

Misra, R.N. et al., 2004. N-(Cycloalkylamino)acyl-2-aminothiazole Inhibitors of Cyclin-Dependent Kinase 2. N-[5-[[[5-(1,1-Dimethylethyl)-2-oxazolyl]methyl]thio]-2-thiazolyl]-4- piperidinecarboxamide (BMS-387032), a Highly Efficacious and Selective Antitumor Agent. *J. Med. Chem.*, 47(7), pp.1719–1728.

Mochida, S. et al., 2010. Greatwall Phosphorylates an Inhibitor of Protein Phosphatase 2A That Is Essential for Mitosis. *Science*, 330(6011), pp.1670–1673.

Mochida, S. et al., 2009. Regulated activity of PP2A–B55δ is crucial for controlling entry into and exit from mitosis in Xenopus egg extracts. *EMBO J.*, 28(18), pp.2777–2785.

Moorhead, G.B.G., Trinkle-Mulcahy, L. & Ulke-Lemée, A., 2007. Emerging roles of nuclear protein phosphatases. *Nature Reviews Molecular Cell Biology*, 8(3), pp.234–244.

Morgan, D.O., 2007. *The Cell Cycle: Principles of Control*, New Science Press Ltd.

Mueller, P.R. et al., 1995. Myt1: A Membrane-Associated Inhibitory Kinase That Phosphorylates Cdc2 on Both Threonine-14 and Tyrosine-15. *Science*, 270(5233), pp.86–90.

Munger, K. & Jones, D.L., 2015. Human Papillomavirus Carcinogenesis: an Identity Crisis in the Retinoblastoma Tumor Suppressor Pathway F. Goodrum, ed. *J. Virol.*, 89(9), p.4708.

Nagel, R., Semenova, E.A. & Berns, A., 2016. Drugging the addict: non-oncogene addiction as a target for cancer therapy. *EMBO Reports*, 17(11), pp.1516–1531.

Network, T.C.G.A. et al., 2012. Comprehensive molecular portraits of human breast tumours. *Nature*, 490, pp.61 EP –.

Nguyen, T.B. et al., 2002. Characterization and Expression of Mammalian Cyclin B3, a Prepachytene Meiotic Cyclin. *Journal of Biological Chemistry*, 277(44), pp.41960–41969.

Nguyen, V.Q., Co, C. & Li, J.J., 2001. Cyclin-dependent kinases prevent DNA re-replication through multiple mechanisms. *Nature*, 411(6841), pp.1068–1073.

Nigg, E.A., 2001. Mitotic kinases as regulators of cell division and its checkpoints. *Nature Reviews Molecular Cell Biology*, 2(1), pp.21–32.

O'Neil, N.J., Bailey, M.L. & Hieter, P., 2017. Synthetic lethality and cancer. *Nature Reviews Genetics*, 18(10), pp.613–623.

Oaks, J.J. et al., 2013. Antagonistic activities of the immunomodulator and PP2A-activating drug FTY720 (Fingolimod, Gilenya) in Jak2-driven hematologic malignancies. *Blood*, 122(11), pp.1923–1934.

Obaya, A.J. et al., 2002. The Proto-oncogene c-myc Acts through the Cyclin-dependent Kinase (Cdk) Inhibitor p27Kip1to Facilitate the Activation of Cdk4/6 and Early G1Phase Progression. *Journal of Biological Chemistry*, 277(34), pp.31263–31269.

Ocasio, C.A. et al., 2016. A first generation inhibitor of human Greatwall kinase, enabled by structural and functional characterisation of a minimal kinase domain construct. *Oncotarget*, 7(44), pp.71182–71197.

Oki, T. et al., 2014. A novel cell-cycle-indicator, mVenus-p27K−, identifies quiescent cells and visualizes G0–G1 transition. *Scientific Reports*, 4, pp.4012 EP –.

Olsen, J.V. et al., 2010. Quantitative Phosphoproteomics Reveals Widespread Full Phosphorylation Site Occupancy During Mitosis. *Science Signaling*, 3(104), pp.ra3–ra3.

Ortega, S. et al., 2003. Cyclin-dependent kinase 2 is essential for meiosis but not for mitotic cell division in mice. *Nature Genetics*, 35, pp.25–31.

Ortega, S., Malumbres, M. & Barbacid, M., 2002. Cyclin D-dependent kinases, INK4 inhibitors and cancer. *Biochimica et Biophysica Acta (BBA) - Reviews on Cancer*, 1602(1), pp.73–87.

O'Connor, C.M. et al., 2018. Therapeutic targeting of PP2A. *The International Journal of Biochemistry & Cell Biology*, 96, pp.182–193.

O'Connor, M.J., 2015. Targeting the DNA Damage Response in Cancer. *Molecular Cell*, 60(4), pp.547–560.

Pajcini, K.V. et al., 2010. Transient inactivation of Rb and ARF yields regenerative cells from postmitotic mammalian muscle. *Cell stem cell*, 7(2), pp.198–213.

Parker, L. & Piwnica-Worms, H., 1992. Inactivation of the p34cdc2-cyclin B complex by the human WEE1 tyrosine kinase. *Science*, 257(5078), pp.1955–1957.

Parry, D. et al., 2010. Dinaciclib (SCH 727965), a Novel and Potent Cyclin-Dependent Kinase Inhibitor. *Molecular Cancer Therapeutics*, 9(8), pp.2344–2353.

Patnaik, A. et al., 2016. Efficacy and Safety of Abemaciclib, an Inhibitor of CDK4 and CDK6, for Patients with Breast Cancer, Non-Small Cell Lung Cancer, and Other Solid Tumors. *Cancer Discovery*, 6(7), pp.740–753.

Payton, M. et al., 2006. Discovery and Evaluation of Dual CDK1 and CDK2 Inhibitors. *Cancer Res.*, 66(8), pp.4299–4308.

Pearl, L.H. et al., 2015. Therapeutic opportunities within the DNA damage response. *Nature Reviews Cancer*, 15(3), pp.166–180.

Peng, A. et al., 2010. A novel role for Greatwall kinase in recovery from DNA damage. *Cell Cycle*, 9(21), pp.4364–4369.

Peng, A., Wang, L. & Fisher, L.A., 2011. Greatwall and Polo-like Kinase 1 Coordinate to Promote Checkpoint Recovery. *Journal of Biological Chemistry*, 286(33), pp.28996–29004.

Perez de Castro, I., de Carcer, G. & Malumbres, M., 2006. A census of mitotic cancer genes: new insights into tumor cell biology and cancer therapy. *Carcinogenesis*, 28(5), pp.899–912.

Pernas, S. et al., 2018. CDK4/6 inhibition in breast cancer: current practice and future directions. *Therapeutic Advances in Medical Oncology*, 10, p.1758835918786451.

Perrotti, D. & Neviani, P., 2013. Targeting A Tumor Suppressor To Suppress Tumor Growth: News and Views on Protein Phosphatase 2A (PP2A) as a Target for Anti-cancer Therapy. *The lancet oncology*, 14(6), pp.e229–e238.

Perry, J.A. & Kornbluth, S., 2007. Cdc25 and Wee1: analogous opposites? *Cell Division*, 2, pp.12–12.

Petri, E.T. et al., 2014. The Crystal Structure of Human Cyclin B. *Cell Cycle*, 6(11), pp.1342–1349.

Pines, J. & Hunt, T., 1987. Molecular cloning and characterization of the mRNA for cyclin from sea urchin eggs. *EMBO J.*, 6(10), pp.2987–2995.

Pines, J. & Rieder, C.L., 2001. Re-staging mitosis: a contemporary view of mitotic progression. *Nature Cell Biology*, 3(1), pp.E3–E6.

Plasilova, M.L. et al., 2016. Features of triple-negative breast cancer: Analysis of 38,813 cases from the national cancer database H. Oshiro, ed. *Medicine*, 95(35), p.e4614.

Polk, A. et al., 2017. Specific CDK4/6 inhibition in breast cancer: a systematic review of current clinical evidence. *ESMO Open*, 1(6), p.e000093.

Poon, R.Y. et al., 1994. Cell cycle regulation of the p34cdc2/p33cdk2-activating kinase p40MO15. *J. Cell Sci.*, 107(10), p.2789.

Poon, R.Y. et al., 1993. The cdc2-related protein p40MO15 is the catalytic subunit of a protein kinase that can activate p33cdk2 and p34cdc2. *EMBO J.*, 12(8), pp.3123–3132.

Pozarowski, P. & Darzynkiewicz, Z., 2004. Analysis of Cell Cycle by Flow Cytometry. In *Checkpoint Controls and Cancer*. Checkpoint Controls and Cancer: Volume 2: Activation and Regulation Protocols. New Jersey: Humana Press, pp. 301–312.

Rao, H. & Stillman, B., 1995. The origin recognition complex interacts with a bipartite DNA binding site within yeast replicators. *Proceedings of the National Academy of Sciences of the United States of America*, 92(6), pp.2224–2228.

Rao, P.N. & Johnson, R.T., 1970. Mammalian Cell Fusion : Studies on the Regulation of DNA Synthesis and Mitosis. *Nature*, 225(5228), pp.159–164.

Remus, D. & Diffley, J.F., 2009. Eukaryotic DNA replication control: Lock and load, then fire. *Current Opinion in Cell Biology*, 21(6), pp.771–777.

Rieder, C.L., 2003. Mitosis Through the Microscope: Advances in Seeing Inside Live Dividing Cells. *Science*, 300(5616), pp.91–96.

Rieder, C.L. et al., 1995. The checkpoint delaying anaphase in response to chromosome monoorientation is mediated by an inhibitory signal produced by unattached kinetochores. *The Journal of Cell Biology*, 130(4), pp.941–948.

Robinson, T.J.W. et al., 2013. RB1 Status in Triple Negative Breast Cancer Cells Dictates Response to Radiation Treatment and Selective Therapeutic Drugs A. Ahmad, ed. *PLoS One*, 8(11), p.e78641.

Rogers, S. et al., 2018. MASTL overexpression promotes chromosome instability and metastasis in breast cancer. *Oncogene*.

Rogers, S. et al., 2016. PP1 initiates the dephosphorylation of MASTL, triggering mitotic exit and bistability in human cells. *Journal of Cell Science*, 129(7), pp.1340–1354.

Rottenberg, S. et al., 2008. High sensitivity of BRCA1-deficient mammary tumors to the PARP inhibitor AZD2281 alone and in combination with

platinum drugs. *Proceedings of the National Academy of Sciences*, 105(44), pp.17079–17084.

Rowley, A. et al., 1995. Initiation complex assembly at budding yeast replication origins begins with the recognition of a bipartite sequence by limiting amounts of the initiator, ORC. *EMBO J.*, 14(11), pp.2631–2641.

Russell, P. & Nurse, P., 1986. Schizosaccharomyces pombe and saccharomyces cerevisiae: A look at yeasts divided. *Cell*, 45(6), pp.781–782.

Russo, A.A., Jeffrey, P.D. & Pavletich, N.P., 1996. Structural basis of cyclin-dependent kinase activation by phosphorylation. *Nature Structural & Molecular Biology*, 3(8), pp.696–700.

Ruvolo, P.P., 2016. The broken “Off” switch in cancer signaling: PP2A as a regulator of tumorigenesis, drug resistance, and immune surveillance. *BBA Clinical*, 6, pp.87–99.

Saldivar, J.C., Cortez, D. & Cimprich, K.A., 2017. The essential kinase ATR: ensuring faithful duplication of a challenging genome. *Nature Reviews Molecular Cell Biology*, 18(10), pp.622–636.

Santamaría, D. et al., 2007. Cdk1 is sufficient to drive the mammalian cell cycle. *Nature*, 448, pp.811 EP –.

Santos, S.D.M. et al., 2012. Spatial Positive Feedback at the Onset of Mitosis. *Cell*, 149(7), pp.1500–1513.

Schachter, M.M. et al., 2013. A Cdk7-Cdk4 T-Loop Phosphorylation Cascade Promotes G1 Progression. *Molecular Cell*, 50(2), pp.250–260.

Schellens, J.H.M., Shapiro, G. & Pavlick, A.C., 2011. Update on a phase I pharmacologic and pharmacodynamic study of MK-1775, a Wee1 tyrosine kinase inhibitor, in monotherapy and combination with gemcitabine, cisplatin, or carboplatin in patients with advanced solid tumors. *J Clin Oncol*, 29(SUPPL.).

Schmitz, M.H.A. et al., 2010. Live-cell imaging RNAi screen identifies PP2A–B55α and importin-β1 as key mitotic exit regulators in human cells. *Nature Cell Biology*, 12(9), pp.10.1038/ncb2092.

Schneider, B.P. et al., 2008. Triple-Negative Breast Cancer: Risk Factors to Potential Targets. *Clinical cancer research : an official journal of the American Association for Cancer Research*, 14(24), pp.8010–8018.

Sciortino, S. et al., 2001. The cyclin B1 gene is actively transcribed during mitosis in HeLa cells. *EMBO Reports*, 2(11), pp.1018–1023.

Sedlacek, H. et al., 1996. Flavopiridol (L86 8275; NSC 649890), a new kinase inhibitor for tumor therapy. *International Journal of Oncology*, 9, pp.1143–1168.

Sharma, P., 2016. Biology and Management of Patients With Triple-Negative Breast Cancer. *The Oncologist*, 21(9), pp.1050–1062.

Sharma, S.V. & Settleman, J., 2007. Oncogene addiction: setting the stage for molecularly targeted cancer therapy. *Genes & Development*, 21(24), pp.3214–3231.

Sherr, C.J. & Roberts, J.M., 1999. CDK Inhibitors: positive and negative regulators of G1-phase progression. *Genes Dev.*, 13(12), pp.1501–1512.

Sigl, R. et al., 2014. Development of a Multipurpose GATEWAY-Based Lentiviral Tetracycline-Regulated Conditional RNAi System (GLTR) R. Tripp, ed. *PLoS One*, 9(5), p.e97764.

Sigoillot, F.D. & King, R.W., 2011. Vigilance and Validation: Keys to Success in RNAi Screening. *ACS Chemical Biology*, 6(1), pp.47–60.

Smith, J. et al., 2010. Chapter 3 - The ATM–Chk2 and ATR–Chk1 Pathways in DNA Damage Signaling and Cancer. In G. F. Vande Woude & G. Klein, eds. *Advances in Cancer Research*. Advances in Cancer Research. Academic Press, pp. 73–112.

Speck, C. et al., 2005. ATPase-dependent cooperative binding of ORC and Cdc6 to origin DNA. *Nature Structural & Molecular Biology*, 12(11), pp.965–971.

Spencer, S.L. et al., 2013. The Proliferation-Quiescence Decision Is Controlled by a Bifurcation in CDK2 Activity at Mitotic Exit. *Cell*, 155(2), pp.369–383.

Stirzaker, C. et al., 1997. Extensive DNA Methylation Spanning the *Rb* Promoter in Retinoblastoma Tumors. *Cancer Res.*, 57(11), p.2229.

Stockmans, G. et al., 2008. Triple-negative breast cancer. *Current Opinion in Oncology*, 20(6).

Strauss, B. et al., 2018. Cyclin B1 is essential for mitosis in mouse embryos, and its nuclear export sets the time for mitosis. *The Journal of Cell Biology*, 217(1), pp.179–193.

Swinnen, E. et al., 2006. Rim15 and the crossroads of nutrient signalling pathways in Saccharomyces cerevisiae. *Cell Division*, 1, pp.3–3.

Takeda, D.Y. & Dutta, A., 2005. DNA replication and progression through S phase. *Oncogene*, 24(17), pp.2827–2843.

Tanaka, S. & Araki, H., 2010. Regulation of the initiation step of DNA replication by cyclin-dependent kinases. *Chromosoma*, 119(6), pp.565–574.

Tanaka, T.U., 2005. Chromosome bi-orientation on the mitotic spindle. *Philosophical Transactions of the Royal Society B: Biological Sciences*, 360(1455), pp.581–589.

Tang, Z. et al., 2006. PP2A Is Required for Centromeric Localization of Sgo1 and Proper Chromosome Segregation. *Developmental Cell*, 10(5), pp.575–585.

Tassan, J.P. et al., 1994. Cell cycle analysis of the activity, subcellular localization, and subunit composition of human CAK (CDK-activating kinase). *The Journal of Cell Biology*, 127(2), pp.467–478.

Teo, Z.L. et al., 2017. Combined CDK4/6 and PI3Kα Inhibition Is Synergistic and Immunogenic in Triple-Negative Breast Cancer. *Cancer Res.*, 77(22), pp.6340–6352.

Toyoshima, F., 1998. Nuclear export of cyclin B1 and its possible role in the DNA damage-induced G2 checkpoint. *The EMBO Journal*, 17(10), pp.2728–2735.

Tripathy, D., Bardia, A. & Sellers, W.R., 2017. Ribociclib (LEE011): Mechanism of Action and Clinical Impact of This Selective Cyclin-Dependent Kinase 4/6 Inhibitor in Various Solid Tumors. *Clinical cancer research : an official journal of the American Association for Cancer Research*, 23(13), pp.3251–3262.

Turner, N.C. et al., 2015. Palbociclib in Hormone-Receptor–Positive Advanced Breast Cancer. *N Engl J Med*, 373(3), pp.209–219.

Turner, W., 1890. The Cell Theory, Past and Present. *Journal of Anatomy and Physiology*, 24(Pt 2), pp.253–287.

Vairapandi, M. et al., 2002. GADD45b and GADD45g are cdc2/cyclinB1 kinase inhibitors with a role in S and G2/M cell cycle checkpoints induced by genotoxic stress. *Journal of Cellular Physiology*, 192(3), pp.327–338.

Venkitaraman, A.R., 2002. Cancer susceptibility and the functions of BRCA1 and BRCA2. *Cell*, 108(2), pp.171–182.

Vera, J. et al., 2015. Greatwall promotes cell transformation by hyperactivating AKT in human malignancies. *eLife*, 4, pp.e10115–24.

Verlinden, L. et al., 2007. The E2F-Regulated Gene Chk1Is Highly Expressed in Triple-Negative Estrogen Receptor−/Progesterone Receptor−/HER-2− Breast Carcinomas. *Cancer Res.*, 67(14), pp.6574–6581.

Vigneron, S. et al., 2009. Greatwall maintains mitosis through regulation of PP2A. *EMBO J.*, 28(18), pp.2786–2793.

Voets, E. & Wolthuis, R.M.F., 2010. MASTL is the human ortholog of Greatwall kinase that facilitates mitotic entry, anaphase and cytokinesis. *Cell Cycle*, 9(17), pp.3591–3601.

Vora, S.R. et al., 2014. CDK 4/6 inhibitors sensitize PIK3CA Mutant Breast Cancer to PI3K inhibitors. *Cancer Cell*, 26(1), pp.136–149.

Wang, L. et al., 2014. Mastl kinase, a promising therapeutic target, promotes cancer recurrence. *Oncotarget*, 5(22), pp.11479–11489.

Wang, X.W. et al., 1999. GADD45 induction of a G(2)/M cell cycle checkpoint. *Proceedings of the National Academy of Sciences of the United States of America*, 96(7), pp.3706–3711.

Weinberger, M. et al., 2007. DNA replication stress is a determinant of chronological lifespan in budding yeast. *PLoS One*, 2(8), pp.e748–e748.

Weinstein, I.B., 2002. CANCER: Enhanced: Addiction to Oncogenes--the Achilles Heal of Cancer. *Science*, 297(5578), pp.63–64.

Welburn, J.P.I. et al., 2007. How Tyrosine 15 Phosphorylation Inhibits the Activity of Cyclin-dependent Kinase 2-Cyclin A. *Journal of Biological Chemistry*, 282(5), pp.3173–3181.

Wiese, K.E. et al., 2013. The role of MIZ-1 in MYC-dependent tumorigenesis. *Cold Spring Harbor perspectives in medicine*, 3(12), pp.a014290–a014290.

Wittenberg, C. & Reed, S.I., 1989. Conservation of function and regulation within the Cdc28/cdc2 protein kinase family: characterization of the human Cdc2Hs protein kinase in Saccharomyces cerevisiae. *Molecular and Cellular Biology*, 9(9), pp.4064–4068.

Wlodarchak, N. & Xing, Y., 2016. PP2A as a master regulator of the cell cycle. *Critical reviews in biochemistry and molecular biology*, 51(3), pp.162–184.

Wong, P.Y. et al., 2016. MASTL(Greatwall) regulates DNA damage responses by coordinating mitotic entry after checkpoint recovery and APC/C activation. *Scientific Reports*, 6, pp.22230 EP –.

Woo, R.A. & Poon, R.Y.C., 2003. Cyclin-Dependent Kinases and S Phase Control in Mammalian Cells. *Cell Cycle*, 2(4), pp.315–323.

Wooster, R. et al., 1995. Identification of the breast cancer susceptibility gene BRCA2. *Nature*, 378(6559), pp.789–792.

Yekezare, M., Gomez-Gonzalez, B. & Diffley, J.F.X., 2013. Controlling DNA replication origins in response to DNA damage - inhibit globally, activate locally. *Journal of Cell Science*, 126(6), pp.1297–1306.

Yim, E.-K. & Park, J.-S., 2005. The role of HPV E6 and E7 oncoproteins in HPV-associated cervical carcinogenesis. *Cancer research and treatment : official journal of Korean Cancer Association*, 37(6), pp.319–324.

Yoon, Y.N., Choe, M.H., Jung, K.-Y., Hwang, S.-G., Oh, J.S. & Kim, J.-S., 2018a. MASTL inhibition promotes mitotic catastrophe through PP2A activation to inhibit cancer growth and radioresistance in breast cancer cells. *BMC Cancer*, 18(1), p.716.

Yoon, Y.N., Choe, M.H., Jung, K.-Y., Hwang, S.-G., Oh, J.S. & Kim, J.-S., 2018b. MASTL inhibition promotes mitotic catastrophe through PP2A activation to inhibit cancer growth and radioresistance in breast cancer cells. *BMC Cancer*, 18, p.716.

Yu, J. et al., 2004. Greatwall kinase: a nuclear protein required for proper chromosome condensation and mitotic progression in Drosophila. *The Journal of Cell Biology*, 164(4), pp.487–492.

Yu, Q. et al., 2006. Requirement for CDK4 kinase function in breast cancer. *Cancer Cell*, 9(1), pp.23–32.

Yu, Q., Geng, Y. & Sicinski, P., 2001. Specific protection against breast cancers by cyclin D1 ablation. *Nature*, 411(6841), pp.1017–1021.

Zhao, H. et al., 2012. Loss of Cyclin-Dependent Kinase 2 (CDK2) Inhibitory Phosphorylation in a CDK2AF Knock-In Mouse Causes Misregulation of DNA Replication and Centrosome Duplication. *Molecular and Cellular Biology*, 32(8), pp.1421–1432.

Zhao, Y. et al., 2008. Roles of Greatwall Kinase in the Regulation of Cdc25 Phosphatase M. Solomon, ed. *MBoC*, 19(4), pp.1317–1327.

Zhu, L. & Skoultchi, A.I., 2001. Coordinating cell proliferation and differentiation. *Curr. Opin. Genet. Dev.*, 11, pp.91–97.

Zhu, Y. et al., 2004. Intra-S-Phase Checkpoint Activation by Direct CDK2 Inhibition. *Molecular and Cellular Biology*, 24(14), pp.6268–6277.

Zou, L. & Stillman, B., 2000. Assembly of a Complex Containing Cdc45p, Replication Protein A, and Mcm2p at Replication Origins Controlled by S-Phase Cyclin-Dependent Kinases and Cdc7p-Dbf4p Kinase. *Molecular and Cellular Biology*, 20(9), pp.3086–3096.